The Influence of Material and Process Parameters on High-Energy Electron Beam Curing of Polymer Composites

by

R. Mark Baillie

A Thesis

Submitted to the Faculty of Graduate Studies

in Partial Fulfillment of the Requirements

for the Degree of

MASTER OF SCIENCE

Department of Mechanical and Industrial Engineering

University of Manitoba

THE UNIVERSITY OF MANITOBA

FACULTY OF GRADUATE STUDIES

*****

COPYRIGHT PERMISSION PAGE

The Influence of Material and Process Parameters on High-Energy Electron Beam Curing of Polymer Composites

BY

R. Mark Baillie

A Thesis/Practicum submitted to the Faculty of Graduate Studies of The University of Manitoba in partial fulfillment of the requirements of the degree of Master of Science

Abstract

High-energy electron beam (EB) curing of advanced composites is a novel alternative to conventional thermal processing. It offers the possibilities of both cost reduction and technical improvements when compared to autoclave curing. The purpose of this thesis is to present a critical examination of the process of EB curing, with the intent of developing a better understanding of its potential for commercial use. Specifically, this study describes EB curing, and then identifies and examines the influence of important material and process parameters on curing and material properties. A resin system consisting of a high-temperature epoxy and a cationic photoinitiator is investigated. The material and process parameters of radiant dose, initiator concentration, temperature, dose rate, and reinforcement are analyzed for their effect on cure extent and glass transition temperature, T_g. Experimental investigation is performed by differential scanning calorimetry (DSC), and dynamic mechanical analysis (DMA). Properties are also compared between EB and thermally cured samples of the identical resin formulation by mechanical testing. The most notable result of this research is that incomplete curing (less than 80% cure extent) occurs for the epoxy formulation irradiated at room temperature, even at EB doses as high as 500 kGy. Also significant is that the ultimate cure extent is strongly influenced by the temperature and dose rate during processing. These results may curtail some of the proposed advantages of EB processing such as the ability to EB cure at a selectable temperature. Additional results are presented and discussed which are important to the further development of predictive models for high energy EB curing of composites.

Acknowledgements

This thesis would not have been possible without the support of

my advisor, Dr. Raghavan Jayaraman,

Vince Lopata of Acsion Industries Inc.,

and most of all Terry Fulton.

Thanks so much for everything.

Table of Contents

List of Figures

List of Tables

Chapter 1

Introduction

High-energy electron beam curing of advanced polymer composites is a unique and potentially revolutionary processing technology. It involves the application of radiant energy, rather than the traditional thermal energy, to induce crosslinking of the polymer matrix. Both fundamentally and practically, this represents a significant departure from conventional processing of polymer composites.

In the past two decades, high-energy electron beam (also referred to as E-Beam or EB) curing of composites has progressed from general concept, to interesting possibility, to a viable alternative to conventional processing. Since the mid-1980's, a notable amount of research on electron beam curing has been done by the Radiation Applications Group at Atomic Energy of Canada in Pinawa, Manitoba. In 1998, this group became Acsion Industries Incorporated and has continued to be a leader in the field. Despite advances made by this team, high-energy EB curing technology has remained largely overlooked by industry until very recently. Two factors contributing to new-found interest in the process have been the demonstration that EB curing can be used to produce

high performance aerospace composites [1-5] and the prevailing trend in the aerospace industry to seek out novel approaches to problem solving and cutting costs [6]. Presently, there is a clamouring of attention and excitement about the growing potential of electron beam curing in the aerospace industry and beyond into other application areas of the polymer composite industry.

Recent studies have been done on the feasibility and potential benefits of high energy EB curing of composites [7-13] and on suggesting and testing new applications [14-17]. As well, new polymeric formulations have been developed for EB, which perform well when compared to conventional thermal formulations [18-20]. Such studies have been necessary to 'sell' the technology to established composites manufacturers. However, very little work has been done on advancing the fundamental understanding of the process itself, both from an engineering and scientific perspective. The lack of information in this area is the motivation for this investigation.

1.1 Advanced Thermoset Polymer Matrix Composites

Simply described, an engineered composite material is the union of two or more distinct components, which together yield a new material with enhanced properties and capabilities. Composites generally consist of a binder or **matrix** material within which **reinforcement** is embedded. Polymer matrix composites (PMCs) are the most widely used and versatile type of composite. PMCs have the chemical stability, low density, and impact resistance of a polymer and obtain improved strength and stiffness from

reinforcing fibres. Polymer matrix composites are commonly used in a variety of diverse fields and applications from fishing rods to boat hulls to rocket casings.

An **'advanced PMC'** is a combination of high performing, temperature resistant polymers and high-strength, high-stiffness, continuous fibre reinforcement resulting in a material with exceptional thermal and mechanical properties. Advanced PMCs possess extremely favourable values for specific strength (strength to density ratio) and specific modulus (modulus to density ratio). Typical specific tensile strengths for aligned fibre PMCs are more than five times those for structural steel [21]. Graphite/carbon fibre reinforced advanced PMCs are used extensively by the aerospace industry because their high specific properties lead directly to weight reduction of aircraft, which is of principle importance in reducing operating (fuel consumption) costs.

For advanced aerospace composites, thermosetting resins* (**thermosets**) are the predominant matrix material. Thermoset PMCs are shaped or molded into form, and then must be 'cured' before being used. The process of **curing** transforms the resin from a liquid or pliable semi-solid into a non-tacky, insoluble, infusible solid. Curing is a chemical process and is shown in schematic form at the molecular level in Figure 1.1. An energy input causes permanent crosslinking bonds (crosslinks) to form between molecules, transforming the resin into a three-dimensional polymer network. The matrix is then dimensionally stable and is able to transfer and evenly distribute external loads to the reinforcing fibres, giving the PMC its resiliency and strength. Once it has been cured or crosslinked, a thermoset cannot be softened or melted by any application of heat.

---

* for a more complete introduction to polymers and composites, including a description of polymer and PMC terminology please refer to appendix 1

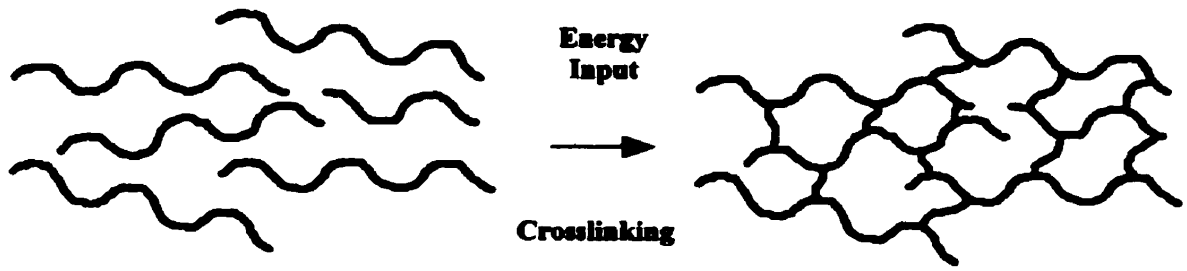

Figure 1.1: Curing of a thermoset polymer

By far the most common matrix material for advanced thermoset composites and for a variety of demanding applications is **epoxy** [21]. Epoxies have taken this major role because of their excellent adhesion, strength, low shrinkage, corrosion protection, processing versatility, and many other properties. Epoxies are thermoset polymers characterized by the presence of the epoxide group – two carbon atoms and an oxygen atom, arranged as shown in Figure 1.2. This epoxide group is typically the site of the crosslinking reactions during curing.

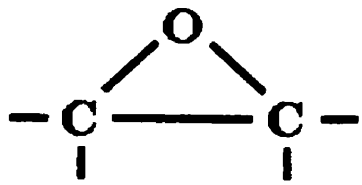

Figure 1.2:
Epoxide Group

The investigation of the curing process for thermoset resins, such as epoxies, is an important subject in the composite industry. For curing of a composite to take place, energy must be supplied to the resin to stimulate the reaction. A reduction in the time required for processing or the energy-input necessary for complete curing leads directly to cost savings. Material characteristics and process conditions influence the kinetics of

curing of the polymer matrix, and effect the thermal and mechanical characteristics of the cured PMC. Consequently, optimization of material and process parameters is essential for reasons of economy and performance.

1.2 Conventional (Autoclave) Processing

Although there are a variety of conventional manufacturing methods for PMCs, advanced aerospace composites are normally produced by the process of autoclave curing of molded laminates. A **laminate** PMC is made up of a number of thin individual layers or plies of composite which are consolidated on a steel or aluminium mold to form a structure of desired shape and thickness. An **autoclave** is a large vessel with a programmable, controlled environment of high temperature and high pressure. Autoclaves range in size from lab-scale autoclaves (Figure 1.3) which are able to accommodate small molds, to giant warehouse-scale autoclaves (Figure 1.4) which accommodate a number of large aerospace structures at one time. Autoclave curing produces composite parts with exceptional properties, but is expensive and has some notable technical drawbacks.

Molded laminates are fabricated by using **prepreg**, a single layer of unidirectional or woven fibres that has been preimpregnated with resin. A number of prepreg layers (lamina) are stacked and shaped on a mold (layed-up) according to design requirements to form the composite part. Prepreg laminates are **bag-molded** before autoclaving, by taping a thin plastic bag to the mold covering the composite part. A vacuum is drawn within the bag to consolidate the prepreg and remove entrapped air and other gaseous

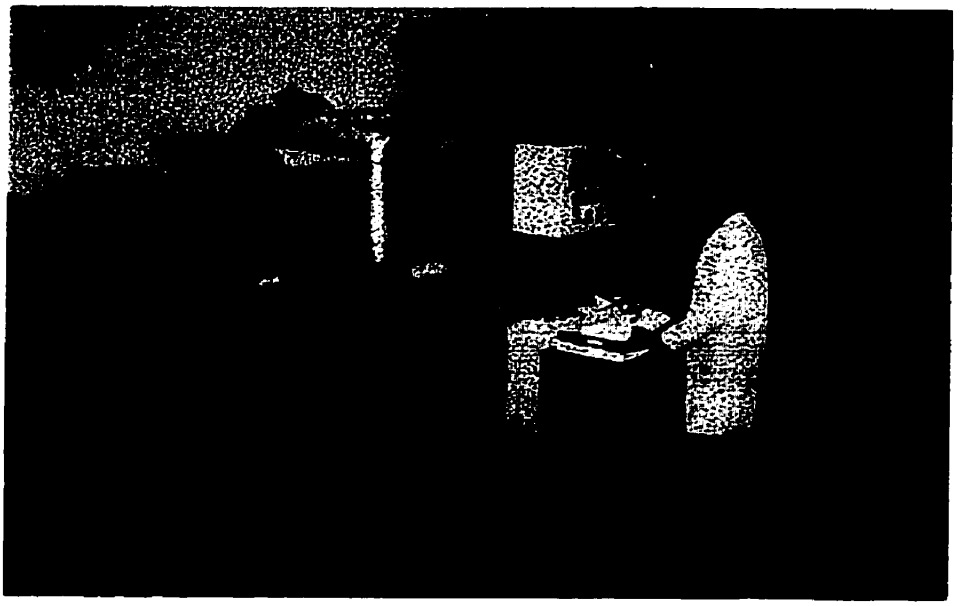

Figure 1.3: Lab-scale autoclave (1 m diameter)
[source: Cranfield University Aerospace Composites Group]

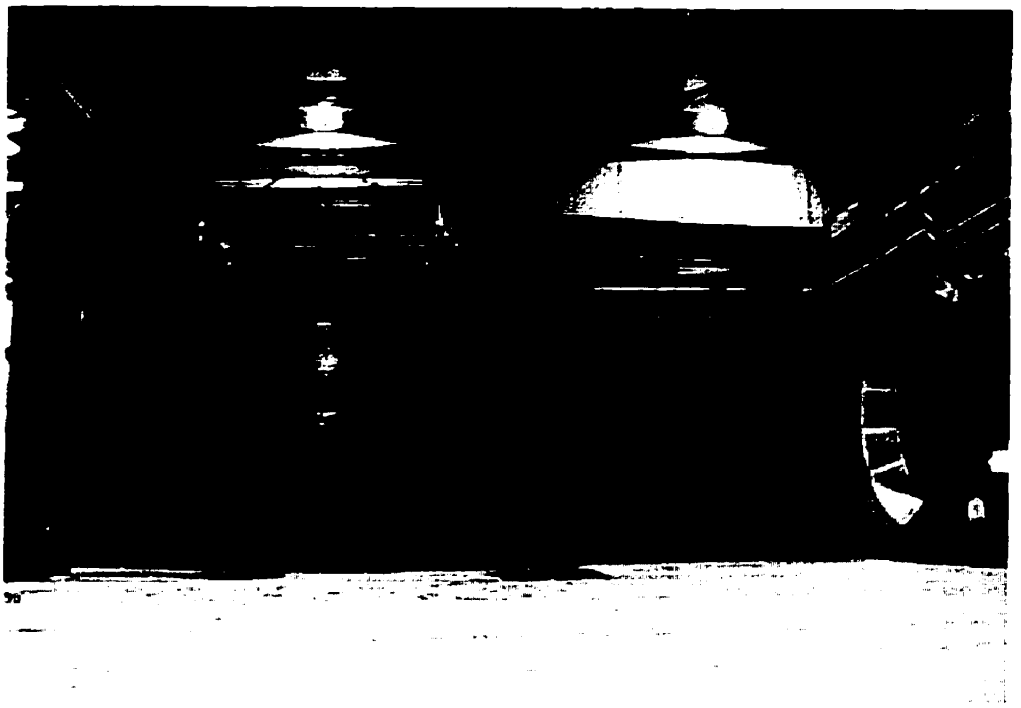

Figure 1.4: Large industrial autoclaves (15.5 m diameter)
[source: Thermal Equipment Corporation]

volatiles. Usually, a number of bag-molded PMCs are placed in the autoclave for processing at the same time. Manufacturing steps prior to the actual curing stage are, for the purpose of this thesis, referred to as 'pre-processing' steps

In autoclave processing, the temperature of the autoclave is ramped up slowly to ensure even heating of the uncured composite and mold. The resin softens and releases gaseous volatiles as it flows between the fibres of the prepreg layers. The application of high pressure in the autoclave helps to further consolidate the laminate and minimize porosity in the composite. Crosslinking reactions begin to occur during the temperature ramp and eventually the autoclave reaches the **cure temperature** that is optimum for the curing reaction. For epoxies, this cure temperature is typically 177°C (350°F) or 121°C (250°F). After holding this temperature for a required period of time to ensure that crosslinking is complete, the autoclave is cooled slowly to avoid residual thermal stress in the cured PMCs. The entire autoclave curing cycle takes a number of hours, depending on the size of the autoclave and the kinetics of the curing reaction.

In conventional curing of a thermoset resin, the addition of a hardening agent is required as well as the application of heat energy. The hardener/resin combination is referred to as the **cure formulation**. Both the cure formulation and cure conditions are important in determining the physical and mechanical properties of the cured composite. For epoxies, the hardener reacts with the epoxy ring during curing to form a reactive site that can then react with another epoxy group leading to crosslinking of the chains. As the thermoset cures, the hardener becomes an integral part of the polymer network so the relative concentration of resin to initiator is an important consideration [22]. An excess of resin leads to undercuring, in which physical properties are less than ideal. An excess

of hardener leads to an adduct of low molecular weight also leading to poor physical properties for the PMC.

Once the resin and hardener are mixed, the curing reaction begins immediately, but typically is very slow at low (near ambient) temperatures. The increase in temperature in the autoclave accelerates the cure process, and curing occurs at a faster rate and to a further degree (more crosslinks). In general, the cure temperature will influence the temperature capabilities of the cured resin. The **glass transition temperature, T_g,** is a rheological* property of a thermoset polymer that influences maximum practical service temperature. Below T_g, a thermoset behaves like a glass and is rigid and dimensionally stable, while above T_g, a thermoset becomes rubber-like, and has lower modulus and strength. Hence the maximum service temperature of a composite is always below the glass transition temperature. The T_g of a composite is proportional to the extent of cure of the matrix and increases during curing as the curing reaction proceeds. For epoxy matrix composites, the resulting T_g of the cured composite part is very near the process cure temperature [22].

Autoclave processing of bag molded laminates is a well-established method that results in PMCs of excellent quality suitable for advanced aerospace applications. However there are a number of disadvantages to this type of conventional thermal processing. One drawback of autoclaves is their high capital cost, which increases rapidly with increasing size requirements. Also, since thermal curing is slow, a bottleneck is often created in the autoclave step of the manufacturing process. Batch

* rheology – the science of plastic deformation and flow in solid materials

processing may also lead to a compromise in the curing conditions to accommodate different parts using different resin systems. Other disadvantages to thermal curing include the high cost of heat resistant tooling materials (molds), and warping of parts due to coefficient of thermal expansion (CTE) mismatch within the composite or between the composite part and tool.

1.3 Electron Beam Processing

Electron beam curing is an emerging alternative to thermal processing which has many potential benefits compared to autoclave curing. In EB curing, the process centres on an electron accelerator rather than an autoclave. A photograph of the electron accelerator used for EB curing in this study is shown in Figure 1.5. Instead of heat energy, **radiant energy** in the form of accelerated electrons is used to initiate and propagate the curing reaction. For a polymer matrix composite (PMC) to be suitable for EB curing, specially designed resin formulations must be used, which utilize unique radiation sensitive **initiators** rather than traditional hardeners [1].

Many of the traditional pre-processing steps in the composite industry such as prepreg lay-up and bag molding remain the same for electron beam processing, however there are significant differences in the curing cycle. In EB curing, the *stationary* autoclave and enclosed heating elements are replaced with *moving* conveyor belts and a continuously scanning electron gun. Rather than curing a composite part in *bulk* by raising the temperature of the entire part, EB processing cures only that *section* of the composite under the influence of the electron beam at any given time. Conventional

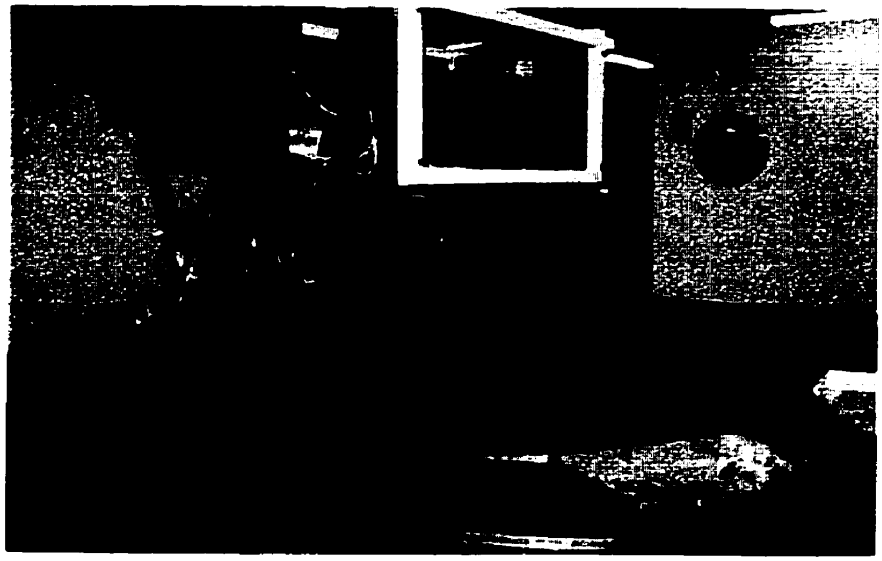

Figure 1.5: High-energy accelerator used for electron beam curing of polymer matrix composites

batch-processing of a number of parts in the autoclave at one time is replaced by repetitive one-after-the-other (*continuous*) processing. A programmed *time-temperature cycle* is replaced by a scheduled scanning *electron beam pattern*. In thermal curing, the time-temperature cycle is designed with *viscosity and resin flow considerations* in mind due to the increase in temperature in the autoclave. In EB processing, curing of a semi-solid pre-polymer may be designed to take place with little temperature rise and *no resin flow* (consolidation and resin flow become pre-processing steps). Finally, possible concerns about *thermal degradation* caused by high temperatures or over-curing in the autoclave are replaced by concerns about *radiation damage* at high radiation doses.

In EB processing, a stream of electrons, collimated into an intense beam, is aimed at the composite part. The electrons penetrate the part and interact at the molecular/atomic level. Curing reactions begin immediately and occur at a very fast rate [23]. High-energy electrons (typically in the order of 10 MeV) are used because they penetrate deep enough (2 to 3 cm) to cure most laminated composites [24]. The electron beam is scanned back and forth continuously as a conveyor moves the composite part by the beam. The cure extent (and hence the glass transition temperature) increases with increasing exposure to the electron beam. Multiple passes under the electron beam are required for maximum curing. The entire process is normally performed at room temperature with no more than vacuum bag pressure applied. Glass transition temperatures far exceeding room temperature are achieved. This is contrary to conventional processing, where the maximum glass transition temperature achieved is highly dependent on cure temperature.

The advantages of EB curing over autoclave curing have been the subject of much speculation and discussion in the aerospace industry. Foremost in any analysis is the advantage of potential immediate and/or long term cost savings compared to conventional processing. Curing at selectable ambient conditions (temperature, pressure) yet obtaining very high T_g values is a revolutionary possibility. Curing at room temperature allows the use of inexpensive molds such as foam, wood, and plaster, replacing steel or other high temperature tooling materials. Although capital costs of E-beam facilities are high (similar to autoclaves) there are no restrictions on size of composite parts and there is no bottleneck at the autoclave step.

With EB curing, improvements in part quality and new technical advantages are possible. The thermal curing process must account for the deformation of the tool and composite part due to coefficient of thermal expansion (CTE) mismatch during processing and cool-down. E-Beam curing at ambient temperature (or potentially at a selected optimum temperature) avoids this problem. In a large autoclave, for different parts to be cured together, they must be subjected to the same curing cycle. In E-Beam, each composite part is processed separately and may have different curing cycles. Furthermore, integrated structures made up of different composites can be E-Beam cured in sections – according to any co-curing requirements. Reduced manufacturing costs, significantly reduced curing times, improvements in part quality and performance, reduced environmental and health concerns, and improvements in material handling, are all potential benefits of EB curing.

1.4 Scope of This Study

The motivation for this study is the relatively limited amount of scientific literature available regarding technical aspects of high energy EB curing. The purpose of this thesis is to help to fill this void by providing an intensive examination of the EB curing process. As a prelude to the experimental work, the development of EB curing is presented, and a detailed description of the process is furnished. Following this, the critical material and process parameters are identified, examined and evaluated for their influence on EB curing and on quality of the processed parts. These critical material and process parameters of high-energy EB curing are:

1) Radiation Dose
2) Initiator concentration
3) Temperature
4) Reinforcement
5) Radiation Dose Rate

To examine these parameters, a case study of one epoxy resin formulation was undertaken. The formulation was studied in its neat (un-reinforced) form and in composite form, with IM7 graphite fibres. Of critical importance is that the formulation selected for this study is both thermally and radiation curable, which allows thermal analysis of the EB formulation and permits a direct comparison between thermal and EB curing.

The formulation examined consists of a proprietary combination of an **epoxy resin** and **cationic photoinitiator.** Analysis of the formulation is done by thermal and mechanical testing of samples at various stages of the EB process. Thermal analysis is done by **dynamic mechanical analysis (DMA)** and **differential scanning calorimetry (DSC).** Mechanical properties are analyzed by DMA as well as by tensile testing. Evaluation of the influence of the material and process parameters is based on their effect on **cure extent** and **glass transition temperature (T_g).** Additional information about the EB curing process is uncovered in an investigation of the **reaction kinetics** by a method of thermal analysis following EB treatment. The mechanical properties of tensile modulus and fracture strength are compared between identically prepared thermally and EB cured samples to develop a better understanding of the contribution of thermal curing during EB irradiation.

After the initial enterprise of describing the process of EB curing, the specific objectives of the experimental work are presented at the end of Chapter 4. Based on the experimental results on **the influence of material and process parameters on EB curing,** meaningful contributions are made towards developing a predictive model of the process. As well, conclusions are drawn on the relative merits and drawbacks of EB curing.

1.5 Organization of Thesis

A background report on the history and evolution of radiation curing of polymers is presented in the next chapter. Also discussed in Chapter 2 is some elementary chemistry

of radiation polymerization and curing. Chapter 3 contains a description of the high-energy EB curing process and a typical EB facility. As well, an explanation of the specific technical aspects of EB curing such as radiant dose and dose delivery is provided in Chapter 3. This technical discussion is lacking from literature on EB curing of composites, and is expected to serve as groundwork not only for this thesis, but also for future studies.

An examination of the results of existing research related to high energy EB curing of advanced composites is presented in a literature review in Chapter 4. Specifically, studies relating to cationic epoxy systems are discussed. The experimental work performed for this study on EB curing is presented and described in Chapter 5. Results and discussion of this experimental work is presented in Chapter 6. Finally, conclusions of this research are summarized and presented in Chapter 7.

A general introduction to polymers and composites is presented in Appendix A. This appendix is intended to serve as an overview of some of the terminology used within this thesis, and may be read for general interest. It generally discusses polymers and plastics, and specifically discusses thermosetting epoxies, crosslinking reactions, PMC processing, and properties of PMCs. Since a great deal of experimental work for this study involves thermal analysis using differential scanning calorimetry (DSC) and dynamic mechanical analysis (DMA), an introduction to the subject has been included in Appendix B.

Chapter 2

Background

This chapter describes the historical development of radiation curing and explains the fundamental concepts of the interaction of radiation with polymers. Since expertise from a number of fields has been borrowed to form the knowledge base on EB curing of composites it is necessary to review, at least briefly, those fields. Also, before commencing with an in-depth description and critical examination of the EB process, it is necessary to briefly describe some chemistry of radiation curing.

2.1 Radiation and Polymers

The study of radiation commenced with the first detection of x-rays by W.K. Roentgen in 1895. Soon after, discoveries by Becquerel, Rutherford, and the Curies established the existence and nature of nuclear radiation in its three forms α, β, and γ. Since these early days, the effects of radiation on matter have been studied by physicists, chemists and materials engineers.

The first evidence of radiation causing the formation of chemical bonds can be attributed to W.D. Coolidge, who in 1925 subjected various organic substances to 'cathode rays' and noticed solid deposits formed on the glass walls of his apparatus [26,27]. In the same year, W. Mund et al. made similar observations when bombarding gaseous hydrocarbons with α-particles [26,28]. Systematic studies on the effects of radiation on different materials became more widespread in the years following the Second World War. The development of nuclear power gave increased motivation to quantify the effects of radiation on biological molecules for safety reasons, and on materials used in the construction of nuclear power plants including moderating-water, concrete, metals, elastomers, and plastics.

During the late 1940's and throughout the 1950's, **radiation chemistry** research became common in university laboratories throughout the world. Radiation chemists are interested in the study of primary products and intermediates caused by radiation interaction with matter, as well as the kinetics of radiation-initiated reactions. The majority of research during this period focussed on understanding the chemistry of the electron, and the differences between reactions in solids, liquids and gases [29]. In the 1950's, a new field emerged from radiation chemistry research, the *commercial development* of products using radiation processes. Because they are more susceptible tc radiation than crystalline metals or ceramics, it was the study of the irradiation of *polymers* for commercial products that grew quickly. It is from these beginnings that high-energy curing of composites as a potential commercial process has emerged.

2.1.1 Radiation Chemistry vs. Photochemistry

Radiation comes in the form of accelerated particles or electromagnetic radiation. Accelerated particles are usually electrons (β-rays), helium nuclei (α-rays), or hydrogen nuclei (protons). Electromagnetic radiation is classified according to its energy and frequency. The electromagnetic spectrum from lowest to highest energy and frequency is made up of:

Radiowaves
Microwaves
Infra-red (IR)
Visible light
Ultra-violet (UV)
X-rays
γ-rays

In a broad sense, the phrase 'radiation chemistry' implies the study of the chemical actions (the making and breaking of chemical bonds) caused by the interaction of all forms of radiation with materials. In practice, the formal research field of radiation chemistry has come to represent only the study of chemical effects caused by **ionizing radiation**. Ionizing radiation has sufficient energy to cause the creation of multiple ions as it passes through matter. It includes energetic electrons and alpha particles, as well as x-rays and γ-rays. Ionizing radiation comes from substances undergoing nuclear transformations, from outer space in the form of cosmic rays, and from particle accelerators such as those that produce electron beams. Generally, radiation chemists

study ionizing radiation with energies in the range of thousands or millions of electron volts (keV or MeV).

Chemical reactions caused by ultraviolet and visible radiation make up the field of **photochemistry**. Photochemists are normally concerned with radiation with in the electron volt (eV) range. Although not classified as ionizing radiation, UV light may have sufficient energy to create ions (photoionization) above approximately 10 eV [30]. High-energy EB curing of composites has developed to its current state because of research breakthroughs by both photochemists and radiation chemists.

2.1.2 Radiation Effects in Polymers

Both ionizing and electromagnetic radiation may initiate various chemical changes in polymers [31]. Radiowaves and microwaves are not powerful enough to cause any significant chemical alterations. Infrared light initiates some chemical change but is generally used more as a heating source. Visible and UV light induce many identifiable chemical reactions and are studied by photochemists. X-rays and γ-rays, as well as accelerated electrons cause many prominent changes in polymers and are studied by radiation chemists.

There are several, distinct chemical effects that may result from the irradiation of polymers. The result can be main chain scission, grafting, polymerization or crosslinking. Each of these is shown in simple schematics in Figure 2.1. Different polymers, in varying irradiation environments generally show an affinity for one result or

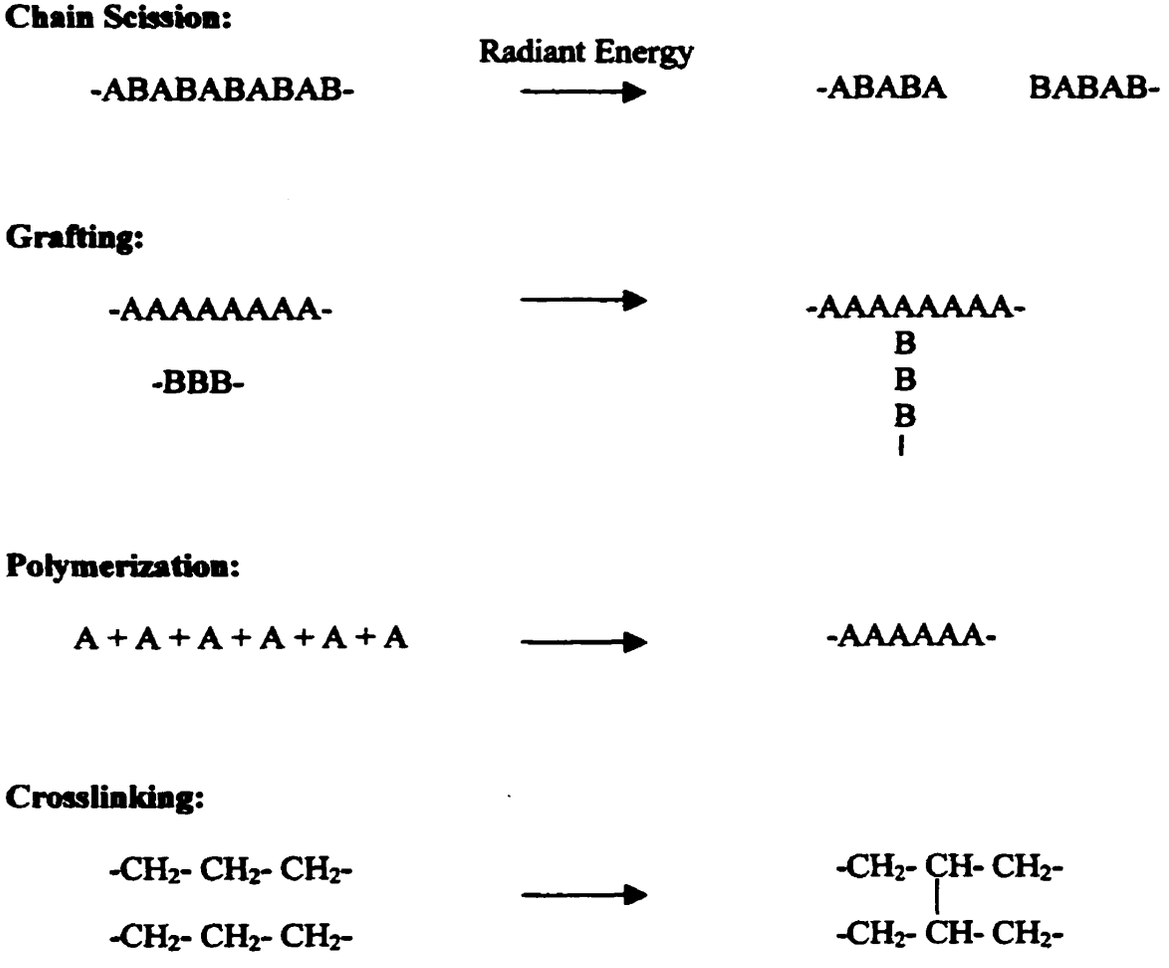

Figure 2.1: Radiation-induced reactions in polymers

another, but under some conditions the effects may compete with one another. An early pioneer of radiation chemistry of polymers, A. Charlesby has published a great deal of research on radiation-induced changes in simple polymers [32].

2.2 Radiation Induced Polymerization

The most commercially useful effects of radiation on polymers are that of polymerization and crosslinking. The term *polymerization* is generally reserved for addition-type reactions in thermoplastic polymers, while the term *curing* is used for crosslinking thermoset polymers. Both of these effects basically consist of the formation of chemical bonds between organic molecules, which serve to raise the molecular weight and change (improve) the properties of the bulk system. Hence it is useful to describe the simple reactions of low-energy radiation polymerization first, and then to discuss high-energy radiation curing next, as a similar but more complex form of the same phenomenon.

2.2.1 Photochemical Polymerization

The most straightforward form of radiation polymerization is simple direct chain growth by UV light. Direct polymerization implies that the UV light influences the monomer directly, and not through a series of other reactions. In photochemical polymerization, each incident photon is absorbed by a single reacting molecule. The molecule is excited to a definite, known excited state. From this excited and energetic state, reactive species in the form of ions or radicals are produced.

The formation of reactive species on the monomer by light absorption is the first step. When the species are free radicals (highly reactive molecular fragments of fleeting existence), a simple chemical representation of the reaction would be [33]:

$$M \xrightarrow{h\nu} M^{*} \longrightarrow M\bullet \xrightarrow{M} (M)_n\bullet \longrightarrow P$$

Where M is the monomer, hν represents a quantum of incident radiation energy of frequency ν, * implies an energetic transitory state, • implies a free radical species, $(M)_n$ represents the growing polymer chain, and P the final polymerized state. If photoionization were to take place, then the reaction would correspondingly be cationic and a representation of the reaction would be:

$$M \xrightarrow{h\nu} M^{*} \longrightarrow M^{+} \xrightarrow{M} (M)_n^{+} \longrightarrow P$$

It has been proven that direct polymerization or crosslinking is not an efficient route. Hence to be useful, the initiation step of the polymerization reaction requires the presence of a **photoinitiator**, I, which under light excitation is capable of generating reactive species:

$$I \xrightarrow{h\nu} I^{*} \longrightarrow R\bullet$$

Where I^{*} is an excited or energetic state for the photoinitiator which precedes its decomposition or transformation to the free radical R•. Simultaneously, the free radicals are produced by initiation and are consumed by the polymerization reaction:

$$R\bullet + M \longrightarrow RM\bullet \xrightarrow{M} P$$

A further complication in the reaction would be due to the addition of photosensitizers, which are added to absorb luminous energy at a wavelength where I is

unable to operate and to transfer the excitation energy to I. These mechanisms are identifiable and are the subject of much study by photochemists such as Foussier [34].

Often, the wavelength of the incident light is matched to the peak absorption spectrum of the polymer or photoinitiator. Additional light sensitive chemicals are used extensively in UV curing, and their reactivity when exposed to UV light is a subject of much study. Much work has been done to develop formulations that utilize photoinitiators, photoaccelerators and photocatalysts. With the addition of such chemical additives, a number of intermediate steps are added to polymerization. With a large, multifunctional (multiple polymerization sites on the same molecule) monomer which forms crosslinks, the reaction becomes increasingly more difficult to describe, although the same principles of simple polymerization apply.

2.2.2 Curing with High Energy Radiation

In contrast to photochemical curing, each particle or ray of ionizing radiation produces a large number of ionized and excited molecules in the polymer along its track. The ionizing radiation is not selective as in photopolymerization, and may interact with any molecule in its path, and raise it to any of its possible ionized and/or excited states. Primary and intermediate reactions quickly become very complex.

The interaction of high-energy radiation with a molecule AB may take one of two paths, either primary ionization (resulting in a molecular cation) or some form of excitation [30]:

$$AB \xrightarrow{EB} AB^{+} + e^{-} \quad \text{(ionization)}$$

$$AB \xrightarrow{EB} AB^{*} \quad \text{(excitation)}$$

The electrons ejected during the ionization will lose their excess kinetic energy by initiation of further ionization and excitation until the electrons reach thermal energies. At this point, neutralization of a cation or attachment can occur:

$$e^- + AB^+ \longrightarrow AB \text{ or } AB^*$$

or attachment to a neutral molecule resulting in a molecular anion:

$$e^- + AB \longrightarrow AB^-$$

Cationic species may also have sufficient excess energy to decompose further by a number of mechanisms including:

$$AB^+ \longrightarrow A^+ + B$$

$$AB^+ \longrightarrow A^+ + B\bullet + e^-$$

The end result of these reactions, in whatever form they take, is the creation of reactive intermediate species – radicals, cations, and anions. These reactive species cause a number of competing curing mechanisms. The result of which is the transformation of the pre-polymer into a three-dimensional network. From a practical perspective, this can mean the transformation from a liquid or semi-solid, unusable state into a crosslinked solid state, to be used as an engineered, load bearing material. The demonstration of the curing of low molecular weight polymers has been shown by a number of authors, notably A. Charlesby [32]. The specific mechanisms of radiation-induced polymerization and crosslinking are increasingly complicated and no attempt is made to describe them further in this thesis. This role is reserved for the radiation chemists of the scientific world.

2.3 Commercial Developments in Radiation Curing

Since the earliest experimental demonstrations of radiation curing, the challenge has been to apply it commercially and prove its continued development to be beneficial. The engineering perspective has been to develop the technology with only a passing concern for describing reactions at the molecular level.

2.3.1 UV Curing

Commercial applications of UV curing were developed early, and today are not particularly uncommon. The use of ultraviolet (UV) light to cure polymers is used extensively for applications such as lithography and thin coatings. For example, some manufacturers use UV inks or printing on toothpaste tubes, cosmetic packaging, plastic bottles, magazine covers, credit cards, and compact disks. Printed circuit boards often use UV marking inks and conformal coatings. PVC or parquet flooring, along with furniture and doors may use UV curable laminates to protect them. UV curing is not the only way to produce, nor is it limited to, these products. In fact, in 1990 the world-wide market share for UV curing of resins was only about 0.5 % for coatings and 3.0 % for graphic arts [31] compared to conventional processes. These market share figures are small but remain significant in terms of tons of product, and continue to grow each year.

The use of UV light for curing polymers is now a fairly mature technology, having been around for more than 50 years. The first patent was granted to Inmont in 1946 for UV cured ink based on unsaturated polyester (UPE) resin [31]. Theoretical discussions were published in the early 1950's, and the first commercial application of thin coatings occurred in the 1960's. This application was a UV cured particle-board

filler based on UPE [31]. Radiation curing continued to expand in graphic arts through the 1970's, when radiation curable acrylic systems became popular. In the 1980's and 1990's the technology has continued to grow and is now only in poorly industrialized countries where it is not used. Traditionally, the only reason for a company to go to radiation curing was cost savings. Progressively, industries have gone to radiation curing for performance reasons and to avoid new and more numerous regulations on solvents used in conventional thermal curing.

Two pictures of UV curing machines are shown in Figure 2.2. A tabletop research unit and an on-line industrial application. There are a number of companies that sell UV machines commercially for straightforward or custom operations. These types of low energy machines do not require any protective shielding from radiation.

2.3.2 Low-Energy EB Curing

Low energy electron beam curing of polymers is often considered as very similar technology to UV curing. Low energy electrons (less than 300 keV) have been proven to initiate polymerization when applied to the identical resin systems with photosensitive additives designed for UV curing. The UV curing industry has adopted the use of low energy electrons because they have better penetration characteristics than UV in opaque resins. For example, a laminate or coating of up to 0.5 mm in thickness may be cured with low energy EB radiation, while UV light penetrates less than 30 μm.

Worldwide, there have been a small number of EB curing applications where a facility has been built to produce product. Usually, these applications were originally designed for UV curing, but were adapted for low energy EB due to design challenges.

Figure 2.2: Industrial (printing) UV curing operation [source: Cold UV Ltd.]

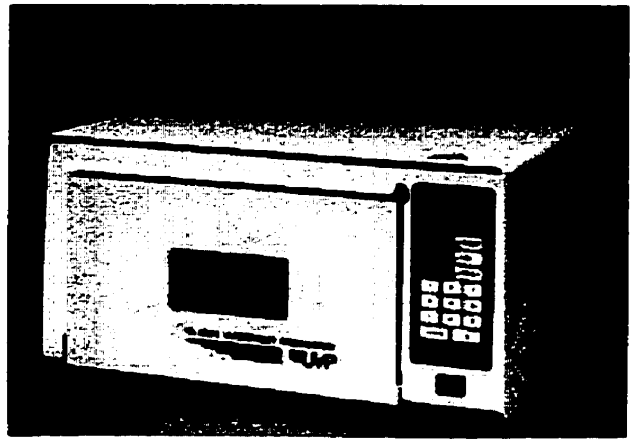

Figure 2.3: Tabletop UV curing chamber [source: UVP, Inc.]

Typically 300 to 500 keV is the maximum energy possible for these types of applications. One reason for this is because above this level, accelerator technology changes dramatically in design and style. As well, for electron energies above this, shielding from radiation becomes a major and expensive safety and design concern. A 300 keV lab-scale EB machine is shown in Figure 2.3.

2.3.3 High-Energy EB Curing of PMCs

The era of radiation curing of composites began at **Aerospatiale** of France in 1979. Until this time, commercial radiation curing had been strictly low-energy, and mostly photochemical in nature. Higher energy radiation was largely reserved for laboratory studies by radiation chemists. Aerospatiale began doing experimental work with both high and low energy radiation in an attempt to cure polymer composite casings for solid propellant motors without thermal treatment [4]. They determined that the use of a high-energy *electron accelerator* was more suitable than any low-energy radiation source, mainly because of its penetration capabilities. Matrix formulations investigated by Aerospatiale were acrylated epoxies, polyesters, and urethanes.

High-energy EB curing became more widely known in the mid-1980's, when **Atomic Energy of Canada's Whiteshell Laboratory** got involved in EB curing of composites as a potential growth market for use of their high-energy Impella line of industrial accelerators [35]. Using a pilot scale electron accelerator and a radiation chemistry knowledge base they began to publish a steady stream of articles on the electron beam curing of polymer composites [36-40]. Early resin formulations studied by AECL were mostly acrylated epoxy systems, which typically had poor properties that

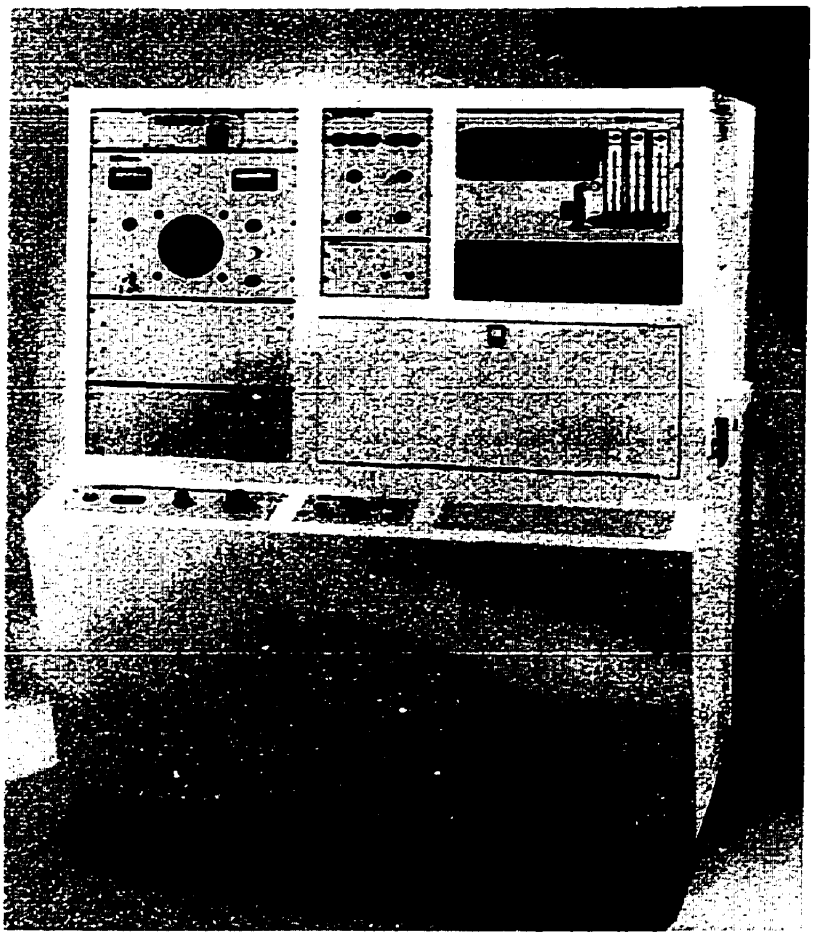

Figure 2.4: Low-energy (175 keV) lab-scale EB curing chamber [source: Energy Sciences Inc.]

made them unsuitable for the aerospace industry, which dominated the composites industry.

The next critical development in high energy EB curing came from a photochemist. In 1992, **J.V. Crivello** described a new, efficient mechanism for the radiation curing of epoxy resins by **cationic polymerization** in the presence of unique initiators [1]. Radiation curing of epoxy resins had been described as early as 1968 by Williams [41], and other notable contributions on the subject had been made by Omel'chenko and Bokalo in 1978 [42] and in 1982 by Laricheva [43]. However, Crivello developed the first efficient initiators, which could be used with no solvents, in low concentrations and could readily be applied to existing, commonly used aerospace epoxy matrix resins. The resulting EB cured composites had good thermal, physical and mechanical properties. It was at this point, that the composites and especially aerospace industries took note.

In 1994 a **Co-operative Research and Development Agreement (CRADA)** between the U.S. Department of Energy and 10 industrial partners was formed to investigate the feasibility of electron beam curing of advanced composites for aerospace applications [44]. From this time onwards, a number of companies in North America have been working on developing the technology. An increased amount of attention for EB curing of composites has created a need for better development of the technology. It can be said with certainty that the 1994 CRADA marked the start of the modern era of high-energy electron beam curing of advanced composites.

2.4 Summary

This chapter has described some of the history and development of high energy EB curing of composites up to the most recent state at which the technology finds itself. As well, some elementary radiation-induced chemical reactions have been described. At this point it is necessary to provide a more complete description of the EB process, something that has been lacking in the current outbreak of articles and studies on the subject. Only once this groundwork has been laid can the EB curing process be scrutinized from a practical perspective.

Chapter 3

High-Energy EB Processing

This chapter contains a functional description of high-energy electron beam processing of composites. The intention is to include an informative report on the basic features of EB processing, including describing processing facilities and process parameters. This description is something that is conspicuous by its absence in current literature on EB curing. In the first part of this chapter, the logistics and layout of an EB processing facility are described, as is the accelerator used for the experimental work in this thesis. Following this, a detailed description of the important processing parameters is provided which is essential in understanding the discussion that follows in chapters 4, 5, and 6.

3.1 High-Energy EB Processing Facilities

High-energy EB processing is easily distinguished from low energy radiation processing by the physical scale of the operation. While low-energy EB or UV curing equipment can be adapted into existing production or laboratory facilities, high-energy EB processing requires a considerable amount of shielding from harmful radiation, and hence

a specially designed facility is required. The electron beam produces x-rays from scattering interactions while online, and so the accelerator must be operated remotely, with the technician separated from the electron beam by thick concrete or lead reinforced walls.

A schematic of a high energy EB facility is shown in Figure 3.1. This schematic is of the existing facility in operation by Acsion Industries in Pinawa, Manitoba (39), which was used in this study. It was designed by AECL as a demonstration prototype for industrial use of an electron accelerator. The accelerator is contained within a concrete bunker covered by an earth berm for additional radiation protection. The facility has a moving conveyor belt that reaches the accelerator after moving through a labyrinth of concrete walls, so that product can be moved to and from the accelerator while it is online. Projected down towards onto the conveyor from above by a fixed *horn* is a scanning electron beam. When the composite part passes under the horn, it is imparted with radiant energy from the electron beam. A technician operates the accelerator and conveyor remotely, and monitors the process by closed circuit TV.

Acsion's accelerator building is a multipurpose production facility designed for continuous irradiation of similar sized objects. No facility has yet been designed specifically for composite processing although there is speculation on the form that it would take. A facility designed for E-Beam curing of large aerospace composites might have a moving accelerator or EB gun rather than a moving composite part. This would facilitate curing of massive or geometrically complicated structures. A spinning mandrel could also be used for parts that are spherical or cylindrical or need to be turned as they are cured.

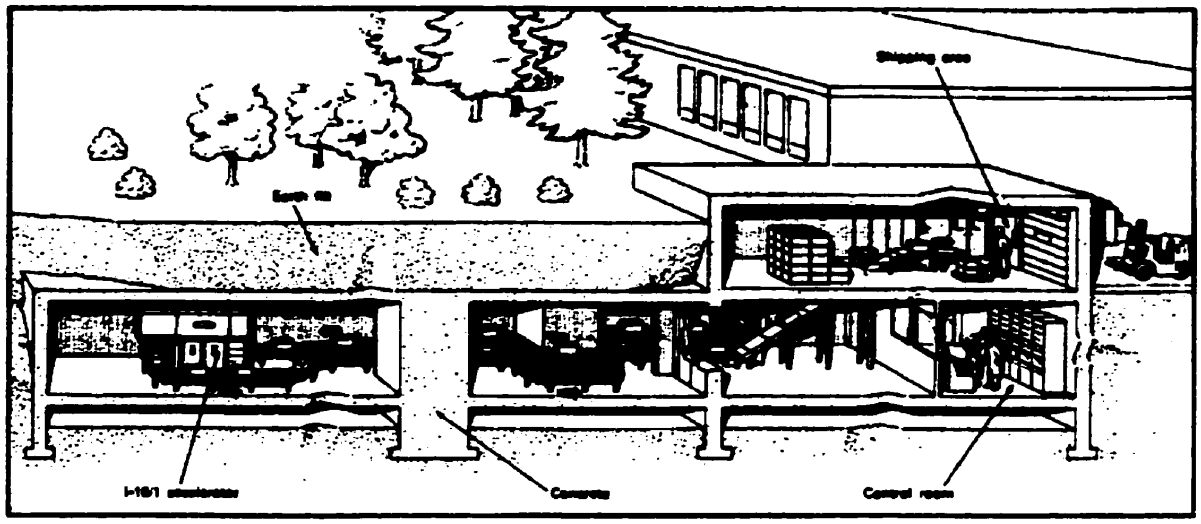

Figure 3.1: Schematic of high-energy EB processing facility in Pinawa, Manitoba

[Source: Acsion Industries Inc.]

Such design possibilities have been discussed in feasibility studies but nothing permanent has yet been implemented.

A number of other facilities and a variety of electron accelerators and building layouts have also been used for high energy EB curing of composites. Universities, aerospace companies and the U.S. military have been active in EB curing research, and normally use a third party contractor, with expertise in accelerator operation and safety, to perform the high energy EB curing services. Acsion Industries Inc., a major contractor for this service, utilizes an AECL pilot scale I-10/1 accelerator (10 MeV, 1 kW), with the facility shown. Other high-energy electron curing contractors use I/10-1 accelerators, or other accelerators such as the AECL Impella™ (10 MeV, 50 kW), the IBA Rhodotron™ (10 MeV, 1-150 kW), Electron Solutions 3 MeV (1 kW) accelerator, or the Titan Scan 10 MeV (15 kW) accelerator. The specifics of electron accelerators vary between facility and service contractor, but they share a number of common features. A closer look at Acsion's E-Beam facility gives some insight into the processing operation and technical aspects of the procedure.

3.1.1 The Accelerator Facility Used for this Study – Acsion Inc.

In March of 1985, Atomic Energy of Canada Research Company formed the Radiation Applications Research Branch at Whiteshell Nuclear Research Establishment in Pinawa, Manitoba. The objective of this group was to carry out the R&D required to encourage further industrial applications of ionizing radiation and to showcase AECL's accelerator technology (45). A facility was designed and built (Figure 3.1), and originally equipped for studies in food chemistry, microbiology, materials properties and dosimetry. In June

of 1998, a group of Radiation Applications (AECL) employees, facing closure of their branch, bought the equipment, took over the facility and formed Acsion Industries Incorporated. It was at this facility, which includes an I-10/1 (10 MeV, 1 kW) electron accelerator that the EB irradiation for this thesis was performed.

The facility was designed to allow experimental irradiation of solids, liquids and gases in various configurations, as well as test quantities of various products. A conveyor system moves the product from the receiving area, through a maze, past the electron beam at a controlled rate and finally to the shipping area. Experimental samples may be assembled in the control room and then moved through the maze to the accelerator room for irradiation. In Figure 3.2, a photograph of the control room is shown. Figure 3.3 shows the I-10/1 accelerator body, the EB horn above the conveyor, and two irradiation trays, used to carry product along the conveyor. In practical operation of single composite parts, the conveyor is not normally used. The composite is placed in the target room under the horn while the accelerator is off-line (not producing electrons). Then the operator retreats to the control room, and monitors the process of the irradiation through closed circuit television. After the irradiation, the accelerator is turned off-line again, and the material/experiment is retrieved.

Figure 3.4 is a photograph of AECL's model 220 Gammacell, which is an additional piece of equipment at Acsion's Whiteshell Laboratory used in high-energy radiation curing experiments. This gamma cell produces high-energy (1.25 MeV) gamma rays from a Cobalt-60 source and is a calibrated source of high-energy radiation. The use of the gamma cell in experimental studies on EB curing of composites will be discussed in the next chapter, in section 4.1.1.

Figure 3.2: Accelerator control room

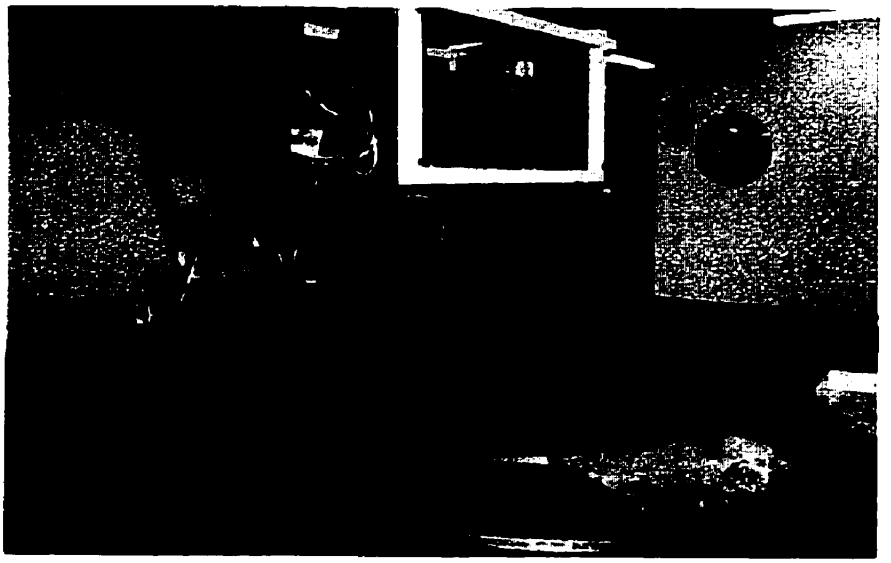

Figure 3.3: The I-10/1 accelerator

Figure 3.4: The Gammacell-220

3.2 The I-10/1 Electron Accelerator

The I-10/1 Accelerator was designed by Atomic Energy of Canada to be an accurately calibrated source of high-energy electrons for research and pilot-scale electron processing studies [46]. This electron accelerator produces 10 MeV electrons and the beam power is nominally 1 kW.

Features attributed to the I-10/1 accelerator by AECL are accurate energy and dose control, and simple automatic operation control and monitoring [46]. The actual specifications listed for the accelerator are [46]:

Maximum Scan Width:	60 cm
Minimum Scan Width:	15 cm
Scan Sweep Rate:	2 Hz
Conveyor Speed Range:	0.01 to 5 cm/s
Mean Energy of electrons:	9.5 ± 0.2 MeV
(at point where they leave accelerator)	
Electron Beam Power:	0.75 (+.25,-.00) kW
Beam Pulse Rate:	300 Hz
Pulse Length:	4 μs

The I-10/1 accelerator is magnetron-driven, short pulsed technology, and only produces electrons during its brief, 4 μs pulses. A diagram of the accelerator beam handling system, Figure 3.5, shows the path the electrons take before they leave the EB horn. As well as being pulsed on and off, the electron beam is continuously scanned back and forth by the scanning coils. The beam emerges from the accelerator at the scanning horn. Upon emerging from the scan horn, the electron beam has a small diameter, but spreads to an significant area by the time it reaches the conveyor, as shown in schematic in Figure 3.6. If the electron beam could be frozen at an instant in time, during one of its

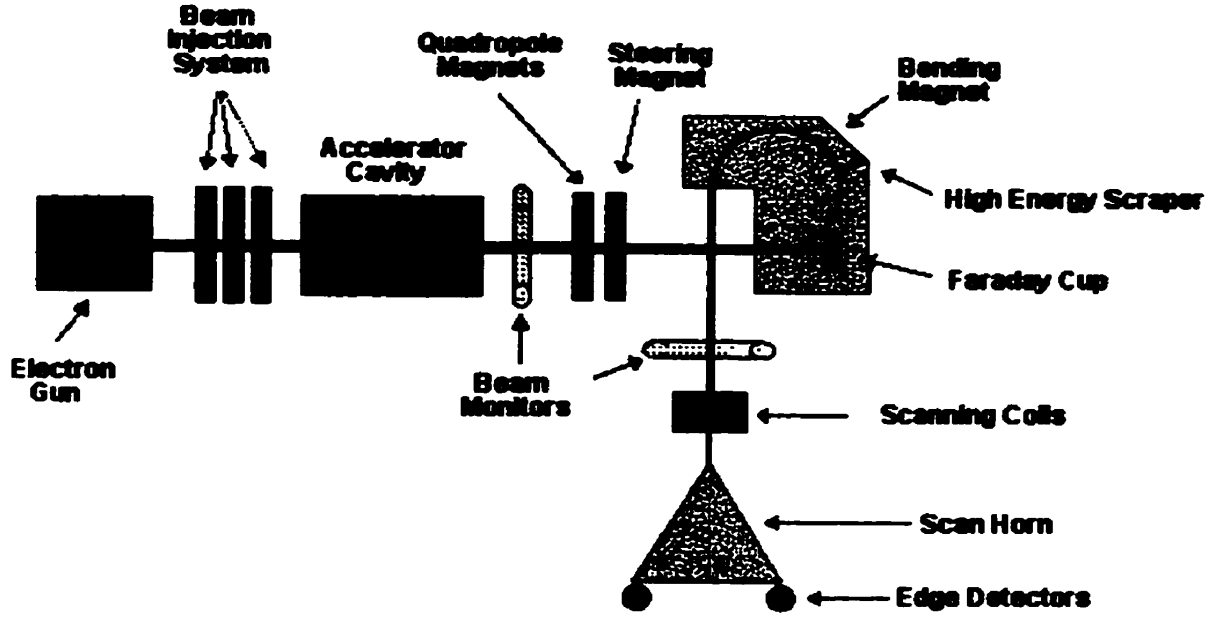

Figure 3.5: Beam handling system for the I-10/1 accelerator

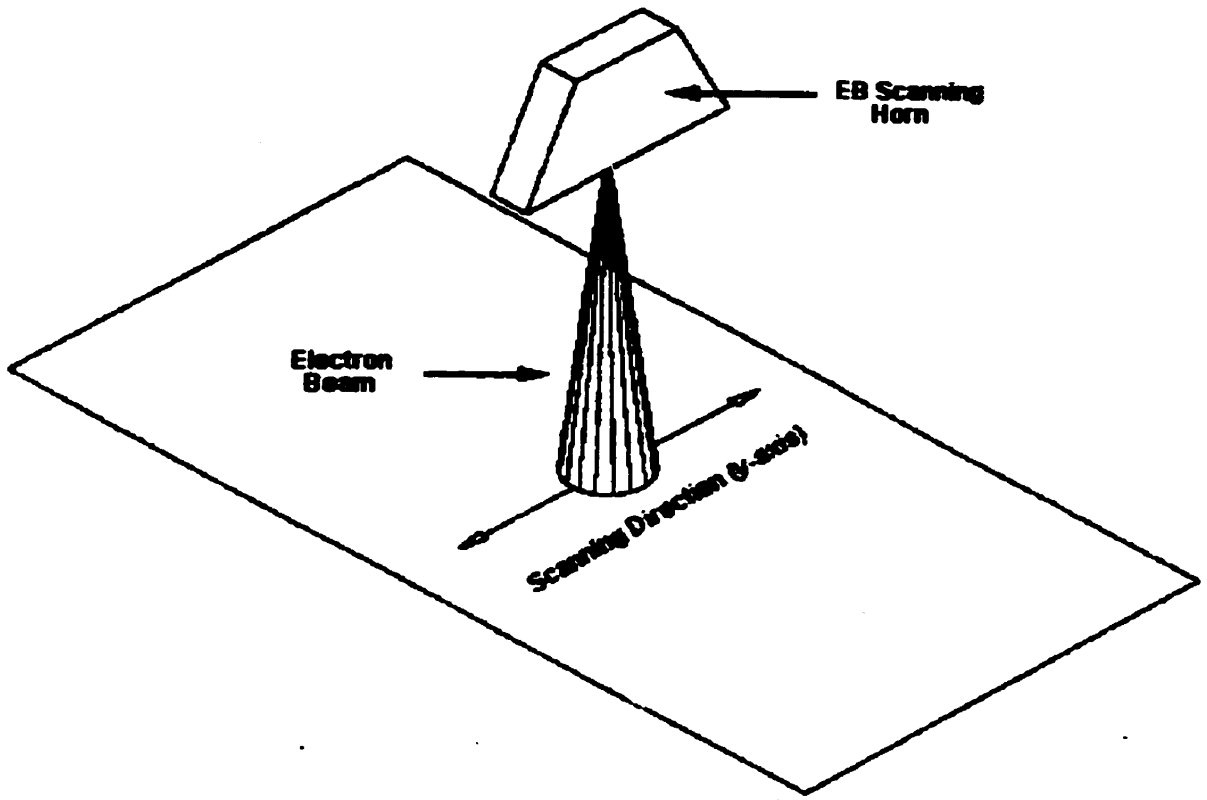

Figure 3.6: Depiction of the electron beam at an instant in time

pulses, and if it was readily visible, the beam would appear as in Figure 3.6. The intensity of the electron beam varies in a normal distribution from beam centre to the periphery, so that the intensity profile of the beam at an instant in time would appear as in Figure 3.7. This Figure shows a contour plot of beam intensity in a cross section of the beam at conveyor height.

A closer view of the electron scanning horn is shown in Figure 3.8. In this photograph three different axis are defined by the author for future reference. The x-axis is the direction of the conveyor movement. The y-axis is perpendicular to this in the same plane as the conveyor. The electron beam is scanned in the y direction by the handling system to simulate a line source. The z-axis moves away from the conveyor and towards the horn. The high pulse repetition rate of the electron production means that any particular region of the sample receives many overlapping pulses (300 per second) as the beam sweeps back and forth in the y-direction, and the conveyor travels in the x-direction.

3.3 Process Parameters and Technical Aspects of E-Beam Curing

In the advanced composite industry, conventional autoclave processing is well established. At its simplest, the autoclave curing cycle involves three design parameters, time, pressure, and temperature. Easy to program and control, a feedback system may be used to control the autoclave heating elements to obtain a desired constant temperature or ramp rate. Resin viscosity and flow, hot-spots due to exothermic heating of resin rich areas, and the production of volatiles are potential cure cycle design concerns. The entire

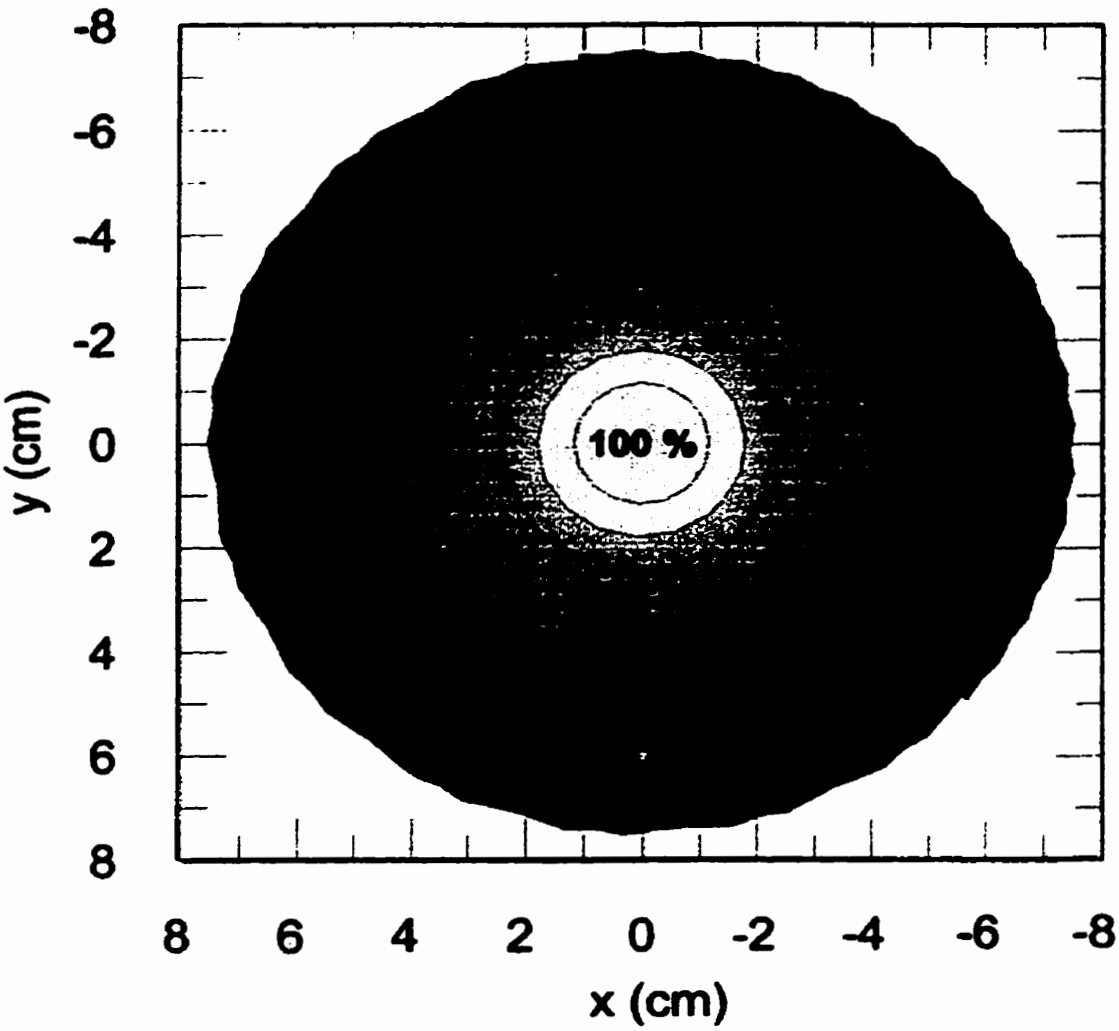

Figure 3.7: Beam cross section intensity profile at conveyor height (size of beam approximately 14 cm in diamter)

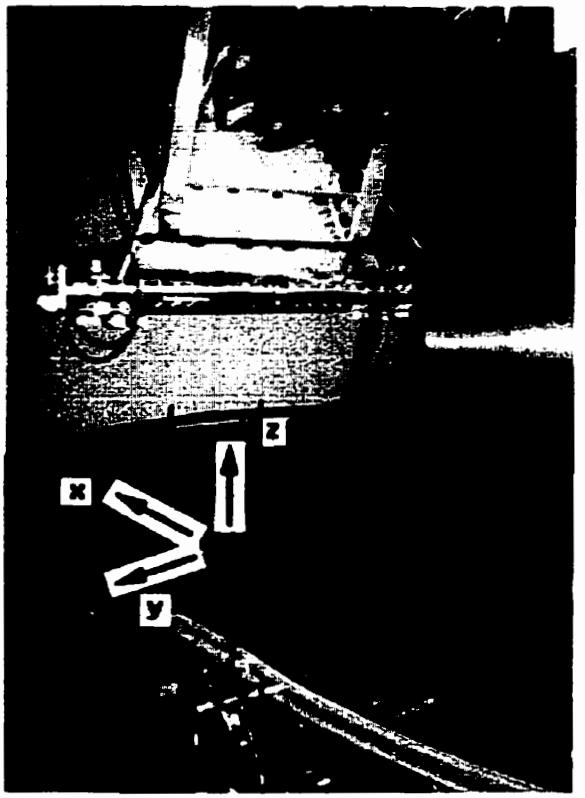

Figure 3.8: Co-ordinate system for EB processing

operation is subject to continual refinement and optimization. To those familiar with conventional processing, the technical aspects of EB curing require some explanation. Instead of autoclave control in terms of time and temperature, radiant dose is of critical importance as well as the time rate of dose delivery. EB curing is presumed to take place at, or very near, room temperature, but indications are that temperature also plays an important role in the curing process. Process control, automation and feedback are currently less refined. Before any comprehensive study on the EB curing process can be undertaken it is crucial to define specific process parameters under the general categories of **dose, dose rate,** and **temperature.**

3.3.1 Dose

Dose is a physical quantity indicating the amount **of radiant energy absorbed per unit mass** [47]. It is analogous to the amount of thermal energy supplied in conventional curing. The higher the E-Beam dose, the more radiant energy supplied to the formulation to induce crosslinking. The absorbed dose to the mass Δm, denoted by D, is defined as the imparted energy, ΔE_d, per unit mass. In symbols,

$$\text{Dose, } D = \Delta E_d / \Delta m.$$

The imparted energy, ΔE_d, is defined by

$$\Delta E_d = E_{in} - E_{out},$$

Where E_{in} and E_{out} are the sum of the kinetic energies of all electrons incident upon and emerging from the volume ΔV, containing Δm. The absorbed dose at a point is the limiting value of D as Δm approaches zero. The SI unit for dose is the Gray (Gy). It is equivalent to 1 Joule per kilogram (J/kg). With respect to EB curing, dose is usually

discussed in units of kGy, which is equivalent to J/g. That is:

$$1\ \text{kGy} = 1\ \text{J/g} = 1000\ \text{Gy} = 1000\ \text{J/kg}$$

The old standard for measuring dose was the rad, an acronym for *radiation absorbed dose*, and has the following equivalence:

$$100\ \text{rad} = 1\ \text{J/kg} = 1\ \text{Gy}$$

$$1\ \text{Mrad} = 10\ \text{kGy}$$

The subject of predicting and measuring absorbed dose is known as **dosimetry.** There are many straightforward techniques available for measuring absorbed dose such as chemical dosimeters. The I-10/1 E-Beam accelerator is designed to simulate a line source of electrons, such that objects moving along the conveyor belt receive the same dose independent of their position, y, along the width of the conveyor. Since the absorbed dose changes with penetration depth in matter, depth-dose determinations can be important. A schematic of the penetration dose profile of electrons is shown in Figure 3.9. Electron interactions cause the production of secondary radiation, which causes the absorbed dose to initially increase. The useful dose is sometimes considered as a simplification of this profile, in which the dose is constant to a certain penetration depth and then zero beyond.

The objective of EB processing is to provide a required dose, uniform over the entire composite part. As will be discussed in the following chapters, the required dose for processing is the dose, D_{cure}, necessary for maximum curing of the composite part. Considering the statistical nature of radiation, heterogeneity of the beam, and possibly of the composite part, and dose-depth dependence, the precision of predicted imparted dose

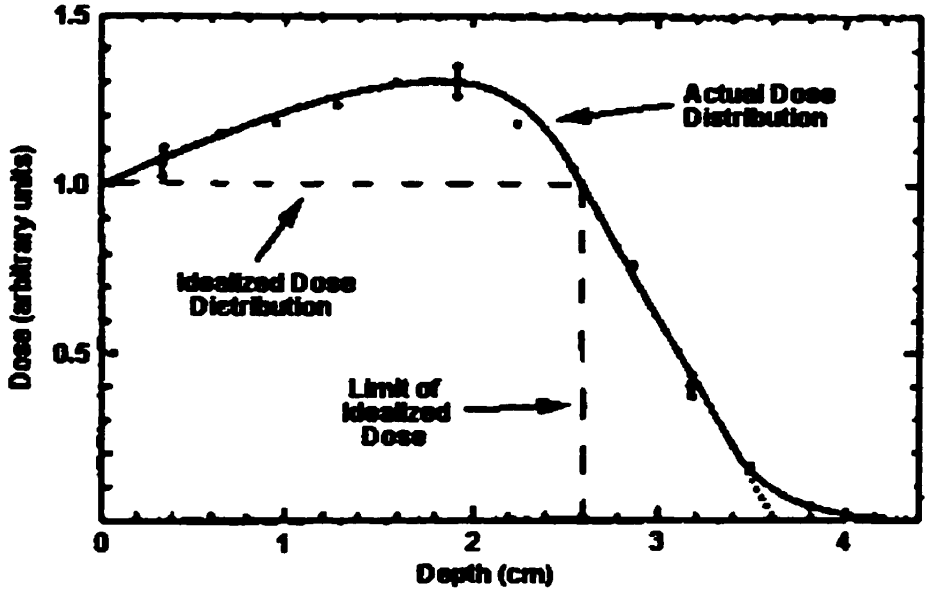

Figure 3.9: Dose distribution with penetration depth

can vary. If accurate dose control is required, it is often necessary to use dosimeters. For a typical chemical dosimeter, measured dose is accurate within 5 to 10%

3.3.2 Dose Rate

The rate at which EB dose is delivered to a composite part is difficult to quantify and describe. The dose rate at a point on a composite part is a property that is changing at each instant in time during EB processing. For an electron beam, the intensity profile during an EB pulse and hence dose rate, varies spatially with x, y and z (the x-y variation for constant z is shown in Figure 3.7). An object in the centre of the beam receives a much higher dose rate than those objects at the beam periphery. Since the electron beam is continually pulsed, scanned in the y-direction, and the conveyor is moving, the dose rate changes drastically with time and position. However, an electron beam accelerator is usually operated so that, although the dose rate varying, all material passing under the beam obtains the same total dose. Since the effect of dose rate is to be investigated in the following chapters, it is necessary to describe and label the quantifiable dose rates (as perceived by the author) for the I-10/1 accelerator.

3.3.2.1 Instantaneous Dose Rate and the Duty Cycle

The I/10-1 accelerator is a magnetron driven, short pulsed accelerator. It produces a short burst of high-energy electrons, followed by a period of dead time. This on-off cycle is often referred to as the duty cycle of the accelerator. At a pulse repetition rate of 300 pulses per second, and pulse length of 4 μs, the duty cycle appears as in Figure 3.10. During the 4 μs burst, the **instantaneous dose rate, d_1,** may be defined. During the

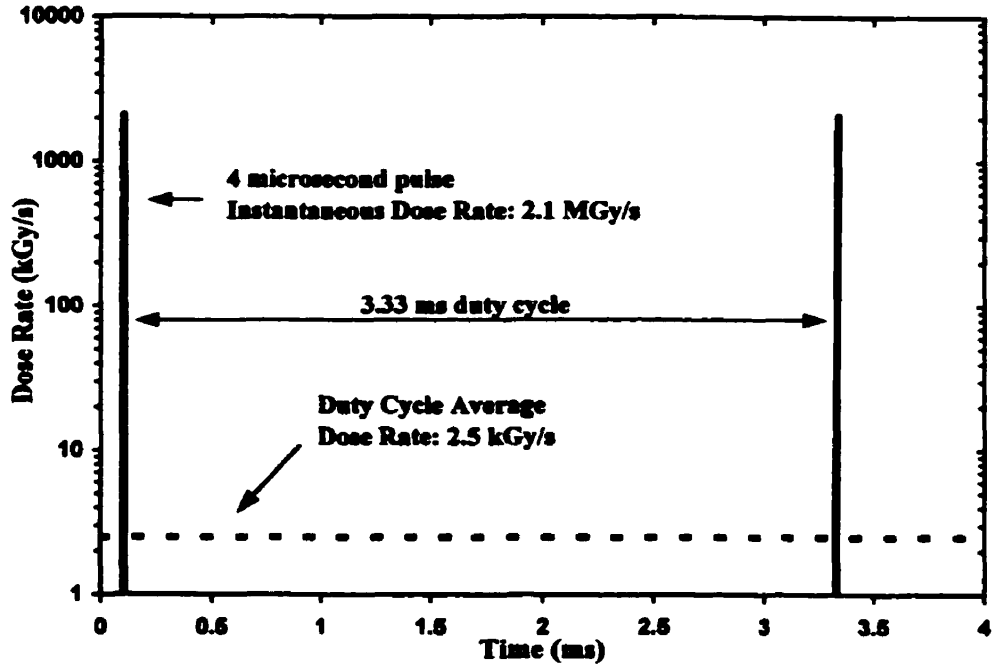

Figure 3.10: Duty cycle for the I-10/1 accelerator (dose rates are at centre of beam)

Height above conveyor (z)	Instantaneous Dose Rate	Duty Cycle Average Dose Rate
0 cm (conveyor)	1.5 MGy/s	1.8 kGy/s
15 cm (typical working position)	2.1 MGy/s	2.5 kGy/s
30 cm	3.5 MGy/s	4.2 kGy/s
45 cm (15 cm from horn)	5.4 MGy/s	6.5 kGy/s

Table 3.1: Dose rates at centre of beam for different sample heights

pulse, the instantaneous dose rate is highest at the centre of the beam, and decreases as one moves away from the centre of the beam in the x-y plane. Also, the instantaneous dose rate increases with increasing distance from the conveyor (+z, towards the horn). The 4 μs burst of electrons is sometimes referred to as a macropulse, because within the pulse are smaller bursts or micropulses, driven by the S-band radio-frequency generator at 3 GHz. During each 30 ps micropulse, approximately 10^8 electrons are produced [48].

For the I-10/1 accelerator, the instantaneous dose rate at the centre of the beam during the macropulse varies from approximately 1.5 MGy/s at the conveyor (z = 0) to approximately 5.4 MGy/s at 15 cm from the horn (z = 45 cm). Figure 3.10 is for a working distance of approximately 15 cm above the conveyor (z = 15 cm). At this nominal height and at the centre of the beam:

$$d_1 = 2.1 \text{ MGy/s} \quad (z = 15 \text{ cm, centre of beam})$$

As well, the dose delivered in one pulse can be averaged over the course of one duty cycle. The **duty cycle average dose rate, d_2,** (*author defined*) is also shown in Figure 3.10. At the centre of the beam and at the working distance of 15 cm above the conveyer:

$$\mathbf{d_2 = 2.5 \text{ kGy/s} \quad (z = 15 \text{ cm, centre of beam})}$$

A summary of peak (centre of beam) instantaneous and duty cycle average dose rates corresponding to various heights above the conveyor is shown in Table 3.1 (previous page).

3.3.2.2 Scanning Average Dose Rate

In practical operation, the electron beam must be scanning in the y-direction at all times. This means that the actual instantaneous and duty cycle average dose rates influencing a

stationary point on the target are constantly changing with time as a point is influenced by one section of the beam during one pulse, and a different section during the next pulse. The frequency of the y-axis scanning pattern is fixed at 2 Hz (4 passes over one position per second), so adjusting the scanning width changes the dose rate profile. Plots of the duty cycle average dose rate for three different scan widths are shown in Figure 3.11, representing the range of adjustment for the I-10/1 accelerator. The dose rates displayed in each of these graphs is for a point on the composite part, directly beneath the scanning horn ($x = 0$), and with the conveyor not moving ($dx/dt = 0$). For each of these scan widths, a **scanning average dose rate, d_3,** is *defined by the author* as the duty cycle average dose rate averaged over a complete scan. The three scanning average dose rates are summarized in Table 3.2. If the conveyor is moving, the scanning average dose rate also changes with time, which complicates the definition of dose rate even further.

Scan Width	Scanning Average Dose Rate
60 cm	0.32 kGy/s
30 cm	0.65 kGy/s
15 cm	1.28 kGy/s

Table 3.2: Scanning average dose rates at conveyor height

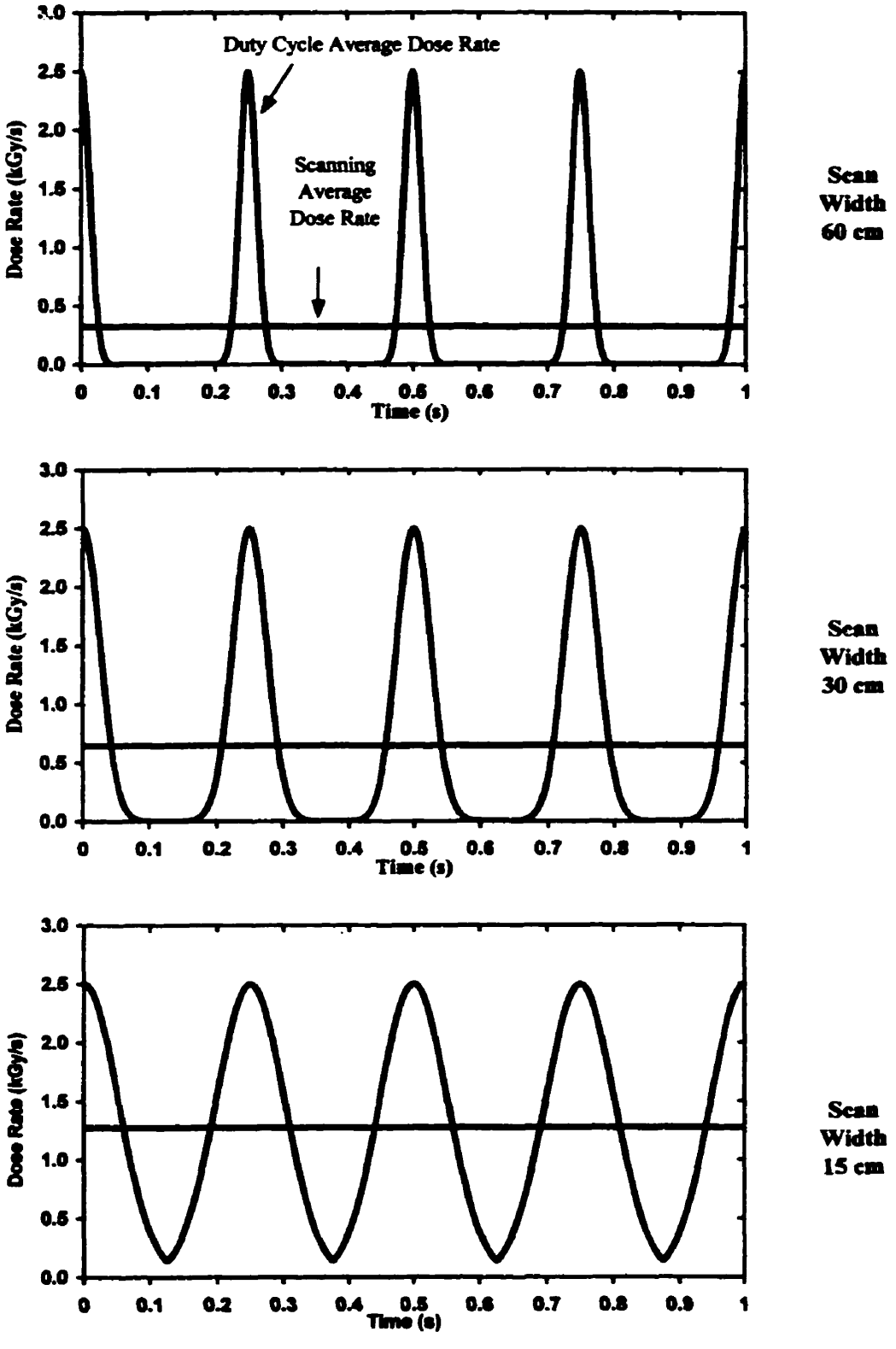

Figure 3.11: Variation in scanning average dose rate with scan width

It is evident that the dose rate during EB processing is difficult to quantify and heavily influenced by the spatial degrees of freedom of EB operation. For example, changing the height above the conveyor (z) changes the instantaneous dose rate, which in turn changes the duty cycle and scanning average dose rates. During any pass under the EB horn, there are in fact **three spatial degrees of freedom: (z, Δy, and dx/dt)** which influence the dose and dose rate profile over time. The next section will show how these degrees of freedom can be changed to produce different EB passes during curing.

3.3.2.3 Dose Per Pass

Dose per pass is a term that refers to the dose imparted to the composite part for one pass under the horn. In fact, dose per pass is not a dose rate but the increment at which dose is provided to the part. Also referred to as the 'engineering dose rate', the dose per pass is the simplest way to describe dose delivery. The dose per pass is controlled by the accelerator operator, by changing the scan width and conveyor speed without changing the height of the composite above the conveyor. The I-10/1 accelerator has reproducible, working limits for dose per **pass from 1 kGy up to approximately 60 kGy** per pass. Nominally, composite parts are given 25 kGy per pass.

Dose per Pass, $d^{\bullet}$ = 1 to 60 kGy per pass

An important distinction should be made here that the dose per pass is often referred to as the dose rate, although it is actually an incremental applied dose. Any applied incremental dose per pass actually has continually changing scanning average, duty cycle average, and instantaneous dose rates. **The dose per pass can be changed by altering the conveyor speed, scan width, or height from the conveyor.**

A plot of the dose rate at a point on a composite sample during one pass under the EB horn is shown in Figure 3.12. This Figure can be referred to as the dose rate profile over the course of one pass. The scanning average and duty cycle average dose rate during this 2 kGy pass are continually changing. The peak scanning average dose rate, $d_{3max} = 0.65$ kGy/s, is set by the scan width of 30 cm. The peak duty cycle average dose rate, $d_{2max} = 2.5$ kGy/s, is set by the height above the conveyor $z = 15$ cm, as is the peak instantaneous dose rate, $d_{1max} = 2.1$ MGy/s. Another characteristic of this dose rate profile is the length of time the EB inflences a point on the composite during one pass under the horn. A simple parameter is *defined by the author*, the **time of influence, t***, of the EB on a point, which is set by the conveyor speed. For this 2 kGy pass:

Time of Influence, $t^* \approx 9$ s (approximate)

A number of similar dose rate profiles can be obtained by manipulating the spatial degrees of freedom. For example, in Figure 3.13, three similar passes are shown, each with the same peak scanning average dose rate (same height above the conveyor, and same scan width). Although the scanning average dose rate peaks at the same value, the time of influence of the electron beam changes, as does the total dose per pass. In Figure 3.14, three similar passes are shown again, this time each of them with the same dose per pass and also the same height above the conveyor. To achieve this, three different scan widths and hence peak scanning average dose rates had to be selected. As well, for a wider scan width (lower peak scanning average dose rate), the time of influence of the beam increased. In Figure 3.15, two similar passes are shown, this time again with the same dose per pass, and the same scan width, but at different heights above the conveyor. To achieve the same dose per pass, two different conveyor speeds were used.

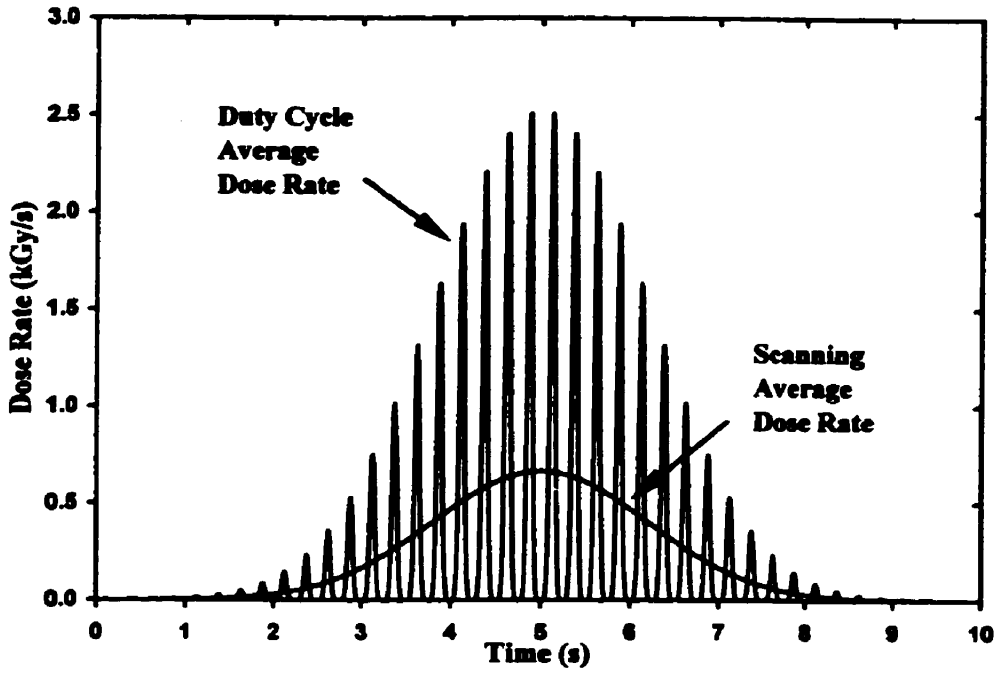

Figure 3.12: Dose rate at a point on moving conveyor during EB pass (30 cm scan width, dx/dt=2.35 cm/s, 2 kGy total dose per pass)

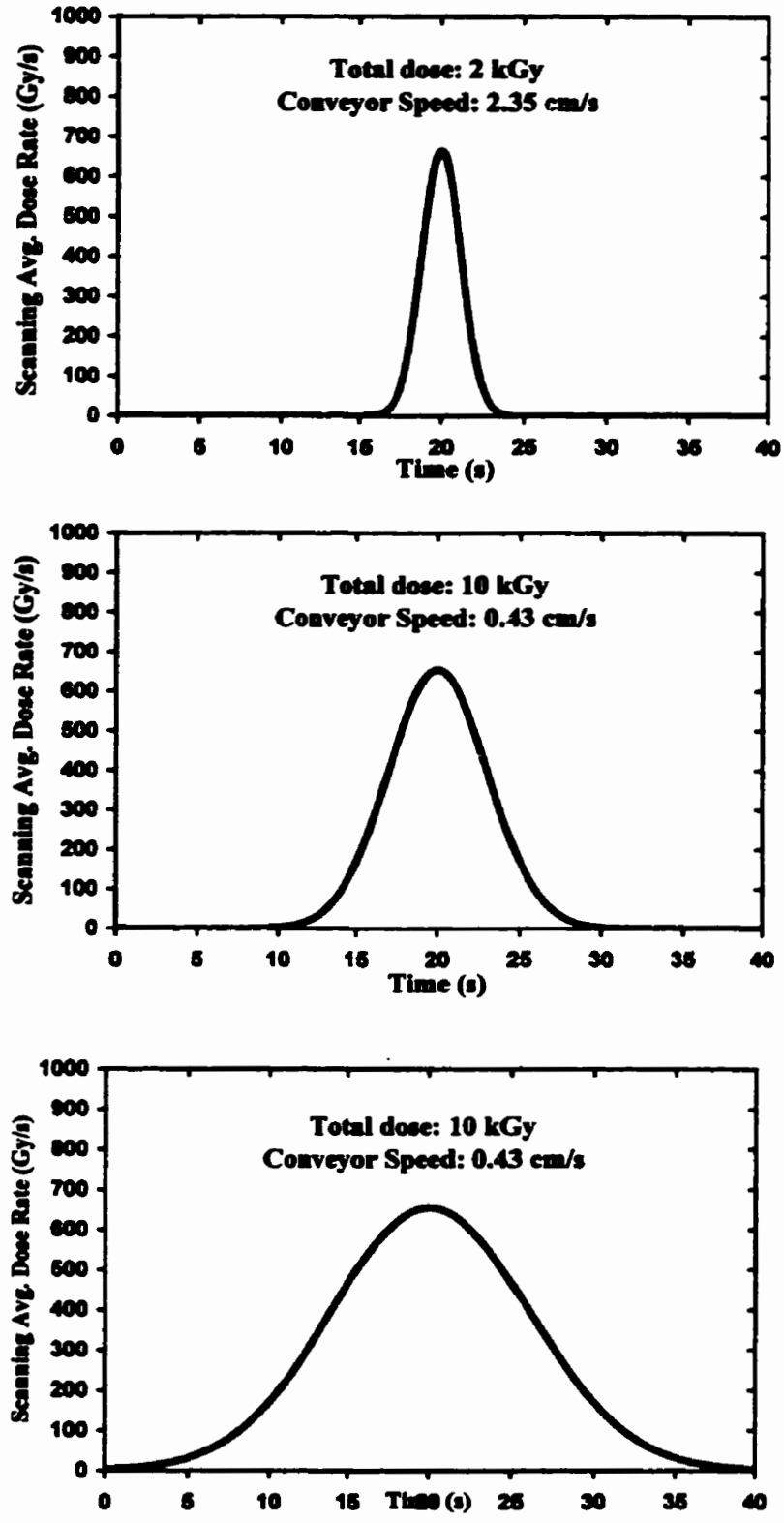

Figure 3.13: Variation in dose per pass for same scan width (scan width = 30 cm, height = 15 cm)

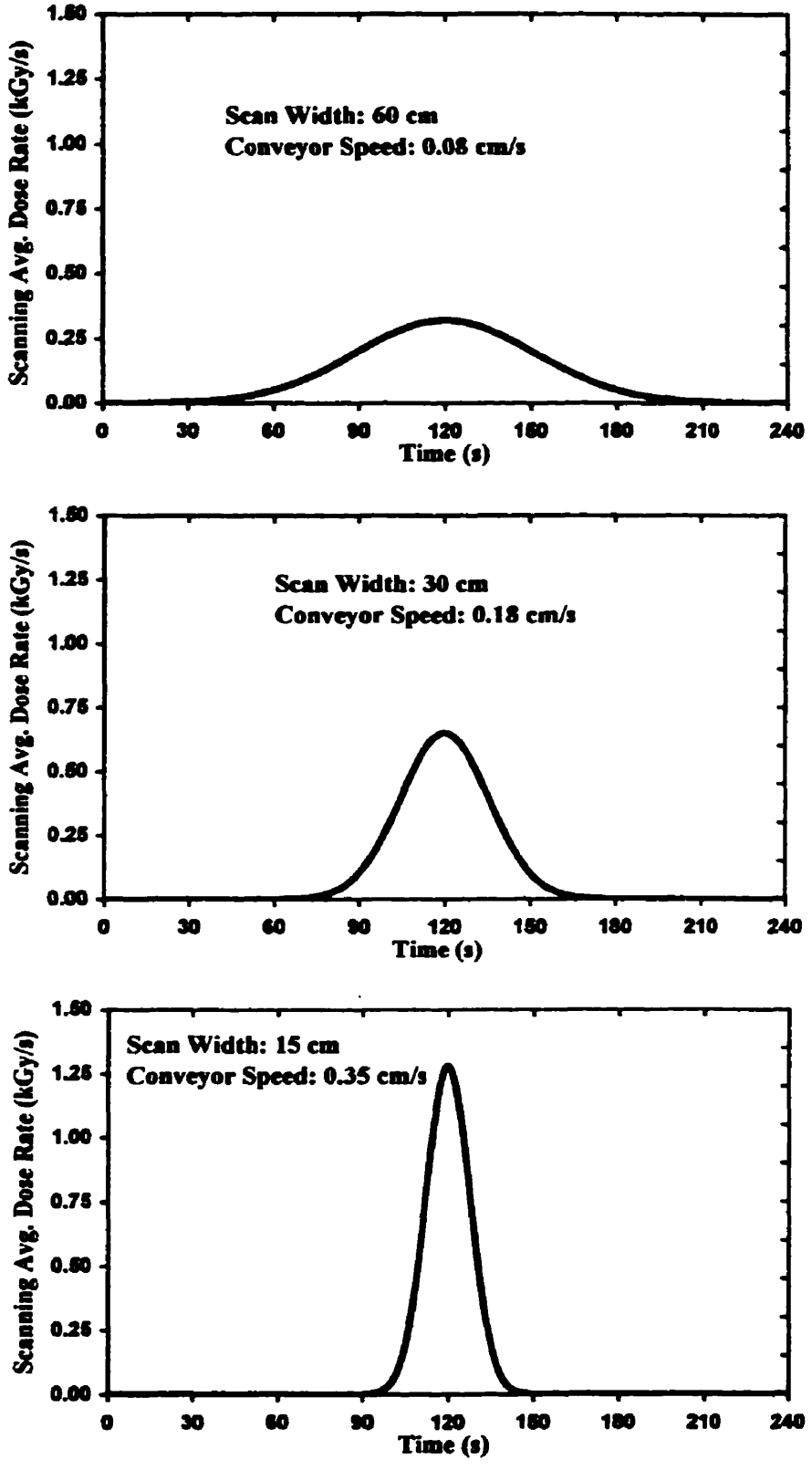

Figure 3.14: Variation in scan width for same dose per pass (Height: 15 cm, Dose per pass: 25 kGy)

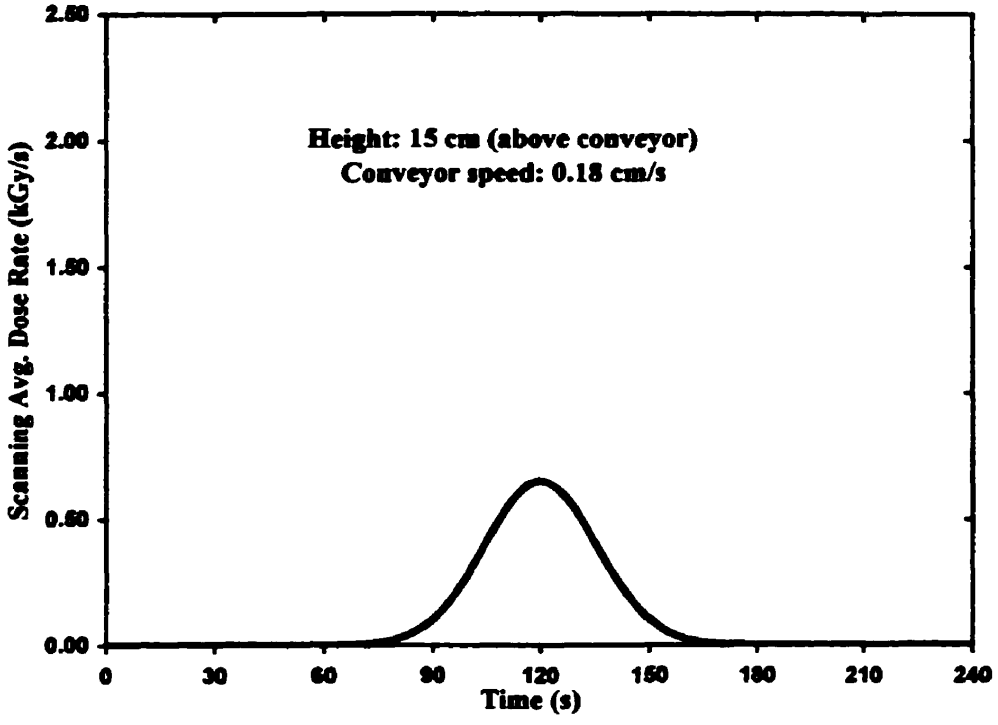

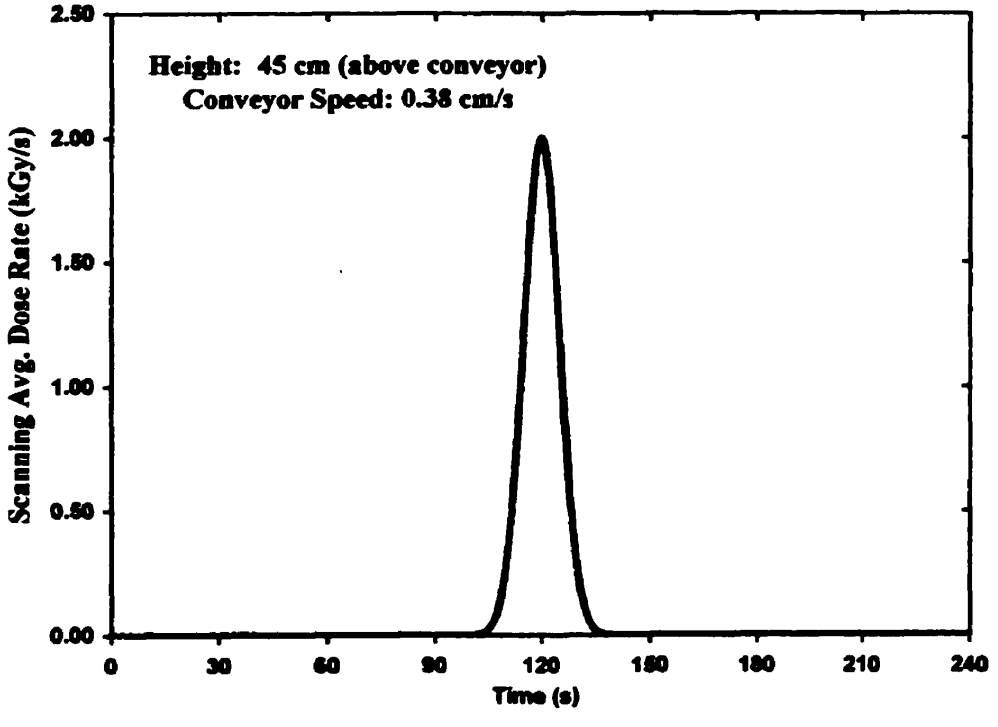

Figure 3.15: Variation in sample height for same dose per pass (Scan Width = 30 cm, Dose per Pass = 25 kGy)

A summary of the three preceding pages (Figures 3.13, 3.14, and 3.15) is presented below in table 3.3 as an aid in understanding how some dose rate parameters can be varied, while others remain the same, for different EB curing passes. This fact is critical for the investigation of dose rate discussed in chapter 6.

	Constant	Varying
Figure 3.13:	scan width (d_{3max}), scan height (d_{1max}, d_{2max})	dose per pass (d^*)
Figure 3.14:	scan height (d_{1max}, d_{2max}), dose per pass (d^*)	scan width (d_{3max})
Figure 3.15:	dose per pass (d^*), scan width	scan height (d_{1max}, d_{2max}, and d_{3max})

Table 3.3: Dose delivery differences and similarities

3.3.3 Temperature

Temperature is another process parameter of EB curing that requires explanation. EB curing is often considered a non-thermal process, which can be performed at selected temperature, but this does not mean that there is no temperature variation during the process. The **temperature of the composite part increases during EB curing due to**

two factors, **exothermic heat** produced from the crosslinking reaction, and **radiation heating** due to scattering reactions of the electrons bombarding the composite and mold. Exothermic temperature rise depends on the resin concentration, reactivity, and the kinetics of the reaction. For a given radiant dose, radiation heating depends only on the density of the material upon which the electron beam is incident. A typical thickness of laminate PMC (2-3 mm), on a thin aluminium mold, being subject to a single 25 kGy pass, the temperature rise may be in the approximate range of 15°C to 25°C. A number of passes under the scanning horn, without adequate time for cooling between passes may cause the temperature of the composite to rise to 75°C, or more. Since these temperature rises are fairly large, it is appropriate to list the **temperature, T**, as a process parameter and to investigate the influence of temperature in the experimental work to follow.

The temperature of the composite during EB processing can not be considered a *bulk* temperature, as it is with autoclave curing. For EB curing, the temperature in the composite varies according to position, dose, dose rate, and time (x, y, z, D, d, t) due to the nature of the process. For simplicity, two process temperatures are defined, which will help to describe and quantify the role of thermal energy during the EB curing process in later discussion. The **ambient temperature, T_a,** is the temperature of the immediate surroundings to the composite part. This ambient temperature may be the temperature of the air in the accelerator room or the '**applied**' temperature if the composite or mold is cooled during the process. For example, if a composite part is packed in ice during curing, the ambient temperature would be 0°C. The **maximum temperature T_{max},** during a pass under the EB horn during curing is also defined as a specific parameter

3.4 Summary

The purpose of the previous discussion was to give the reader a good understanding of *what is involved* in the process of high energy EB curing. Some basic details have been provided on the appearance of an EB processing facility and accelerator. More specifically, the process parameters of dose, dose rate and temperature have been described and specific process variables have been defined. These variables are identified and catagorized as:

Dose:	D, D_{cure}
Dose Rate:	d_1, d_2, d_3, d^*, t^*
Temperature:	T, T_g, T_{max}

It is now appropriate to commence with an examination of literature that is available regarding the influence of these specific process parameters as well as some important material parameters.

Chapter 4

Literature Review

Previous research studies relevant to high energy EB curing are discussed in this chapter, specifically that literature concerning the influence of material and process parameters. Three general process parameters (i.e. dose, dose rate, and temperature) were identified in the previous chapter. This chapter will introduce the reader to the additional considerations of the EB resin formulation and material parameters. As well, a few studies which discuss rheological properties and reaction kinetics are considered. At the end of the chapter, armed with knowledge of the EB process and recent literature, the motivating reasons for this thesis and specific research objectives are revisited.

4.1 Resin Formulations and Material Parameters

Since the earliest research on EB curing of composites, one challenge has been to develop suitable resin systems. Describing their work that began at Aerospatial in 1979, Beziers and Capdepuy [4] stated that radiation induced crosslinking occurred readily for

polymers with double bonds on their chain ends. They suggested acrylate epoxies, acryate polyesters (figure 4.1) and acrylate urethanes were suitable for EB when used with a UV photoinitiator but did not identify any initiators they had used. This and other early research on high energy EB curing of composites was almost exclusively on **acrylated resin systems**.

Dickson and Singh [37] reviewed previous literature to evaluate the potential for EB curing of epoxies in their 1987 paper. They concluded that radiation-induced curing of epoxies via a free cationic mechanism (i.e. without addition of any initiator) was inefficient due to its inhibition by even trace amounts of oxygen or water. They also suggested that "epoxy –like" polymers could be produced by **free radiation curing of acrylated derivatives of epoxy oligomers**. This type of preliminary research on acrylated epoxies was done by many authors including Saunders, et al. [36], Singh and Saunders [49], and Kerluke et al. [24]. More extensive research was done by Singh et al. [50], who described the screening and extensive evaluation of various acrylated resins that cured by free reactions. The objective of systematic research on EB curing of these acrylated systems was for their use as matrix resins in composites, however they were generally found to be unsuitable for high performing advanced aerospace composites. Limitations included low glass transition temperatures, low fracture toughness, and high shrinkage when cured [3,51]. In short, acrylated systems were shown to have **poor ultimate properties**.

Developments by Crivello [1,52] in 1992 suggested that **certain cationic photoinitiators** (diaryliodonium and triarylsulfonium salts) could be used with **conventional epoxies** in very low concentrations to make EB curable formulations.

These cationic formulations were not inhibited by trace water or oxygen and did not require the addition of any solvents and so they offered a very easy mixing and curing routine. This was the first demonstration that epoxies could be efficiently radiation cured and created the possibility for high energy EB curing of conventional aerospace-grade epoxy resins. E-beam researchers quickly moved away from acrylated resins and began to evaluate EB curable epoxies (see figures 4.1 and 4.2).

In 1994, the Cooperative Research and Development Agreement (CRADA) to advance EB curing of PMCs was established in the U.S.A. Resin development and screening was one of the important objectives for this CRADA [53]. The intention of the CRADA was to screen different combinations of existing aerospace epoxies with cationic photoinitiators to produce a comprehensive list of performance and cure characteristics of resin/initiator formulations. AECL Radiation Applications Group was one of the industrial partners in this CRADA and performed most of the irradiation. AECL had been involved in a lot of early research on EB curing, and had practical expertise on screening resin/initiator formulations for their suitability and relative curing characteristics by a method called gamma cell calorimetry. Among the resins evaluated were a number of commonly used aerospace epoxies, including Tactix 123 and EPON 862 (figure 4.2) [3].

4.1.1 Gamma Cell Calorimetry

An empirical method for screening and evaluating EB resin formulations had been developed by AECL prior to the CRADA. Called gamma calorimetry, it involved exposing small test samples to high-energy gamma radiation and monitoring their

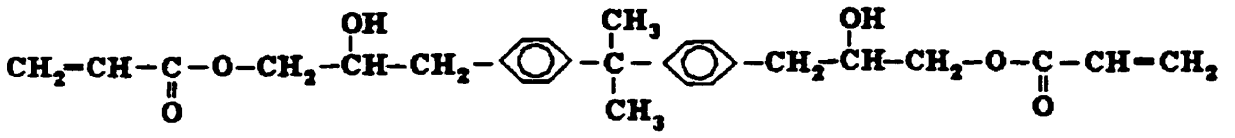

Acrylate Epoxy

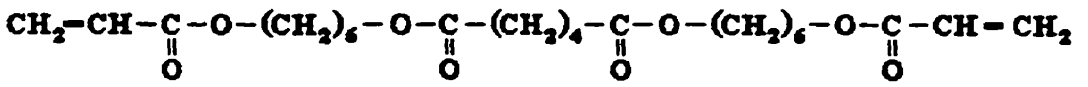

Acrylate Polyester

Figure 4.1: 'Old' EB resins – acrylated systems

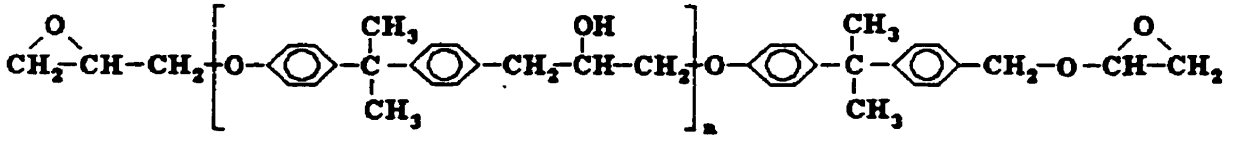

Tactix 123 – bisphenol-A epoxy

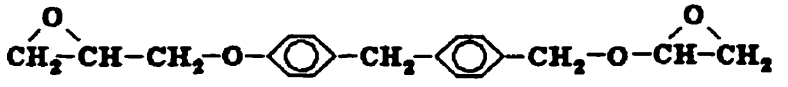

Epon 862 – bisphenol-F epoxy

Figure 4.2: 'New' EB resins – aerospace grade epoxies

temperature over time [3,50]. The resulting temperature rise (due to exothermic heat of curing) versus time data for each sample was analyzed and compared to other test samples. The use of gamma radiation in place of electron radiation was justified by reasons of economy and good experimental control, and a number of precedents [54,55]. Experiments were done with an AECL model 220 Gammacell Cobalt-60 gamma source (photographs of which are shown in the previous chapter in figure 3.7), which produces 1.25 MeV gamma rays. A schematic of the calorimetry setup for gamma cell experimental work is shown in figure 4.3 and an example of output data (dose versus temperature rise) is shown in figure 4.4.

Conventional aerospace matrix resins combined with a number of cationic photoinitiators were tested and evaluated. The temperature difference between an inert reference sample and a resin sample was monitored as a function of radiation dose. Evaluation involved examining the temperature history over 10 kGy dose, and subsequent visual examination of the resin. If the temperature history showed an exothermic peak, it was taken to be evidence of a curing reaction. Visual examination was used as a qualitative way to evaluate the extent of the reaction based on colour change and hardness [3,50]. If there was no evidence of curing, resins were immediately judged inappropriate for EB curing. **Screening of cationic photoinitiators with bisphenol A, bisphenol F, and cycloaliphatic epoxies demonstrated that diaryliodonium salts of weakly nucleophilic anions such as hexafluoroantimonate were particularly effective as initiators for radiation induced cationic epoxy curing [3].**

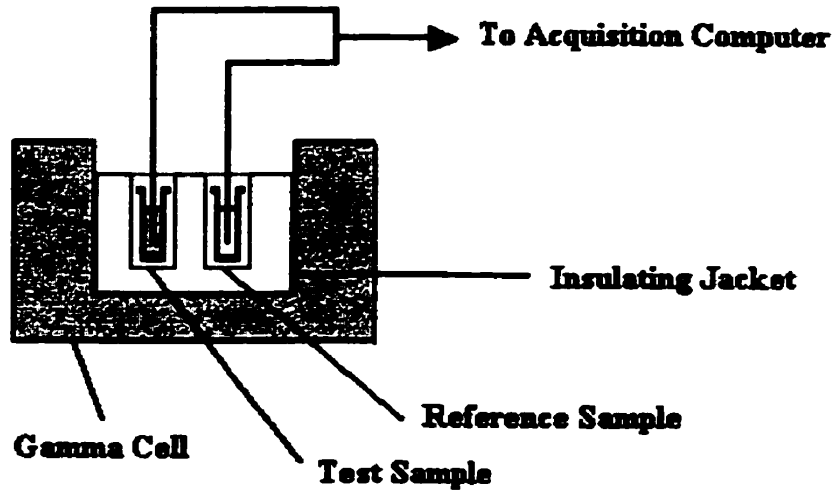

Figure 4.3: Gamma cell calorimetry

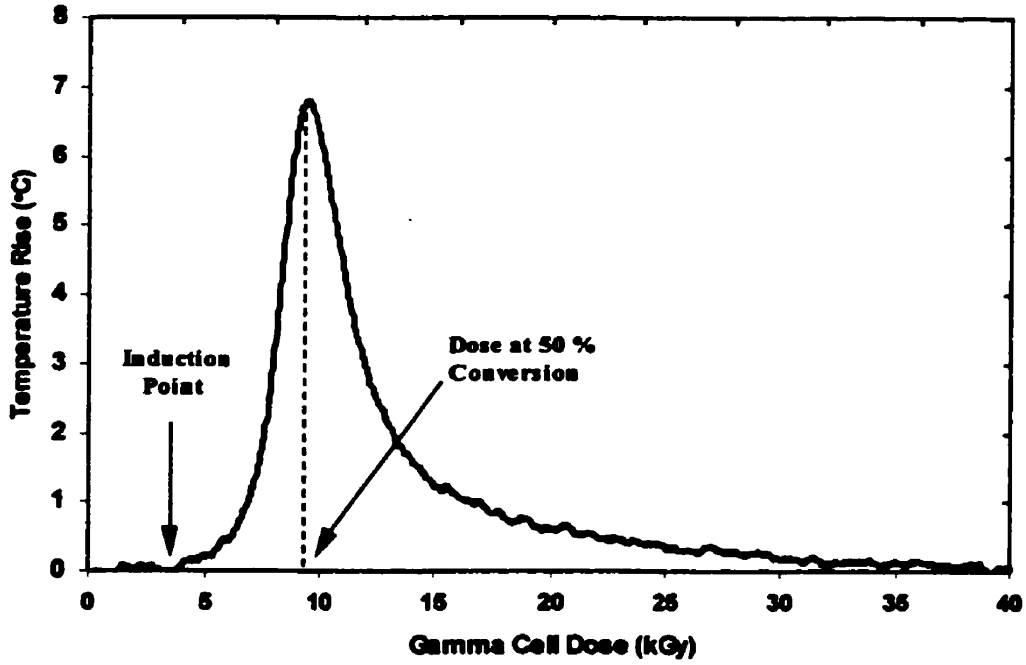

4.1.2 Initiator Concentration

The concentration of initiator mixed with resin to create the cure formulation is an important material parameter. Normally, initiator concentration is expressed in mass parts per hundred of resin, and for the is given the designation:

Initiator concentration, [I] (phr)

It is obviously desirable to optimize the initiator concentration for high physical performance at minimal cost.

Initiator concentration was evaluated by gamma cell methods during the CRADA [53]. A maximum or peak temperature due to the exothermic reaction was observed due to slowing of the reaction and heat loss from the gamma cell. The dose at which this maximum temperature occurred was taken as an indication of efficiency of the reaction. When the maximum temperature occurred at a lower dose the formulation was deemed more efficient than a temperature peak at a higher dose. Once a formulation had been approved for radiation curing, the concentration of initiator was varied and the resulting temperature data from gamma calorimetry were compared. The dose for peak temperature was observed to decrease with rising initiator concentration to a minimum dose and then for higher initiator concentrations the peak began to move to higher doses. The concentration of initiator for which the temperature peak occurred at the lowest dose was presumed to be the optimum (most efficient) initiator concentration [53]. This was found to be between 2 and 3 phr (parts per hundred of resin), depending on the resin/initiator combination. That is:

$$2 < [I] < 3$$

Lopata et al [53] also optimized initiator concentration based on dynamic mechanical analysis (DMA) of epoxy resins with different initiator concentrations. DMA is a thermal analysis method whereby a sample is cyclically stressed while scanning the temperature (see appendix B). The glass transition temperature (T_g) was measured by DMA analysis after EB curing of each sample. Results showed that at a certain initiator concentration the T_g was a maximum and beyond that concentration the T_g decreased. The results of this DMA study were in general agreement with the gamma cell analysis from the same paper, namely that the optimum initiator concentration was specific to each formulation but always between 2 and 4 phr.

$$2 < [I] < 4$$

4.1.3 Reinforcement

Another factor in considering the effect of material parameters on EB curing is the presence of reinforcing fibres in the composite. Resin screening has generally been done with neat resins and subsequently prepreg has been fabricated and EB cured with an approved resin to achieve a composite for analysis of mechanical properties. There has been little mention of the effect of reinforcement on cure kinetics during EB processing.

A unique situation occurs with EB processing where prepreg consolidation and debulking is required before EB curing. In conventional processing, wetting of fibres, resin flow, and debulking occurs during the temperature ramp up to the cure temperature. The resin viscosity lowers with increasing temperature until the gel point has been reached. However, in EB curing, there is no viscosity decrease and hence polymers are cured in the semi-solid, or solid state. Fibre wetting and debulking must be done bfore EB curing, and become pre-processing steps. This is a significant difference between the

difference between the two cure methods which warrants discussion, but will not be dealt with in this thesis. For example, fibre-matrix interface studies are beginning to appear [72] which investigate differences between conventional curing and EB curing.

The only reports on the effect of reinforcement on EB curing have come from the CRADA, which has reported that reinforcement serves to slightly hinder EB curing and slightly higher EB doses are needed when reinforcement is present. This has been reported in a general statement by the CRADA report, but no supporting data has been published.

4.2 Radiation Dose

A critical task in regard to EB processing of composites has been to determine the amount of radiation dose required for curing, D_{cure}. An insufficient dose is undesirable because it would result in incomplete curing and poor rheological properties. An overdose is also undesired for efficiency and economy of the process and could, in extreme cases; result in radiation induced damage (cleavage of bonds).

Studies done on acrylated resins suggested that the D_{cure} for those systems was approximately 25 - 50 kGy [4,39]. The experimental basis for this estimate was the measurement of rheological properties with increasing dose, and when the properties showed no improvement, the system was presumed to be cured. Crivello et al. [1] suggested that the D_{cure} for cationic epoxy systems was in a similar range of 10 - 30 kGy. The evidence for this estimate was based on observing the dose at which samples became tack-free after irradiation.

Singh et al. [50], developed a systematic way to determine the curing dose for each resin formulation. The EB dose required was determined by gamma cell analysis, based on the temperature-versus-dose data. Referring to figure 4.4, the point at which the temperature of the sample first starts to increase above the reference sample was labeled the 'induction point' and Singh assumed this to be the gel point of the formulation. Physically speaking, the gel point occurs when the bulk polymer transforms from the liquid state to the rubbery state, noted by the divergence of the viscosity to infinity (at this point, the polymer network has just extended throughout the entire bulk polymer). Singh also assumed that the peak temperature occurred at 50 % cure extent. An empirical formula was developed that approximated the dose required for complete curing based on this induction point and the peak temperature. If D_{cure} is the dose at 100 % cure, DGP is the dose at the induction point and DTM is the dose at the peak temperature, it was proposed that:

$$\textbf{Singh:} \qquad D_{cure} = DGP + 10(DTM - DGP) \qquad \textbf{(eq. 4.1)}$$

This empirical method for determining curing dose was applied to acrylated resins before the CRADA and during the CRADA was applied to cationic epoxies. For most acrylated resin systems, this formula led to a dose for 100 % cure of 30 to 70 kGy. Janke [56] and Lopata et al. [53], simplified this formula to a 'rule of thumb' that the curing dose was 10 times the dose at peak temperature in the gamma cell. This led to predictions for the **curing dose for cationic epoxy formulations of 70-100 kGy.**

Singh et al. [50], used DMA to determine the curing dose to compare with his gamma cell experimental work on acrylated systems. The glass transition temperature (T_g) was determined for samples at various stages of irradiation and the values for T_g vs.

dose were plotted. The dose at which the T_g reached a plateau was considered the curing dose. Although gamma cell analysis predicted the curing dose would be lower, Singh did not observe the T_g plateau until dose values near 150 kGy, suggesting this was the curing dose.

4.3 Dose Rate Effects

The general process parameter of dose rate, d, is critical for a number of reasons. From a practical point of view, the higher the dose rate, the shorter the processing time. Also, it is important to determine whether differences in applied dose rate change the cure characteristics such as curing dose, or the resulting rheological properties of the composite. Very few studies have been done on this effect for EB curing presumably due to difficulties in quantifying the continuously varying dose rate for an electron accelerator (discussed in chapter 3). In fact, no studies could be found that made any attempt to describe or measure the influence of the continuously varying dose rate during EB irradiation.

Singh et al. [50], briefly discussed the effect of dose rate by comparing EB to gamma cell irradiation. The gel fraction (fraction of polymer which has been crosslinked) by size exclusion chromatography (SEC) analysis was compared with samples irradiated to the same dose in the gamma cell and under the electron beam. The dose rate in the gamma cell was nominally 7.8 kGy/h and the stated dose rate for the electron beam was nominally 5400 kGy/hr. This dose rate for the electron beam is likely the instantaneous dose rate at the center of the beam (d_1 from chapter 3). The resins

resins tested were acrylated systems (among them epoxies, urethanes, butylenes and polypropylenes) cured without addition of an initiator or catalyst. Results showed a distinct difference in gel fraction as a function of dose for the two different dose rates. For three resin systems, increased curing occurred at a much lower dose for the low dose rate (gamma cell curing). Another way of stating this is to say that to reach a similar gel fraction, a higher dose would be needed for EB irradiation (higher dose rate) than for gamma irradiation (lower dose rate). For two acrylated epoxies tested, the opposite was true and the gel point occurred at a lower dose for the higher dose rate (EB curing). For an acrylated epoxy blended system, no difference in gel fraction for the low dose rates was seen for resin samples, but for composite samples EB irradiation was more effective. While no general conclusions can be made from these results, they prove that **dose rate differences have strong implications on the cure progression during irradiation.**

Examples of other dose rate investigations can be taken from research not specifically dealing with the curing of thermosets. Czvikovsky presented a detailed study of dose rate effects for high-energy gamma and low energy EB crosslinking of wood-thermoplastic composites in 1992 [57]. Results for different methyl methacrylate resin purifications and matrices show that the curing dose, D_{cure}, is proportional to dose rate, d. That is:

$$\textbf{Czvikovsky:} \qquad D_{cure} \approx k\sqrt{d}. \qquad \textbf{(eq. 4.2)}$$

This result implies that the total curing dose (energy input) can be lowered by choosing the smallest acceptable dose rate for radiation processing. Different gamma dose rates were easily obtained by moving samples to various distances from the gamma source. Different low energy EB dose rates were achieved by varying the conveyor speed under

the influence of a linear EB source. This suggests that the EB dose rates may be similar in character to the author's definition of peak scanning average dose rates (d_3) as described in chapter 3.

Skraba and Lynn [58] investigated the effect of dose rate on grafting of Polyurethane foam. A Cobalt-60 gamma source (1 kGy/hr) and a Van de Graff electron accelerator were both used in this investigation. The specified accelerator dose rate of 1000 kGy/hr is likely some type of averaged dose rate. The extent of grafting was about seven times **greater at the lower dose rate** than with the accelerator dose rate for similar total doses. Campbell et al. [59], investigated the effect of dose rate on the grafting of vinyl monomers to wool. The dose rate was varied from 7.5 Gy/h to 10 kGy/hr by changing the distance from a Co-60 source. The grafting yields increased as the dose rate decreased. Cambell also performed experiments varying the dose rate on the electron accelerator. In this case, the dose-per-pass was used in place of a dose rate per unit time. Dose-per-pass values of 2.5, 5 and 10 kGy were used to irradiate samples to total doses of 20 and 50 kGy. An insignificant difference in grafting yield was seen between the different dose-per-pass values.

4.4 Temperature Considerations

Little has been published or discussed with regards to the influence of temperature, T, on high energy EB curing of composites. General discussions on EB have often simply stated that it is a non-thermal process that may be performed at any selectable temperature. These discussions have helped attract attention to EB because of the

potential advantages of avoiding the autoclave, inexpensive tooling, and co-curing of dissimilar cure systems. Furthermore, curing at selectable temperature suggests the possibility of avoiding warping due to coefficient of thermal expansion (CTE) mismatch between the tool and composite part, or CTE mismatch between cross directional plies of a laminate. In fact, the initial motivation for pursuing EB curing of composites by Aerospatial [4] was to avoid thermal deformation during curing

For conventional (non-EB) curing of low-performance epoxies, often no application of external heat is required (so-called room temperature curing). In fact, the reaction begins at room temp but the formulation quickly heats up due to exothermic heat produced. This temperature rise then causes the reaction to accelerate, which subsequently produces more heat. During EB curing, a similar exothermic heat rise occurs. The actual amount of exothermic heat and temperature increase depends on the reactivity of the reaction and on the bulk amount of material (i.e. a thin fibre rich laminate will not produce as much heat as a thick resin rich part). Also, the act of bombarding the composite part with radiation energy causes the part to heat up – a phenomenon generally called radiation heating.

Goodman et al. [13], first drew attention to these facts in his 1996 paper. In 1997 Goodman et al. [14], reported temperatures approaching 70°C for the composite part, even with cooling between passes under the EB horn and limited dose-per-pass values. With the observation of significant temperature rises during EB irradiation, a significant factor to consider is that Crivello had suggested that cationic systems could be thermally-initiated [1] as well as radiation-initiated. This implies that simultaneous EB curing and

thermal curing may occur during irradiation, influenced by temperature fluctuations during processing.

Passing references to the possibility of temperature influencing the reaction have been made previously. Singh et al. [50], briefly mentions that the temperature rise in the gamma cell was lower than the temperature rise under EB, potentially influencing dose rate experimental data. Tavlet et al. [60], makes a significant observation that "ambient temperature may be of great importance when irradiating polymers".

4.5 Properties of EB-Cured Composites

A great deal of literature has been published on the mechanical, thermal and rheological properties of EB cured composites. Usually, such literature is the result of an investigation of a new resin formulation, or an initial trial and evaluation of the technology of EB processing. The studies have typically non-technical in nature. However, a number of interesting results and questions have arisen from such studies.

The mechanical and thermal properties of EB cured resins and composites have been studied by DMA analysis and mechanical (tensile, shear, compression) testing. Some studies have been used to determine optimum values for resin formulation and curing dose, as already discussed. Farmer et al. [61], in 1997 compared the rheological properties of EB cured fibreglass/epoxy (cationic EB formulation) prepreg laminates with an autoclave cured conventional formulation. Porosity and tensile strength properties of the EB cured laminates were equivalent to the thermal laminate both at 25°C and 71°C. The moduli of the EB laminates were equivalent to or higher than the conventional laminate. A drawback was that the compressive and flexural strengths of the EB

laminates were 20-30 % lower than the conventional laminate. **Good to favourable comparisons between EB and thermally cured samples** have also been cited by a number of other authors [3,9,55,62-64].

Although Farmer et al. [61] observed very high primary T_g's for EB formulations he also observed **two minor transitions** in flexural modulus while testing all EB samples. He alludes to the fact that minor glass transitions such as those he observed are usually attributable to uncured resin. Walton and Crivello [20] observed high T_g values for EB cured formulations, but their DMA plots appear to have the same type of minor transitions. However, the authors clearly stated that no thermal postcure was necessary for their formulations.

A fact about conventional curing of thermosets is that the temperature properties of the final cured part depend highly on the cure temperature. Studies have shown that the T_g may be limited to a value of approximately 50°C above the cure temperature [65] for thermal curing. This is mainly due to the fact that the when T_g exceeds T_{cure}, the thermoset is in its glassy state, and crosslinking reactions become limited by diffusion. For example, an epoxy composite part cured at 177°C (350°F) obtains a T_g in the range of 175°C to 200°C. Some EB research has contradicted this principle by claiming T_g's as high as 300°C for room temperature EB cure [66]. Goodman [13] challenges such high reported values by suggesting that subsequent thermal testing artificially raises the observed T_g. A number of other authors have suggested that some form of thermal postcuring is required after EB curing to finish off the reaction and raise the T_g [2,13,67]. The questions regarding necessity of thermal postcure, thermal curing during EB irradiation, and very high reported T_gs, have not been resolved in any current literature.

4.6 Reaction Mechanisms and Kinetics

The chemical mechanisms by which cationic curing of an epoxy occurs under electron beam irradiation is the subject of speculation by chemists. Crivello has outlined a possible mechanism for general EB curing based on past experience with photocurable formulations [1,68,69]. However, no formal study has been done which specifically investigates the mechanism(s) or kinetics of EB curing. In formulations that are both radiation curable and thermally curable (previous studies suggest that this is the case with cationic epoxy systems) no research has been published which discusses whether the thermal and EB reactions are identical, similar or unrelated in nature.

4.7 Motivation for New Research

A number of research papers on EB processing have been discussed in this chapter. From this literature, a preliminary level of knowledge has been obtained on the general effects of the material and process parameters of **dose, initiator concentration, temperature, dose rate, and reinforcement.** Studies that have examined the rheological properties of EB cured cationic epoxies and their composites have produced good results when compared to thermal formulations, which indicates that EB curing is a promising technology. However, there are a number of questions about EB processing which have arisen in previous research studies. These are due to lapses in the knowledge of the explicit influence of material and process parameters.

The experimental study to follow was performed with an overall goal: **To make significant contributions towards the development of a processing model for high-**

energy EB curing. An accurate processing model would predict material properties during and following EB curing based on the known inputs of all the material and process parameters. This would facilitate improvements in process control and quality, and allow optimization for cost and performance considerations. An accurate predictive model for EB curing will, in reality, not be fully developed for some time. However, specific details on the nature of high-energy EB curing are required as building blocks for further development. This thesis seeks to investigate the influence of material and process parameters, and to provide insight into the nature of EB curing. Over the course of the experimental investigation, underlying questions about EB curing will be addressed. Each of the following 5 parameters will be investigated:

1) **Electron beam dose, D.** Required is an accurate method of determining the **curing dose** D_{cure}.. Resins that have been reported to require thermal postcuring may not be receiving enough dose, and determination of the minimum dose for maximum curing optimizes the time and energy spent during processing. Furthermore, a study of **cure progression with dose** is required to evaluate the effect of EB radiation on cure extent at various stages of the process. Since EB curing ostensibly takes place with the polymer in the glassy state, the influence of EB dose on diffusion and reaction kinetics also needs exploring. An explanation of how EB processing can achieve such high reported T_gs, when curing at ambient room temperature would be a desirable result of such an investigation.
2) **Temperature, T.** Indications from a number of studies have suggested that **thermal energy** may play an important role in EB processing. Some authors have suggested that **thermal postcuring** is a necessary requirement. Other authors have indicated

that the temperature rise during EB processing may lead to **simultaneous thermal curing**. The influence of temperature during and after EB processing must be determined. Since EB curing has generally been considered a non-thermal process, and many projected advantages of EB curing revolve around its temperature independence, quantifying the influence of process temperature has major ramifications for the future of EB curing.

3) **Initiator concentration, [I].** Methods of evaluating the influence of [I] on material properties require investigation. It should be verified whether gamma radiation screening and analysis is actually valid for EB curing. Also, if the optimum initiator concentration for thermal curing can be determined, it must be resolved as to whether this concentration applies to EB curing as well.
4) **Dose rate, d.** An investigation is needed to determine if the influence of the dose rates conceived of and described in chapter 3 can be quantified. Any changes in cure properties with dose rate will have implications on optimizing the time required for EB curing.
5) Finally, it must be determined how the presence of **reinforcing fibres** effects the curing process, and whether results of EB curing investigations obtained from analysis of neat (unreinforced) resins can be readily applied to composites.

An additional objective of the work to follow is to evaluate the proposed advantages of EB curing. To aid in the evaluation of the process, comparisons are to be made between thermal and EB curing of the same resin formulations. Although mechanical characterization is not the focus of this thesis, some simple mechanical property measurements are to be made and compared.

Chapter 5

Experimental

This chapter outlines the experimental work performed in this thesis. First, the epoxy resin selected for this study is described, along with its EB initiator, and recommended conventional hardener. Next, the sample preparation and curing of the resin formulation are described. Finally, the methods of analysis (namely DSC, DMA and mechanical testing) used to investigate EB curing are explained.

5.1 Description of Materials

A single epoxy resin was chosen for examination of the EB curing process. The formulation chosen is a proprietary formulation developed by the CRADA [70]. Out of professional respect for its developers, the resin will not be identified except to describe it as an aerospace resin desirable for its high service temperature and excellent adhesion. It

will be referred to as 1E for the remainder of this thesis. No additional purification was performed upon receiving this resin.

The initiator that completes the formulation is a cationic photoinitiator approved by the CRADA on EB curing [3,25,53], and first developed by Crivello [1]. It is available from General Electric Silicones and is formally described as (4-octyloxyphenol) phenyliodonium hexafluoroantimonate, but generally referred to by its acronym OPPI. The chemical structure of OPPI is shown in Figure 5.1. As with the resin no additional purification was performed on the photoinitiator once it was obtained.

The initiator was nominally used at a concentration of 3 phr (parts per hundred of resin). The justification for this nominal value was that this was the standard concentration used by other researchers [3,25] and determined as the optimum concentration by Lopata et al. [53]. For initiator concentration experiments, the mixing regime was varied between a minimum of 1 phr and a maximum of 20 phr. For purposes of comparison, a small amount of 1E resin was prepared with a conventional curing agent, the amine hardener 4,4'-sulfonyldianiline (DDS). Reinforcement used in manufacturing of composites was IM7 graphite plain weave fabric.

5.2 Sample Preparation and Curing

5.2.1 Sample Preparation

Resin 1E is a semi-solid at room temperature that softens at approximately 60°C and has a suitably low viscosity for stirring at approximately 80°C to 100°C. Addition of

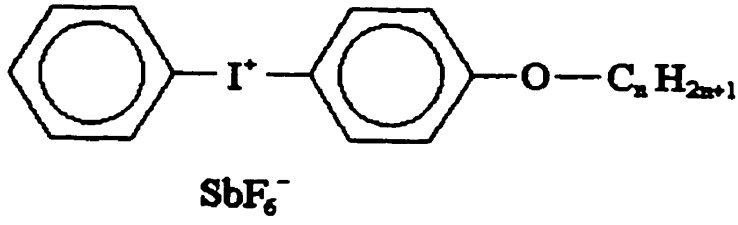

Figure 5.1: Chemical structure of OPPI

initiator to resin was done by heating a known amount of resin to 100°C and adding OPPI according to desired concentration. The formulation was mixed repeatedly to ensure even distribution of OPPI. All transfer of the resin formulation from mixing container to mold or other receptacle was done while the resin was still hot. Resin samples to be EB or gamma cell cured were taken into 1 ml or 3 ml polypropylene syringes. A picture of resin filled syringes ready for EB curing is shown in Figure 5.2. Syringes were weighed before and after filling to determine the mass of resin. Since temperature monitoring during curing was necessary, small chromel-alumel thermocouples were set into the centre of the resin filled syringes as the resin cooled. For EB curing, syringes were taped onto a thin Aluminium plate to secure them in place during conveyor movement.

Resin samples that were to be thermally or EB cured and then DMA tested were cast in aluminium molds. Heated to 100°C, the resin was transferred into a similarly warm mold of 10 cm x 20 cm x 3 mm with aluminium walls of approximately 3 mm thickness. Resin samples to be thermally or EB cured and then tensile tested were cast into a warm mold specially designed for that purpose (Figure 5.3). Both types of molds were kept at 100°C for approximately 2 hours after being filled with resin so that any air bubbles caused by pouring could escape. The resin mold ensured that tensile specimens had dimensions as per recommendations in ASTM D638. The nominal thickness of tensile samples was 4 mm. Thermocouples were placed both on the outside of the molds and also within the cast resin to monitor temperature rise during EB curing.

Composite samples were prepared by lay-up on a 3 mm thick Aluminium plate. One layer of plain weave IM7 graphite fibres was placed on the plate and then brushed with hot resin. This was followed by subsequent layers of composite and resin until a

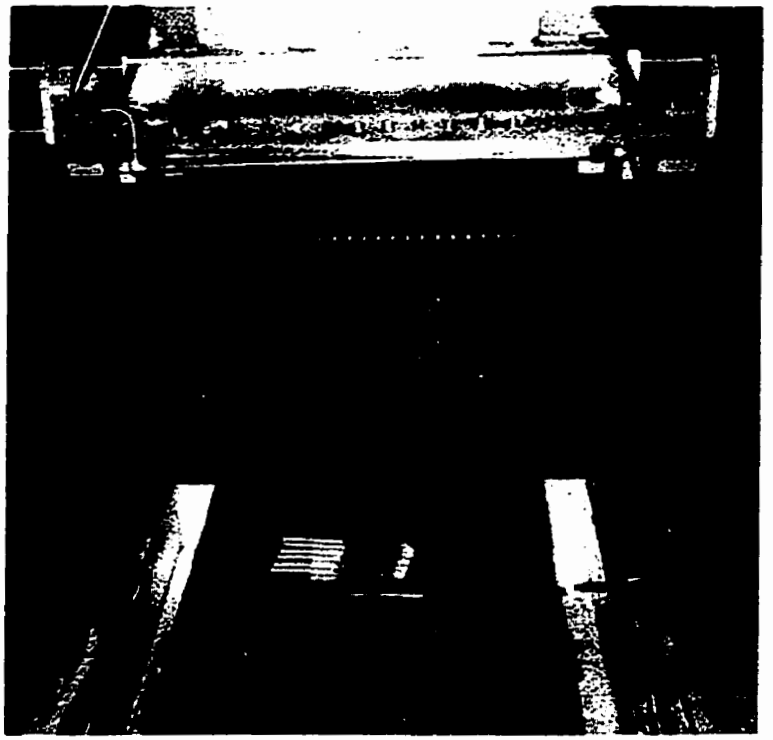

Figure 5.3: Resin samples in polypropylene syringes ready for EB curing

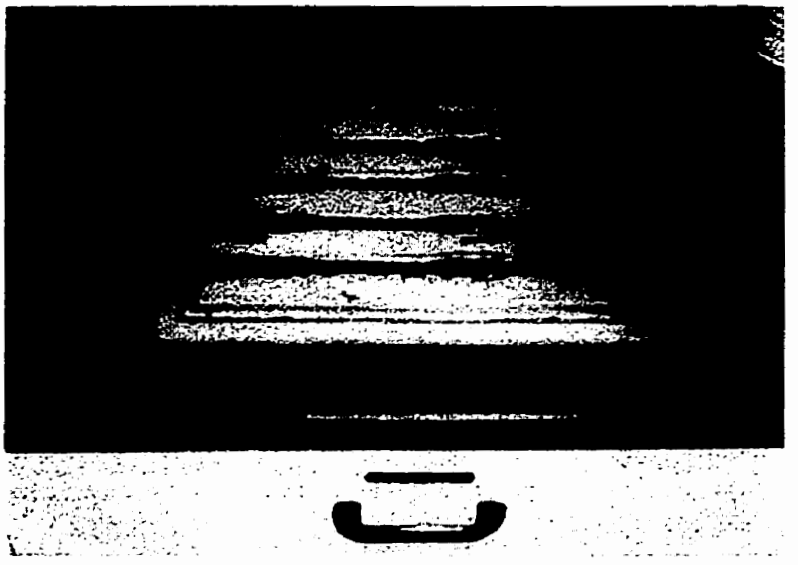

Figure 5.4: Resin mold for tensile samples

laminate of 4 layers was achieved. The laminate was then vacuum bagged with nylon bagging film, and placed in a platen press at 100°C. The vacuum bag was evacuated and the composite was left to consolidate for approximately 1.5 hours.

Upon curing to a desired dose or cure extent, DMA resin and composite samples were dry cut with a slow-speed diamond blade cut-off saw to the required nominal dimensions of 1 cm x 6 cm.

5.2.2 EB Curing

All EB curing was done at Acsion Inc. in Pinawa, Manitoba with the AECL model I-10/1 (10 MeV, 1 kW) accelerator, described at length in chapter 3. EB cured samples were transported to the University of Manitoba for subsequent mechanical or thermal analysis.

A scan width of $\Delta y = 30$ cm was used and a scan height of $z = 15$ cm (15 cm above the conveyor) were used for all EB curing except for dose rate experiments. Normally, both the resin and composite samples were cured in steps of 25 kGy (i.e. 25 kGy/pass). Additional dose rate experiments were also performed at 2, 5, 10, and 20 kGy/pass. The maximum total dose applied to any samples was 500 kGy. The scan widths, sample heights, and conveyor speeds used are summarized in table 5.1, with their corresponding dose rates as defined in chapter 3.

The time required for EB curing of is dependent on a number of factors, and the time scale for curing in the experimental work herein can only be estimated to an approximation. The time for one sample to pass under the EB horn depends only on the conveyor speed, however, the time between successive passes, depended on the number and size of the samples being cured during that pass, the amount of cooling desired

Dose per Pass (kGy)	Scan Width, Δy (cm)	Scan Height, z (cm)	Conveyor Speed, dx/dt (cm/s)	Instantanecus Dose Rate at Beam Centre (MGy/s)	Peak Scanning Average Dose Rate (kGy/s)
80	30	15	0.05	2.1	0.65
50	30	15	0.09	2.1	0.65
25	30	15	0.18	2.1	0.65
20	30	15	0.22	2.1	0.65
20	60	15	0.09	2.1	0.32
20	30	45	0.35	5.4	1.7
10	30	15	0.43	2.1	0.65
5	30	15	0.80	2.1	0.65
2	30	15	2.35	2.1	0.65

Table 5.1: Specifications for EB irradiation

between passes, and whether the accelerator had to be turned off-line to retrieve samples. Typically, no more than 40 cm (Δx) of samples were cured at one time, and the time for one pass can be estimated using the conveyor speeds in Table 5.1. Normally, the progression of EB cure was investigated for all samples, so a dead time of 3 to 5 minutes occurred between incremental passes to retrieve samples from the accelerator room, unless otherwise specified. For samples that were cooled between passes to limit temperature rise, the dead time between passes was an additional 2 to 3 minutes. For example, for a scan width of 30 cm and a dose per pass of 25 kGy, chart 5.1 shows the conveyor speed was 0.18 cm/s. For 40 cm of travel, this equates to approximately 4 minutes (rounding off to the nearest minute). Assuming 5 minutes between passes; 10 passes (a dose of 250 kGy) would have taken approximately 90 minutes.

When curing syringes of resin, the syringes were taped to a thin aluminium sheet or platform and placed on the conveyor. According to applied ambient temperature requirements, either ice (0°C), room temperature air (22°C), or dry ice (approximately -78°C) were used in thermal contact with the aluminium platform during processing. When required, ice or dry ice was placed below and surrounding resin specimens, but not on top, to avoid even the slightest shielding effects. The syringe plunger and cap were kept in place when curing on ice or dry ice to ensure that condensation formed only on the outside of the syringe and no moisture was introduced into the resin. Any samples that were cured at sub-RT cure temperatures were transferred from the accelerator facility to the testing facility at the University of Manitoba in a cooler at the same temperature, and kept at that temperature until they were tested.

All molded samples were cured with the mold in contact with a bag of ice to

ensure a minimum temperature rise during EB irradiation. Bagging film was taped over the open mold to restrict condensation on the resin. After curing in 10 kGy per pass steps, tensile samples were removed from the mold and free cured (no mold) in additional 25 kGy steps up to 200 kGy.

During EB curing, the temperature of resin and composite samples was monitored by wiring thermocouples from the accelerator room to the control room. A panel of thermocouple connections was available in the accelerator room that was wired to a panel in the control room. Voltage signals were obtained with an acquisition board and computer and converted to temperature. In this manner, the temperature of the sample could be monitored during each pass under the EB horn. As well, the curing passes were delayed, if so required for temperature control, to wait for the samples to be cooled before the next pass under the horn was performed. When this procedure was followed, the temperature requirement between successive passes was approximately within 10°C of the applied ambient temperature.

5.2.3 Gamma Cell Curing

The gamma cell at Acsion's facility, described in chapter 3 was also used to cure a number of resin samples. The Gammacell 220 produces high-energy (1.25 MeV) gamma rays from a Cobalt-60 source. The dose rate in the gamma cell was nominally 50 Gy/min (3 kGy/h). Samples were placed in 1 or 3 ml syringes and placed in the gamma cell for a set amount of time to acquire the desired radiation dose. Temperature measurements were also made during gamma cell curing in a similar manner to gamma cell calorimetry experiments described in chapter 4.

5.2.4 Thermal Curing

Thermal curing of resin samples was performed either within the DSC cell, or in a laboratory oven. Ramp curing of small samples was done in the DSC cell, so that cure exothermic reaction could be monitored. Isothermal curing of small samples was also performed in the DSC cell by ramping the sample up to the desired temperature and then curing isothermally for a programmed period of time. If a partial cure was desired, then the sample was removed from the DSC and quench-cooled in air after the desired amount of time.

Tensile samples of resin were prepared in the same mold as for EB curing. The resin was poured in the mold at approximately 100°C and the temperature was kept at 100°C until all visible porosity had risen out. Then the temperature of the oven was ramped at approximately 5°C/min to 177°C. Curing at 177°C for 4 hours. A free-standing postcure (tensile samples out of mold) was performed at 232°C immediately following the initial cure cycle.

5.3 DSC Analysis

The majority of the experimental testing for this investigation was done with a Differential Scanning Calorimeter (DSC). An introduction to thermal analysis and DSC is presented in Appendix Two. Thermal Analysis of the epoxy/photoinitiator combination was made possible by the fact that the formulation could be cured by both thermal energy and radiation energy. This fact is of central importance to all testing and subsequent analysis.

A photograph of the thermal analysis equipment at the U of M is shown in Figures 5.4 and 5.5. The DSC is a heat flux type DSC, model 2910 manufactured by TA Instruments Ltd. Hermetically (airtight) sample pans were used and a nominal sample weight of 14 mg was used. Samples were tested in an inert gas (Nitrogen) environment. For measuring glass transition temperature (T_g), ASTM standard E1356 was followed. At a minimum, two samples of each cure condition were tested to ensure repeatability. For each resin *batch* mixed and *type* of experiment performed, at least 5 identically treated samples were tested to measure and compare experimental error. For heat flow measurements, the average standard deviation of resin samples was 5 %.

A nominal ramp rate of 10°C/min was used for all ramp experiments. This ramp rate was determined by testing a number of identical samples at different ramp rates (from 2.5 to 20°C/min) and selecting 10°C/min for its balance between good sensitivity and good resolution. For all ramp DSC plots, a two-point rotation was used to correct for baseline slope. Temperatures for isothermal DSC testing were selected between the reaction onset and peak heat flow temperatures during ramp curing. For irradiated samples, isothermal analysis was only performed on samples that had received doses less than 14 kGy, for reasons that will be explained in the next chapter.

5.3.1 Degree of Cure Analysis

Ramp curing was used to determine the total exothermic heat of reaction for a formulation that had not been subjected to any radiation (untreated). This total

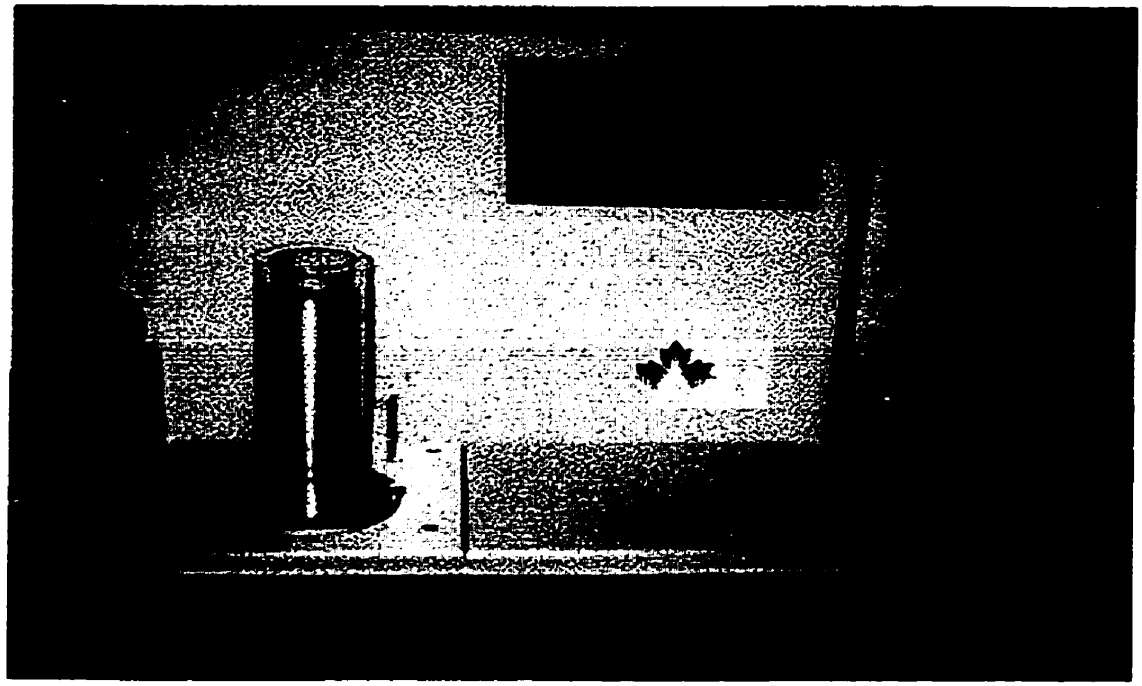

Figure 5.5: TA 2910 Differential Scanning Calorimeter

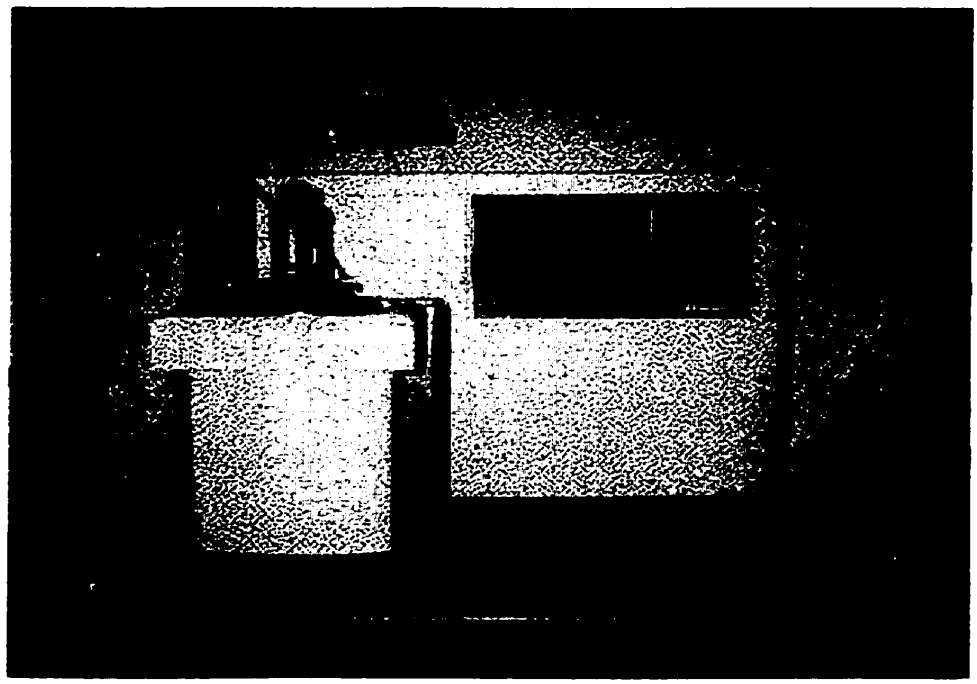

Figure 5.6: TA 2980 Dynamic Mechanical Analyzer

exothermic heat of reaction is given the symbol ΔH_o. Samples were partially cured either by thermal means or by EB, and then were subsequently ramp cured with the DSC to determine the exothermic heat of the remaining crosslinking (residual heat of reaction), ΔH_{pr}. A simple calculation of the degree of cure, c, could be made by:

$$c = \Delta H_{pr} / \Delta H_o \qquad \text{(eq. 5.1)}$$

5.3.2 Kinetic Analysis

Kinetic analysis was done on the DSC by isothermal curing of untreated and EB-treated samples. The cure kinetics can be mathematically modelled by either autocatalytic or nth order analysis. Nth order reactions are characterized by maximum exothermic heat evolution at time t=0, while autocatalyzed reactions show a maximum heat evolution at 30% to 40% cure extent and often show an induction period during which no apparent reaction takes place. A significant portion of the epoxy systems used in industry are autocatalytic. The autocatalytic effect is due to the formation of some intermediate species, which markedly accelerates the reaction. For example, the curing process for an epoxy-amine thermoset is autocatalyzed by the hydroxyl groups formed in the reaction. The induction time for autocatalytic reactions depends on the initial concentration of the catalyst, or the reaction rate constant of the parallel reaction that produces the intermediate species.

Initial experiments showed that the resin formulation studied here followed autocatalytic behaviour during curing. Hence autocatalytic analysis was performed on

the time-heat flow data at a given isothermal temperature. The autocatalyzed model can be described as follows:

$$dc/dt = k\,c^m\,(1 - c^n) \qquad \text{(eq. 5.2)}$$

where:

- c = the fractional conversion after a time t
- k = specific rate constant at temperature T (1/sec)
- dc/dt = reaction rate (1/sec)
- n,m = reaction constants (also know as reaction orders)

And the rate constant may be described by the following equation:

$$k\,(T) = Z\,e^{-E/RT} \qquad \text{(eq. 5.3)}$$

where

- Z = pre-exponential factor or Arrhenius frequency factor (1/sec)
- E = activation energy (J/mol)
- R = gas constant (8.314 J/mol-K)
- T = absolute temperature (K)

Taking logarithms of equation 5.3 yield

$$\ln k(T) = \ln Z - E/RT \qquad \text{(eq. 5.4)}$$

A plot of ln k(T) versus 1/T is called an Arrhenius plot, and should be a straight line if the temperature dependence of the rate constant can be modelled by equation 5.3. The activation energy and pre-exponential factor can be obtained from the slope an intercept respectively.

Taking the logarithms of equation 5.2,

$$\log (dc/dt) = \log k + n \log c^{m/n}\,(1\text{-}c) \qquad \text{(eq. 5.5)}$$

This modified equation can also be solved by a linear fit, with the slope of the line being n, and the intercept equal to log k. The value of m is calculated by substituting n and k, and then solving for m.

The two basic parameters (dc/dt and c) required for analysis can be obtained from the DSC exotherm. The reaction rate is obtained by dividing the peak height dH/dt, at time t by the total heat of reaction, ΔH_o.

$$dc/dt = (dH/dt) / \Delta H_o \qquad \text{(eq. 5.6)}$$

The value of c is determined in a fashion similar to ramp curing, by measuring the partial heat of reaction up to time t, ΔH_{pi}, and dividing by the total heat of reaction (which is usually found by ramp curing), ΔH_o.

$$c = \Delta H_{pi} / \Delta H_o \qquad \text{(eq. 5.7)}$$

At least three isothermal runs at different temperatures are required to obtain kinetic parameters from an Arrhenius plot.

5.4 DMA Analysis

Dynamic Mechanical Analyzer (DMA) tests were performed with a TA Instruments 2980 DMA. The DMA is shown in the photograph in Figure 5.5. The nominal size for resin or composite specimens was 10 mm x 60 mm x 2 mm. The 'dual cantilever' mode was employed in which either end of the rectangular specimen was fixed in place by a clamp while a clamp fixed to a small drive motor was clamped to the centre of the specimen. The specimen was then deformed sinusoidally in a flexural mode with a nominal maximum displacement of 20μm and a frequency of 1 Hz. All DMA experiments were

performed as ramp tests at a 10°C/minute ramp rate. For all DMA experimental work, the guidelines of ASTM standard D4065 were followed.

5.5 Mechanical Testing

Tensile testing was done on a model 8562 Instron test servohydraulic test frame shown in a photograph in Figure 5.6. Tensile testing was performed according to ASTM standards D3039 and D638. Initial samples were tested with two strain gages – one on each side. Following confirmation of equivalent strain on both surfaces of the sample (i.e. no bending), one strain gage was used for subsequent samples. All tensile tests were performed at room temperature. All tensile tests were also performed at a constant rate of extension of 0.01 mm/s. For the tensile specimen described above, this is equivalent to a strain rate of approximately 10^{-4} mm/mm. From tensile tests the ultimate strength, ultimate strain, and modulus were measured.

Figure 5.7: Instron model 8562 at U of M

Chapter 6

Results and Discussion

Experimental results and discussion of these results are presented in this chapter. The analysis of untreated resin and composite samples is presented first, to demonstrate the characteristics of thermal curing of the EB formulation and as a basis for subsequent analysis of EB treated samples. Each material and process parameter of influence is then discussed separately – dose, initiator concentration, temperature, reinforcement, and dose rate. Finally, kinetic analysis and mechanical testing results of both EB and thermally cured samples are presented and discussed.

6.1 Thermal Analysis of Untreated Samples

A number of observations can be made about the resin formulation by thermal analysis of freshly mixed resin that has not undergone any EB irradiation (i.e. *untreated* resin). When EB irradiation is introduced in the next section, the observations made on the untreated resin are used to make comparisons, analyze the data, and to draw conclusions.

The epoxy resin 1E is a *conventional* resin adopted for EB processing, and a brief investigation of its conventional formulation is useful. The recommended mixing schedule for conventional thermal cure is 38 phr of the amine hardener DDS (4,4'-sulfonyldianiline). The 1E resin was mixed with DDS at this concentration and thermally cured in the DSC by ramping the temperature from 22°C to 350°C at a rate of 10°C/min. The DSC scan of this conventional curing reaction is shown in Figure 6.1. As can be seen in the figure, a characteristic exotherm occurs corresponding to the crosslinking reaction, beginning at approximately 130°C and peaking at approximately 220°C. The exotherm ends at approximately 300°C and the increase in heat flow beyond this temperature corresponds to charring and thermal decomposition of the material. Integrating the heat flow exothermic peak, an energy of 418 ± 10 J/g is determined to be the heat of reaction for the thermally cured system.

The EB designed formulation of the photoinitiator OPPI with 1E resin was investigated next. Thermal activation of the photoinitiator OPPI had been reported previously, so it was tested in the DSC cell with no resin present, to observe its thermal characteristics. This DSC scan is shown in Figure 6.2. The endothermic event of melting was observed over the temperature range of 45-60°C. A sharp exothermic peak observed at approximately 210°C indicates a distinct chemical change at that temperature, likely a dissociation reaction. This indicates that the OPPI can be thermally activated, a fact which is critical to further understanding of the remaining results.

OPPI was mixed with 1E resin at 3 phr, a concentration recommended by previous researchers [3,25,53]. This formulation was tested in the DSC to investigate the

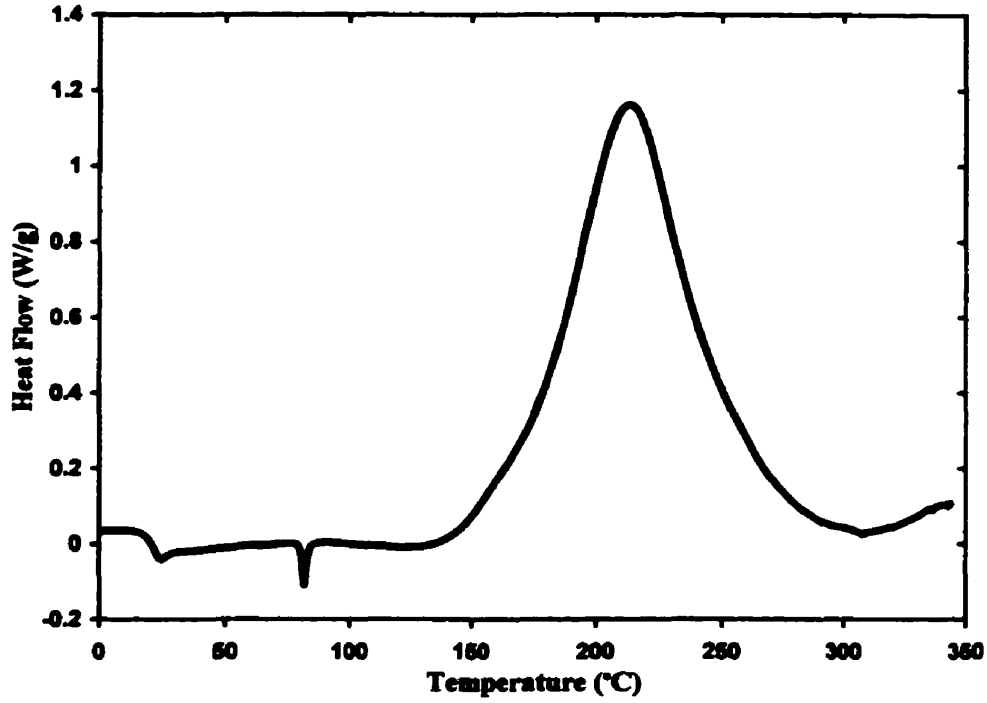

Figure 6.1: DSC curing exotherm of 1E/DDS (conventional formulation)

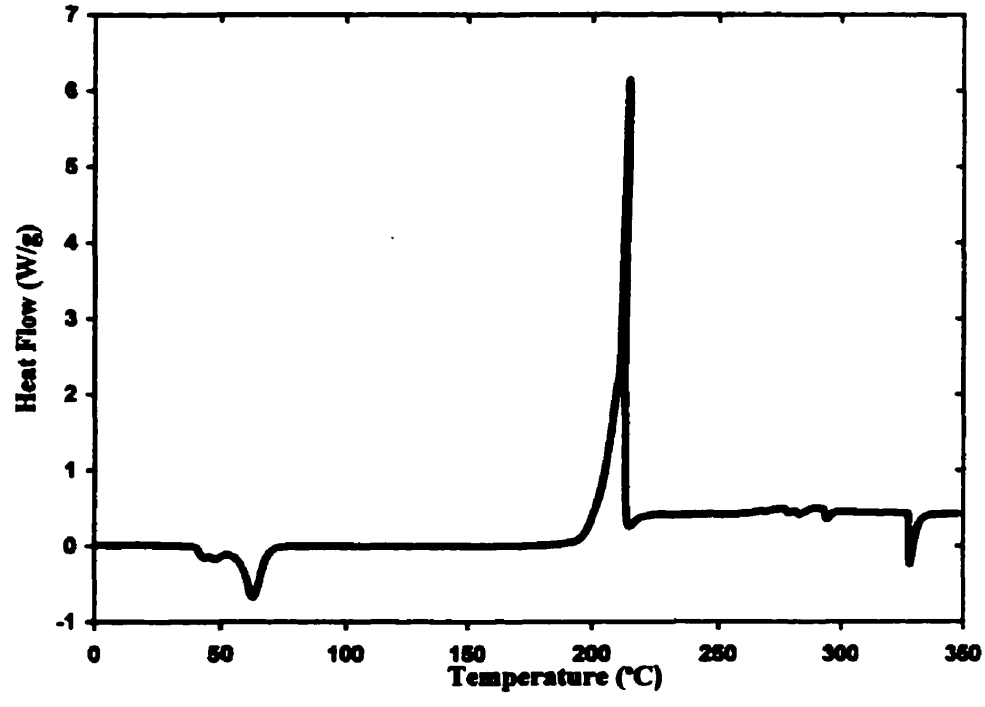

Figure 6.2: DSC scan of photoinitiator OPPI without resin

potential thermal activation and curing of the EB-designed system. The 10°C/min DSC scan shown in Figure 6.3 indicates that the system is thermally curable. A prominent exothermic peak is observed at approximately 180°C followed by a smaller peak at approximately 225°C. Thermal degradation begins at approximately 340°C. The existence of two exothermic peaks indicates that complex curing reactions take place in which at least two distinct mechanisms or reactions contribute to crosslinking. The two prominent temperature peaks (reactions) are given the designations alpha (α) and beta (β) as shown in Figure 6.3. Identification of the chemistry of these reactions would require FTIR (Fourier Transform Infra-Red) spectroscopy, which is outside the scope of this thesis. Figure 6.4 shows an enlarged or exploded view of Figure 6.3 which shows the glass transition temperature of the uncured resin formulation, T_{go} = 19°C. The value for T_g is selected to be the temperature corresponding to the inflection point of the transition, as shown.

Isothermal curing of 1E/OPPI at a temperature of 160°C in the DSC is shown in Figure 6.5. This sample was kept at 160°C for 2 hours and cooled to room temperature. In Figure 6.6, the subsequent temperature scan of the same sample shows that while the alpha peak has disappeared, the beta peak is intact. This is an indication that the temperature of 160°C was not high enough to initiate the beta reaction. Re-examining Figure 6.5, it is evident that there are two exothermic peaks, which implies that two reactions are occurring, apart from the beta reaction. To confirm this, a fresh 3 phr 1E/OPPI sample was ramp cured at a slower ramp rate of 5°C/min. Shown in Figure 6.7, this clearly shows a third, lower temperature peak corresponding to approximately 145°C, that is nearly masked by the alpha peak. This third peak and corresponding reaction are

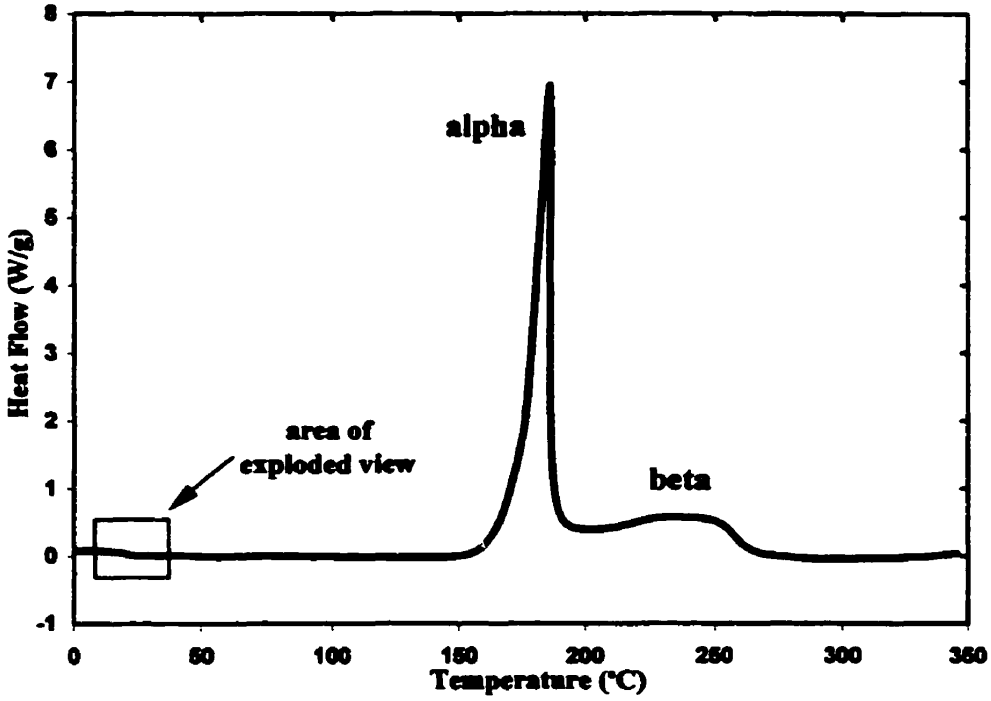

Figure 6.3: DSC ramp curing of 1E resin with 3 phr OPPI

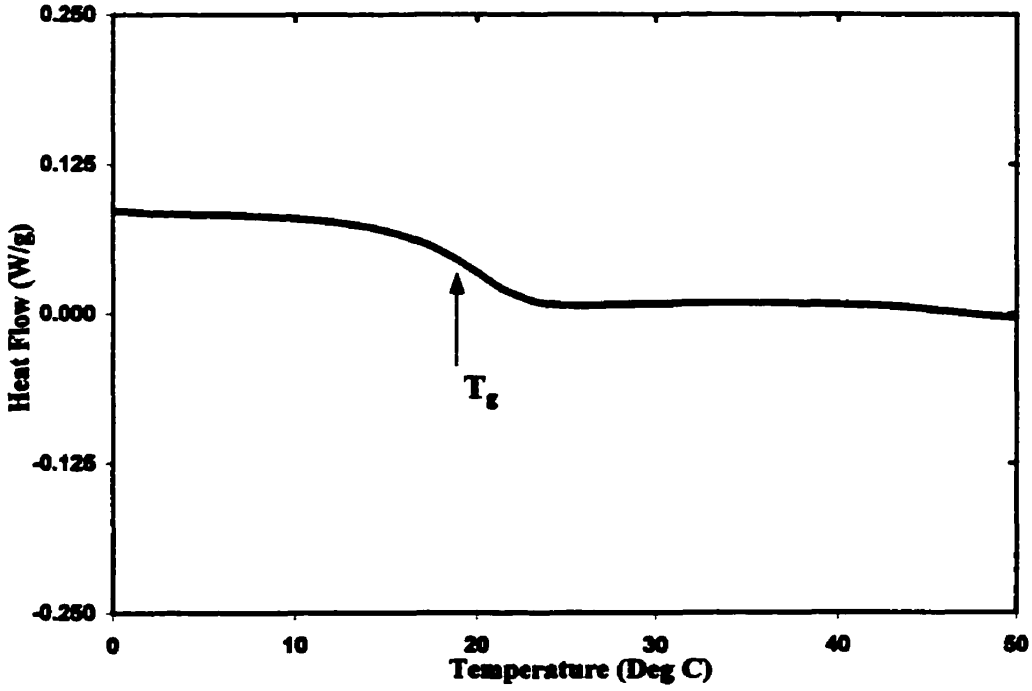

Figure 6.4: Exploded view of Figure 6.3 showing glass transition of uncured 1E/OPPI

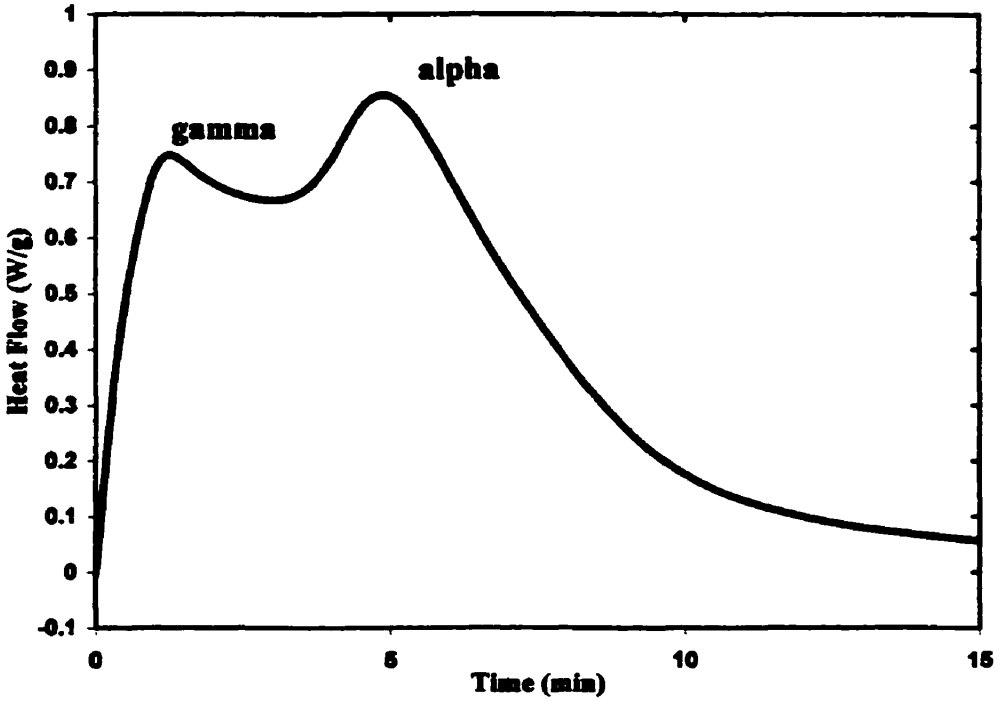

Figure 6.5: DSC isothermal curing of 3 phr 1E/OPPI at 155°C

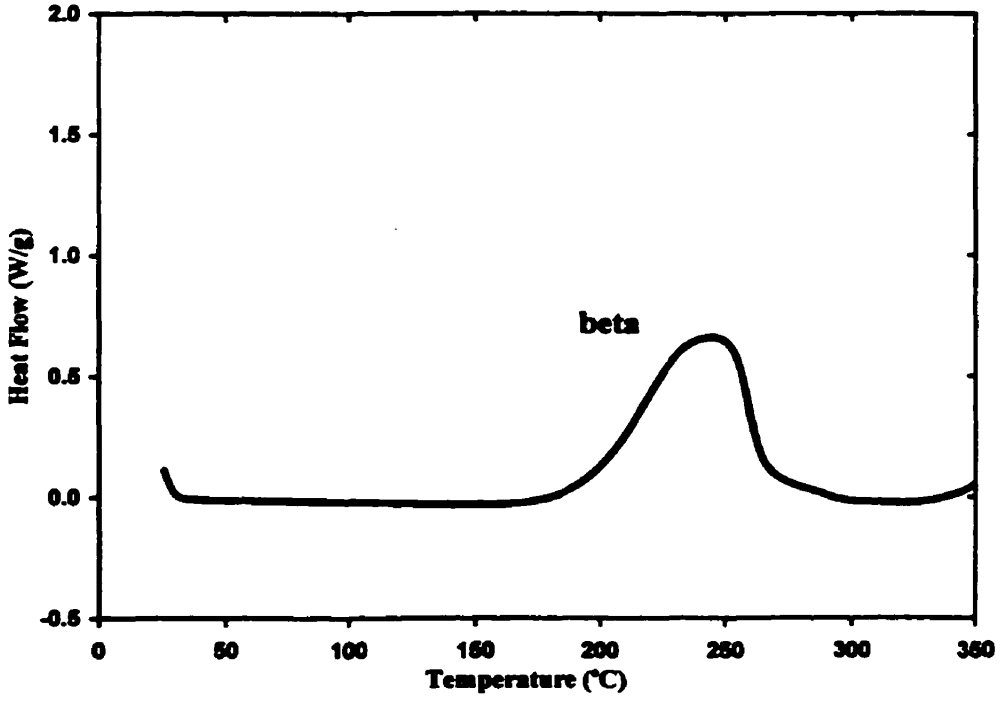

Figure 6.6: Re-ramp DSC scan after isothermal curing at 155°C

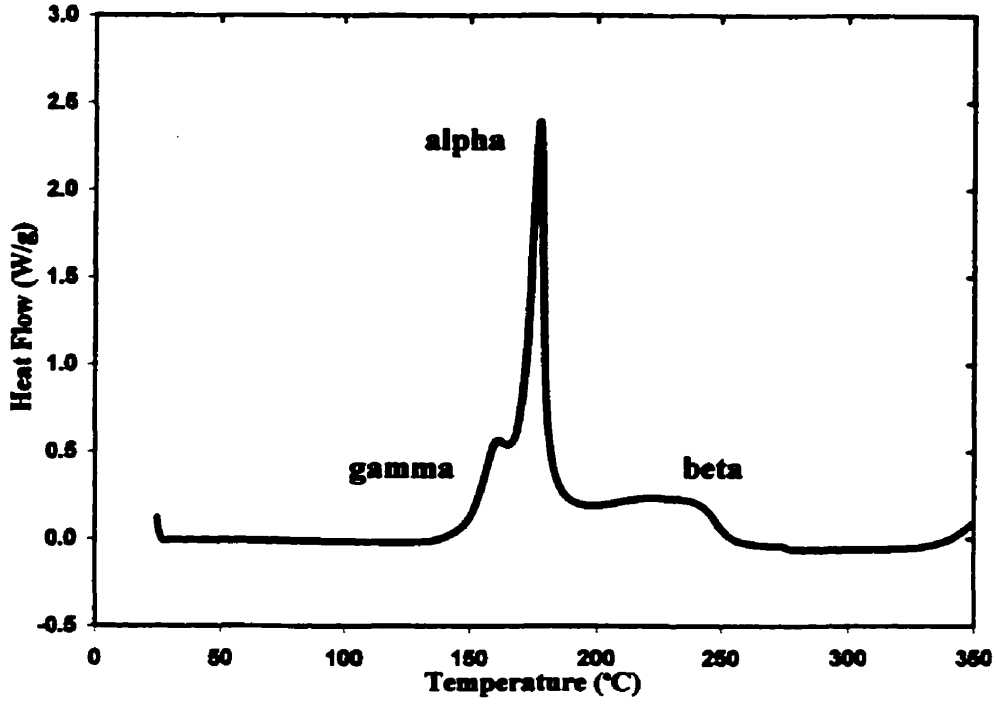

Figure 6.7: DSC ramp curing of 3 phr 1E/OPPI at 5°C/min

given the designation gamma (γ). Integration of the multiple exothermic peaks of 1E/OPPI yields the total amount of energy released during the curing reaction. Fifteen 3 phr resin samples were cured by DSC ramp curing (as in Figure 6.3) and the average **total integrated heat of reaction, H_o, was determined to be 615 ± 10 J/g.** The **glass transition** temperature of the thermally cured 1E/OPPI resin, $T_{g\infty}$, could not be determined by DSC analysis because the transition occurs above the onset of degradation (i.e. $T_{g\infty}$>340°) and is masked by this exothermic event. As an alternative method, thermally cured **resin and composite 1E/OPPI samples were tested by dynamic mechanical analysis (DMA).** A sample 10°C/min DMA scan of a 3 phr 1E/OPPI composite of 58% volume fraction of IM7 graphite fibres is displayed in Figure 6.8. The temperature of the peak in Tan delta or loss modulus is normally taken to be the glass transition, but could not be used in this case due to thermal decomposition in the range where T_g occurs. Hence, the **service temperature, T_s,** defined as the temperature at which the modulus has dropped to 50% of its value at room temperature, was alternatively used. The service temperature of the thermally cured composite was determined to be **T_s = 370°C.** Table 6.1 summarizes the glass transition and heat of reaction comparison between the thermally cured 1E/OPPI and 1E/DDS. Next, the contribution to total exothermic heat of each of the alpha, beta, and gamma reactions during ramp curing was approximated, and the temperature at which they occur for a 10°C/min ramp cure was determined. Table 6.2 shows a summary of this information.

The nature of the progression of glass transition temperature, T_g, with thermal cure extent was investigated next. Resin samples were initially cured isothermally at 177°C for increasing lengths of time, and then cooled to room temperature. The samples

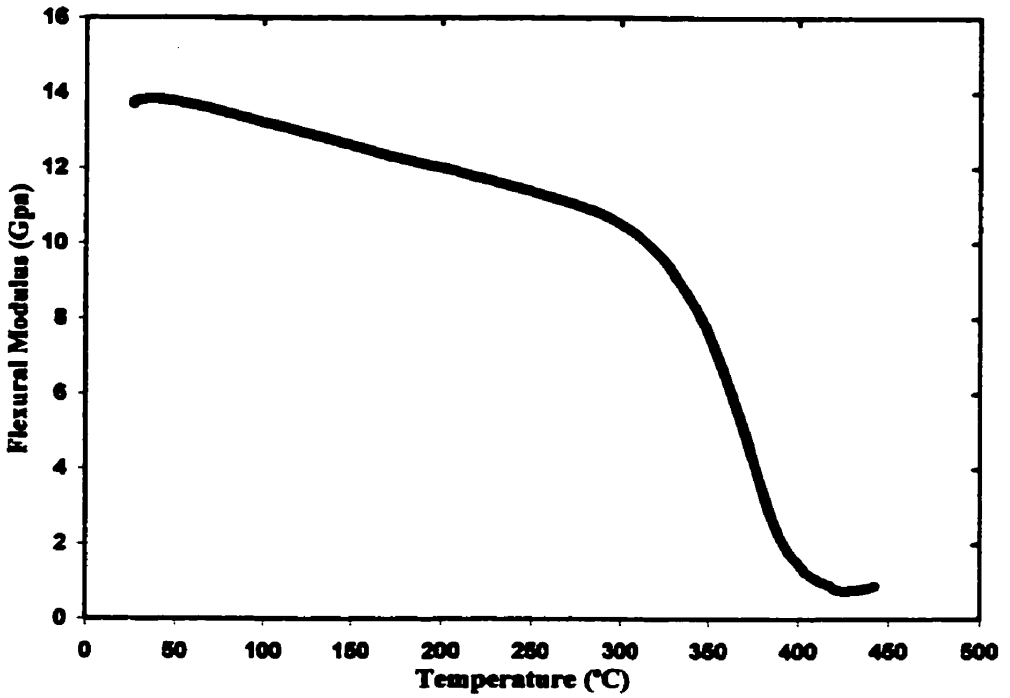

Figure 6.8: DMA scan of cured 1E/OPPI composite showing the glass transition

1E Formulation	Glass Transition Temperature T_g	Exothermic Heat Evolved During DSC Thermal Curing Q_o
3 phr OPPI (EB system)	370°C (DMA Service Temperature)	615 J/g
38 phr DDS (conventional system)	311°C	418 J/g

Table 6.1: Thermal analysis of EB and conventional 1E formulations

Reaction	Peak Temperature (at 10°C/min ramp curing)	Exothermic Heat of Reaction (J/g)
Alpha	177	350
Beta	232	210
Gamma	<177	55

Table 6.2: Analysis of the three reactions observed during DSC curing of 3 phr 1E/OPPI

were subsequently scanned in the DSC to observe T_g and obtain the residual heat of reaction. The known heat of reaction for 100% thermal curing and equation 5.1 were then used to calculate the cure extent. As with all thermally cured resins, as the cure extent increases the glass transition temperature also increases, and there is a one to one correspondence between cure extent and glass transition temperature. The cure extent versus T_g results are displayed in Figure 6.9. During isothermal curing, the T_g increases with increasing cure time at T_{cure}=177°C and eventually surpasses T_{cure}. When this happens, the T_g transition observed by subsequent re-ramp becomes masked by the residual exothermic heat. For this reason, the glass transition at higher temperatures can be more easily observed by DMA analysis. For values of T_g beyond 60% cure extent, data was obtained by DMA analysis of resin and composite samples. The DMA and DSC analysis of resin and composite samples was fitted to a combination of a straight line and exponential curve, as seen in Figure 6.9.

A number of significant observations can be made from the thermal cure analysis of the EB resin formulation 1E/OPPI:

1) The **EB formulation can be cured with thermal energy.** This observation (that the EB formulation can be cured in the same way a conventional formulation is cured) is of fundamental importance to other experimental results. In practice, the thermal curing of epoxies with the use of cationic catalysts is well known, but is much less common than the use of amine hardeners such as DDS, [71].

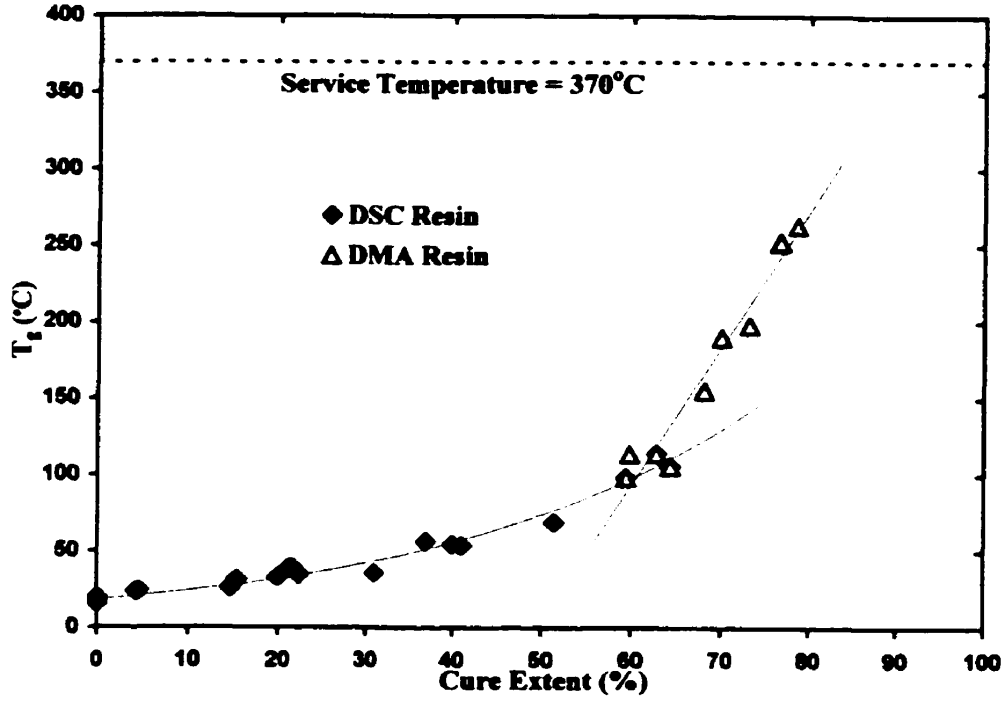

Figure 6.9: The progression of T_g with cure extent for thermally cured 3 phr 1E/OPPI

2) **The complexity of the thermal reaction for 1E/OPPI is significant when compared to the amine formulation of 1E/DDS.** Typically, an increase in temperature causes dissociation of a catalyst, the products of which facilitate ring opening of the epoxy groups. The dominant alpha peak likely corresponds to this reaction, which occurs very quickly once the dissociation of OPPI occurs. No suggestions are made here with regards to identification of the beta and gamma reactions although it can be said that they are likely competing or additional curing reactions, which complicate the analysis of the prominent alpha reaction.

3) Another observation to be made is that the glass transition temperature of the thermally cured cationic EB formulation exceeds the glass transition temperature of the thermally cured amine formulation. This **establishes OPPI as a suitable thermal catalyst** for achieving high T_gs with 1E epoxy under conventional curing. However, no consideration is made here of the comparative cost of the two catalysts.

4) Lastly, **1E/OPPI is more reactive than 1E/DDS.** The concentration of OPPI required is only 3 phr (at this point, this value has been borrowed from previous literature, but is investigated experimentally later), while the mixing regime for DDS is 38 phr. However, the exothermic energy released during curing with OPPI (615 J/g) is nearly 150% of the energy released during curing with DDS (418 J/g).

6.2 Influence of Dose

A critical undertaking during analysis of high energy EB curing is the determination of the effect of EB dose, D, on cure extent of the resin system. A low curing dose, D_{cure}, is desirable, because it can be achieved in a shorter time and with less energy expenditure. Also, the influence of incremental doses at different stages of EB curing must be determined if a predictive model of EB processing is to be developed.

During EB irradiation, the exothermic heat evolved cannot be directly measured, as is the case with thermal curing within the DSC cell. In other words, an EB calorimeter does not exist. However an indirect method of studying EB curing has been developed by the author, which involves examining the residual DSC exotherms following EB irradiation. Analyzing the residual exotherms allows one to infer the cure extent and nature of partial EB curing. This method relies on the 1E/OPPI formulation being thermally curable, which has been established in the previous section.

The 1E/OPPI resin was exposed to EB radiation in small increments, and then postcured in the DSC cell. In Figure 6.10 and 6.11, residual exotherms of EB treated resin are compared with 100% thermal curing ('untreated' resin or 0 kGy dose). All EB treated resin samples in these two figures were EB cured at an ambient temperature of T_a=22°C, and the temperature rise due to the exothermic reaction and radiation heating resulted in a maximum temperature of T_{max}=50°C. Figure 6.10 shows that as EB dose increases from 0 to 25 kGy, the residual alpha peak intensity reduces while the beta peak remains unchanged. From this observation, one can infer that the alpha reaction is effected by EB radiation, and some curing has occurred. This is also a first indication that the alpha reaction is more sensitive to EB radiation than the beta reaction.

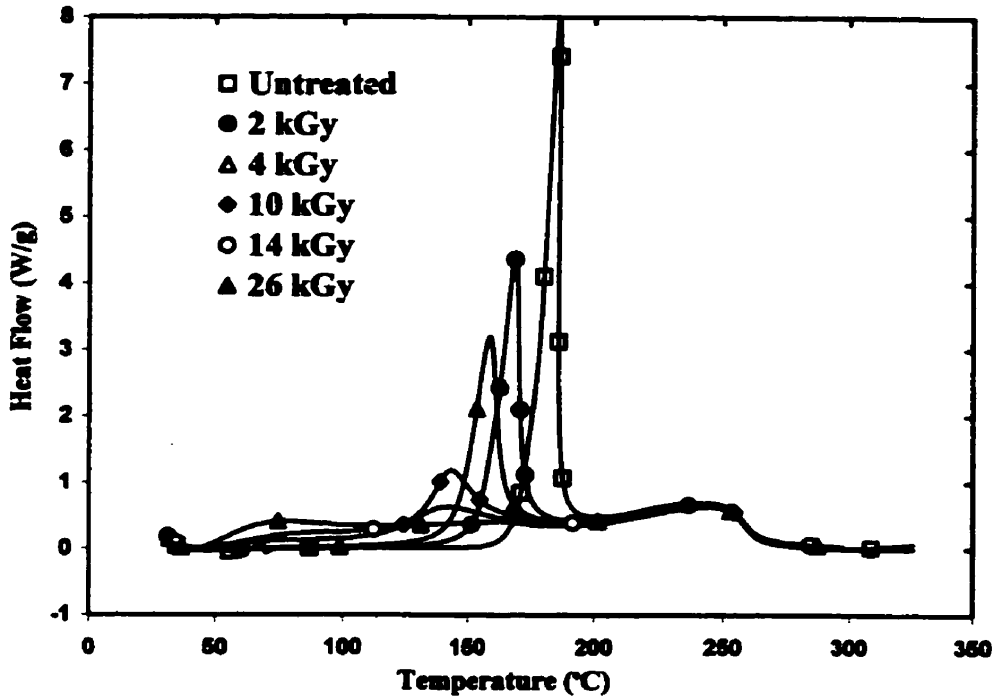

Figure 6.10: The progression of EB cure (residual exotherms) 0-26 kGy

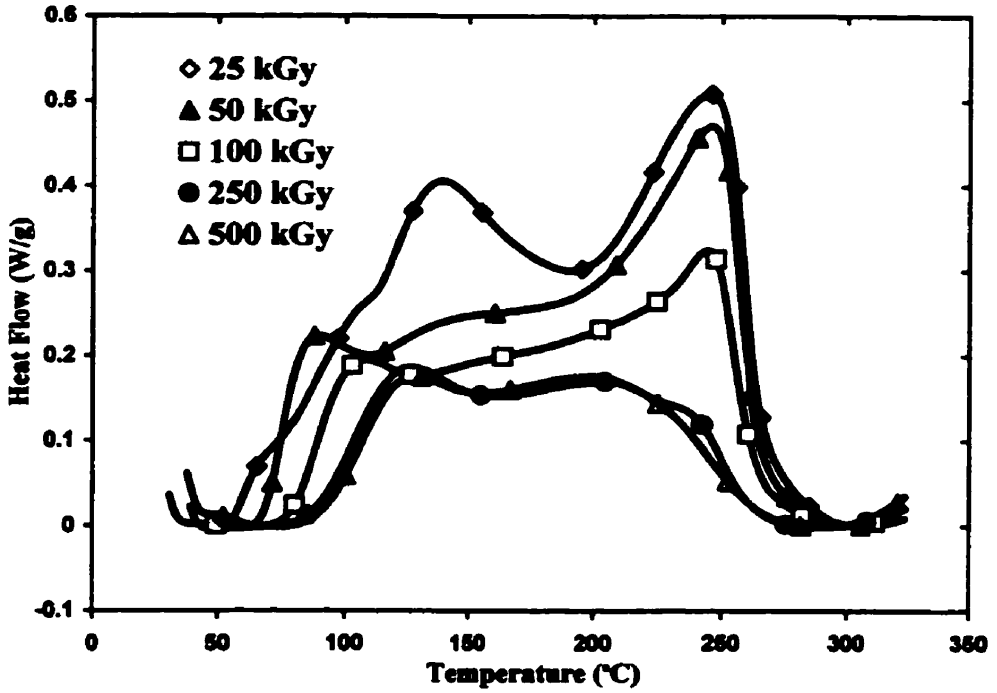

Figure 6.11: The progression of EB cure (residual exotherms) 25-500 kGy

Furthermore, the location of the alpha peak shifts to a lower temperature than it had been for complete thermal curing, indicating that with increasing EB irradiation, less thermal energy is required to initiate the residual thermal alpha reaction. Beyond approximately 10 kGy, the residual alpha peak is no longer prominent compared to the beta peak, and a low temperature peak with **temperature onset less than 50°C** emerges. It is possible that this low temperature peak corresponds with the original gamma reaction that is now at a significantly lower onset temperature than the 150°C observed for the untreated formulation. Between 10 and 25 kGy, it can be observed that a significant amount of low temperature residual curing is present after EB treatment.

From Figure 6.10, it is observed that the EB radiation is particularly effective with respect to the alpha reaction, as indicated by the decreasing alpha peak, but does not effect change in the beta reaction. In Figure 6.11, it can be seen that beyond 25 kGy, the EB radiation progresses the entire reaction, including the beta peak, although the radiation is less effective than it was at lower doses. The most striking result from this analysis is that **at even at 500 kGy, there is a significant amount of undercure**, evident by the existence of residual thermal curing. To quantify the amount of undercuring during EB irradiation of 1E/OPPI, it was assumed that the total heat of reaction for EB curing was the same as that for thermal curing. That is:

$$\Delta H_o \text{ (EB)} = \Delta H_o \text{ (thermal)}$$

With this assumption, the amount of residual cure was determined and subsequently the percentage of curing due to EB irradiation was determined according to equation 5.1. The cure extent with increasing dose is plotted in Figure 6.12. In this figure, the cure extent increases rapidly, to 42% within the first 50 kGy of irradiation. Beyond this dose,

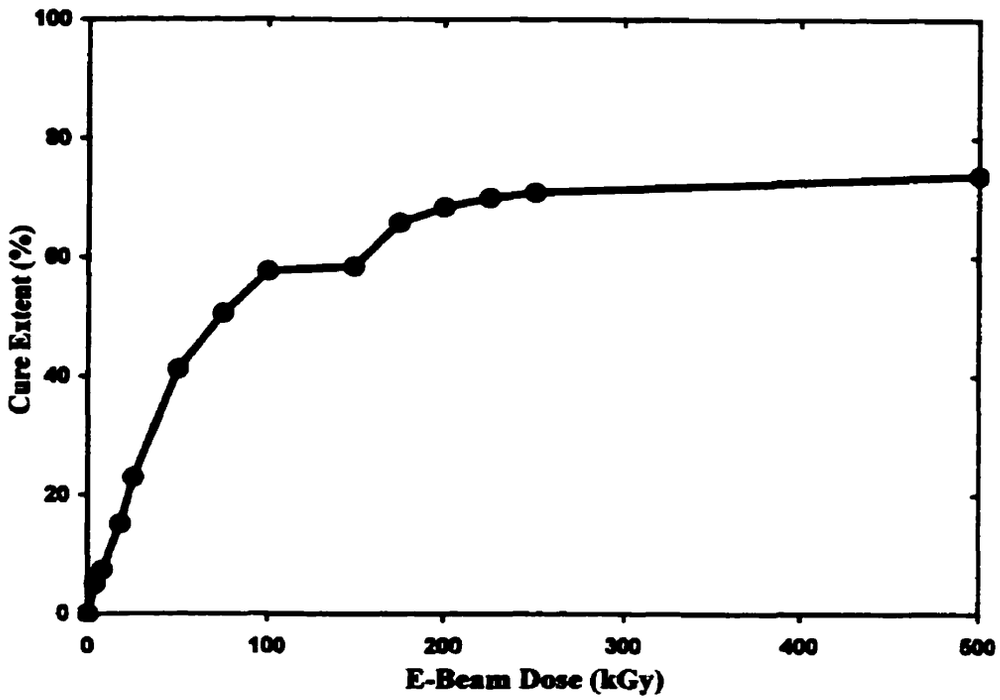

Figure 6.12: Cure extent for increasing EB dose

increase in cure extent is less significant with increasing dose to approximately 100 kGy at which a **plateau in curing** is reached. Small gains in cure extent are made between 150 kGy and 175 kGy, but beyond 175 kGy, cure extent increases are almost insignificant up to 500 kGy. **The maximum cure extent achieved at 500 kGy was 73% (i.e. 27% residual thermal postcure).** This indicates that thermal postcuring is a necessity to complete curing.

Another way of studying the influence of dose is to examine the increasing glass transition temperature with increasing dose. Below 20 kGy EB treatment, the glass transition temperature of resin samples was measured by DSC analysis. Beyond 50 kGy, however, the onset temperature of residual postcuring was less than the glass transition temperature achieved during EB curing. This meant that the glass transition was masked by exothermic heat flow. For samples irradiated beyond 20 kGy, the glass transition temperature was obtained by DMA analysis of composite samples. Composite samples were used because they retain a high modulus until the glass transition making the transition readily observable. Resin samples, on the other hand, exhibit a more subtle DMA glass transition and have a tendency to crack during testing. Although the particular influence of the introduction of reinforcement fibres will be discussed in another section of this chapter, it is useful to examine this data now, for the current discussion. The composite samples were of the identical 3 phr 1E/OPPI resin, with approximately 58 % fibre volume fraction, prepared as described in the previous chapter. One problem with glass transition temperature observation is that as a result of the existence of residual thermal postcuring, the resin formulation actually cures during DMA testing. An example of this is shown in Figure 6.13. This sample was irradiated

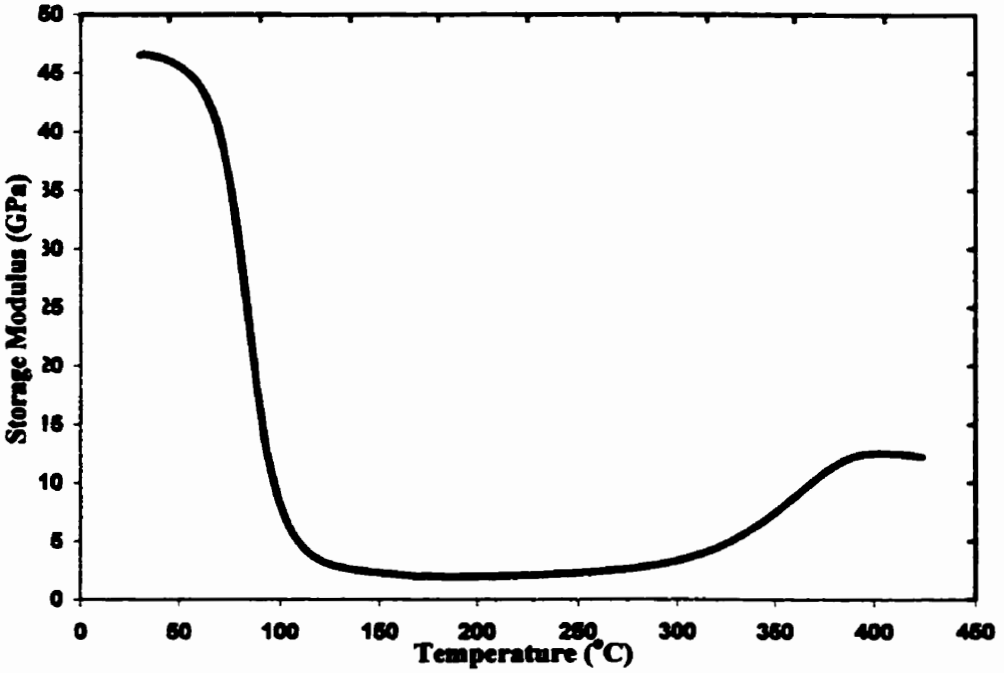

Figure 6.13: DMA scan of undercured EB treated composite sample (50 kGy)

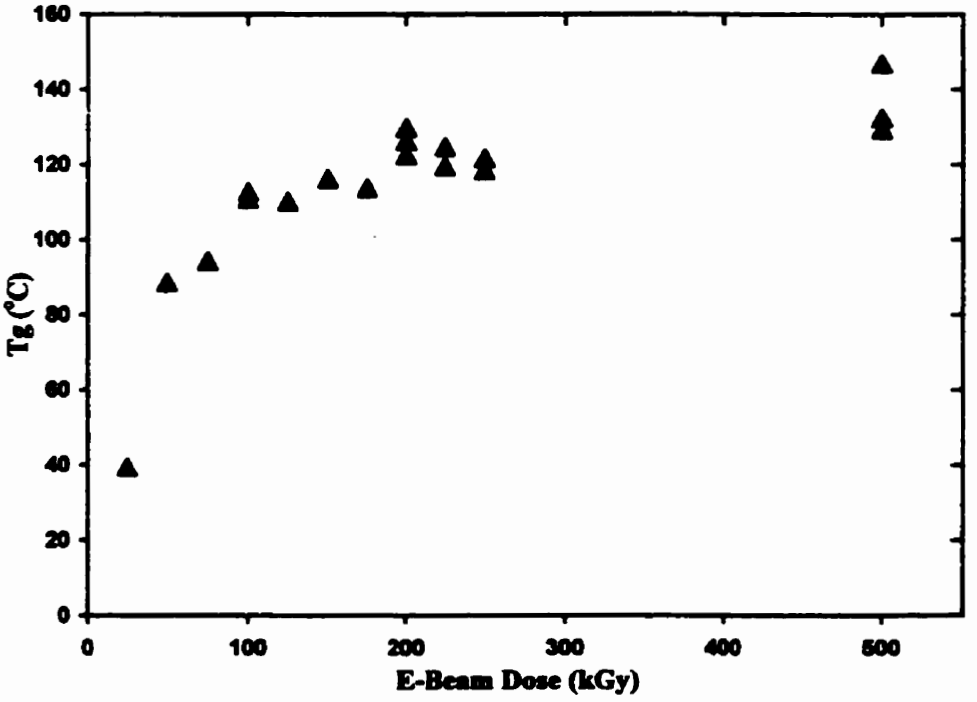

Figure 6.14: Influence of dose on (B) glass transition temperature

to 50 kGy and then tested on DMA. The result is two transitions, A and B. The A transition is seen at 370°C, as it was for the fully cured resin. The B transition is seen at a lower temperature due to the incomplete curing of the resin. Examining this B glass transition, the DMA T_g is plotted as a function of dose as shown in Figure 6.14. The T_g(B) shows significant increases with increasing dose until 100 kGy, at which time it increases marginally with increasing dose until it reaches a plateau at approximately 150-200 kGy. The plateau value for T_g(B) is approximately 125°C. Subsequent DMA analysis after the initial postcure results in a single T_g = 370°C as observed during the A transition and no observation of any minor (B) transitions.

In terms of optimizing the time and cost of the EB process, a low curing dose, D_{cure} is desired. For example, doses below 50 kGy can quickly be imparted in one pass under the EB horn. In practical terms, curing doses over approximately 200 kGy are time consuming, and are to be avoided. For this reason it is important to determine the particular influence of EB dose at various stages of EB irradiation. From the previous experimental investigation, it can be observed that **there are three distinct ranges during EB curing.** These correspond to stages of varying influence of radiation dose. The first range may be referred to as the **excitation and activation**, from 0 kGy up to approximately 50 kGy. It is characterized by approximately linear increases in cure extent and T_g with increasing dose (as seen in Figure 6.12 and 6.15). The second range may be referred to as the **transition region**, from 50-100 kGy. It is characterized by limited gains in cure extent and T_g with increasing dose. The third range may be called the **diffusion region**, above doses of 100 kGy. It is characterized by only very slight

increases in cure extent and T_g with increasing dose. A number of characteristics can be attribututed to each of these regions as follows:

1) **The excitation and activation region. EB energy applied to the formulation at low doses (0 kGy to approximately 50 kGy) goes into exciting or imparting energy to the initiator.** Some initiator is excited to a high enough energy that it dissociates (i.e. is activated). It is likely that **activated initiator in this dose range causes crosslinking** reactions to occur immediately. Evidence of these crosslinking reactions are large gains made in cure extent observed by thermal analysis following EB treatment. **Initiator which has been excited** during EB processing **subsequently requires less thermal energy** to be activated and cause crosslinking reactions. This is evident from the shift in the alpha peak to a lower temperature upon thermal analysis as shown in Figures 6.10 and 6.11.

2) **The transition region.** At approximately 50 kGy, **a lot of the initiator has been excited to activation** by the EB energy, evident by the decrease in dominance of the residual alpha reaction. Some of the activated initiator has produced crosslinking (approximately 40% cure extent), but there is obviously a significant amount of curing that has not occurred. At 50 kGy, T_g has increased to 80°C, and since the polymer is at or near the ambient temperature of T_a=22°C, it is well below the glass transition and in a glassy state. It is probable that **many of the reactive ions from the activated, dissociated initiator are *trapped* in the glassy polymer,** with limited mobility. With most of the initiator dissociated, the

exothermic heat produced in thermal postcuring of a D>50 kGy resin sample is likely due to **increased diffusion** of the reactive ions with temperature rise. The crosslinking reactions do not occur until the reactive ions diffuse to the vicinity of an uncrosslinked epoxy group. Increases in cure extent and T_g for EB doses from 50 kGy to 100 kGy may be due to some additional activation-and-immediate-crosslinking of the initiator; but are likely due to increased thermal energy of the bulk polymer due to additional radiant and exothermic heat produced during EB processing.

3) **The diffusion region**. Beyond 100 kGy, increases in cure extent are limited. It is proposed that the activated initiator is largely trapped in the glassy state of the polymer. Increases made in cure extent in the transition region have increased the T_g (and crosslink density) and put the polymer further into the glassy state. There are small increases in cure extent in this region, which one can contribute to increased time at slightly elevated temperatures due to radiant heating and exothermic heat.

Based on the observations made to this point, it cannot be determined with certainty how much of the residual exotherm at any dose is contributed by diffusion and how much is contributed by thermal excitation and reaction. An effort was made to delineate these two contributions by analysis of the residual reaction kinetics at various dose levels. If the thermal reaction kinetics could be modelled following EB treatment, it follows that they could be predicted and delineated from diffusion related crosslinking.

The kinetic analysis is described in more detail in section 6.7. Unfortunately, due to the complexity of the curing reactions occurring for this specific formulation, and to difficulties in performing residual isothermal kinetic analysis at higher doses, this work could not be completed. It is evident, however, that kinetic analysis may be a useful tool in determining the contribution of diffusion to residual curing and hence to EB cure extent limitations.

It should be noted that the residual beta reaction started to occur in the transition region. This as observed by the decrease in the height of the beta peak (starting at approximately 50 kGy) in Figure 6.11. For 1E/OPPI, the beta peak contributes to the amount of postcure required because it is only weakly dependent of EB dose. This secondary beta reaction continues to progress slowly in the diffusion region, and contributes to small gains made in cure extent in that region.

It is a useful exercise to temporarily consider the primary alpha reaction by itself. The plateau in cure extent observed between 100 and 150 kGy in figure 6.12, and the limited change in residual exotherms as observed in Figure 6.11 indicate that a ceiling has been reached in the amount of EB curing for the alpha reaction. Hence the effective curing dose is defined for maximum achievable crosslinking for the alpha reaction:

$$\mathbf{D_{cure}\ (1E/OPPI,\ alpha\ reaction) = 100\ kGy.}$$

Considering all crosslinking reactions, observable gains in cure extent are made between 100 and 200 kGy, but gains between 200 and 500 kGy are negligible. Hence it can be stated that the practical curing dose for the entire formulation is:

$$\mathbf{D_{cure}\ (1E/OPPI,\ all\ reactions) = 200\ kGy.}$$

These determined values of D_{cure} clearly do not correspond to complete curing, but to the maximum cure extent possible under EB. It is evident that increases in EB dose beyond 200 kGy are not helpful and do not reduce the need for thermal postcuring. The evidence of the first (alpha) plateau indicates that optimization of the EB formulation to eliminate weakly EB dependent reactions (beta) may lead to a lower D_{cure}, and hence more economical processing.

It should also be noted that the glass transition temperature increased significantly beyond ambient curing temperature to a difference of approximately 100°C (125°C compared to 22°C). This confirms the unique character of EB curing as reported by previous authors. However, the T_g of the thermally cured system was much greater still, observed at 370°C. Postcuring (completing the cure extent from 73% to 100%) the EB treated resin brought the T_g up to this value of 370°C as well. This evidence suggests that although T_g may exceed T_{cure} by significant amounts compared to thermal curing, there may still be a ceiling for the maximum T_g achievable by EB curing due to diffusion limitations.

6.3 Influence of Initiator Concentration

The material parameter of initiator concentration, [I], is now considered. Determining the lowest initiator concentration possible for acceptable performance is important to minimize material costs. This is especially applicable to EB formulations because of the high cost of photoinitiators such as OPPI. Balancing this concern, it is also desired to find the initiator concentration which leads to the maximum cure extent and hence the

ultimate physical and rheological properties. Lopata, et. al [53], determined the optimum initiator concentration by gamma cell analysis to be approximately $[I]_{opt}$=3 phr for most EB resin formulations. Because of this determination, this has been the nominal initiator concentration used in this study and in many other studies. Confirmation of this gamma cell determination by an independent method of optimizing initiator concentration is a desired objective.

The 1E/OPPI formulation was analyzed for its thermal curing characteristics under varying initiator concentrations. Resin samples were ramp cured in the DSC and the resulting exotherms were analyzed. Exotherms for concentrations of 1,3,5, and 10 phr are overlayed in Figure 6.15. In this figure it can be seen that the height of the alpha peak increases with increasing initiator concentration, and the alpha peaks overlay at approximately the same temperature (there is only a marginal decrease in peak temperature with increasing [I]). The beta peak height also increases with increasing initiator concentration, but moves to a lower temperature. This is an indication that the cure kinetics of the beta reaction are more strongly influenced by initiator concentration than the alpha reaction. In Figure 6.16, the integrated heat of reaction for the exotherms of Figure 6.15 are plotted. The total heat of the reaction increased with photoinitiator concentration until it reached a plateau value at approximately 5 phr. The exothermic heat corresponding to each of the major alpha peak (alpha and gamma reactions were grouped together for this analysis since they couldn't be separated) and the beta peak was determined by fitting a gaussian curve to each of the peaks. The heat evolved due to both reactions also increased with increasing initiator concentration until a plateau was reached at 5 phr. However, the fraction of the total heat of reaction attributed to the alpha

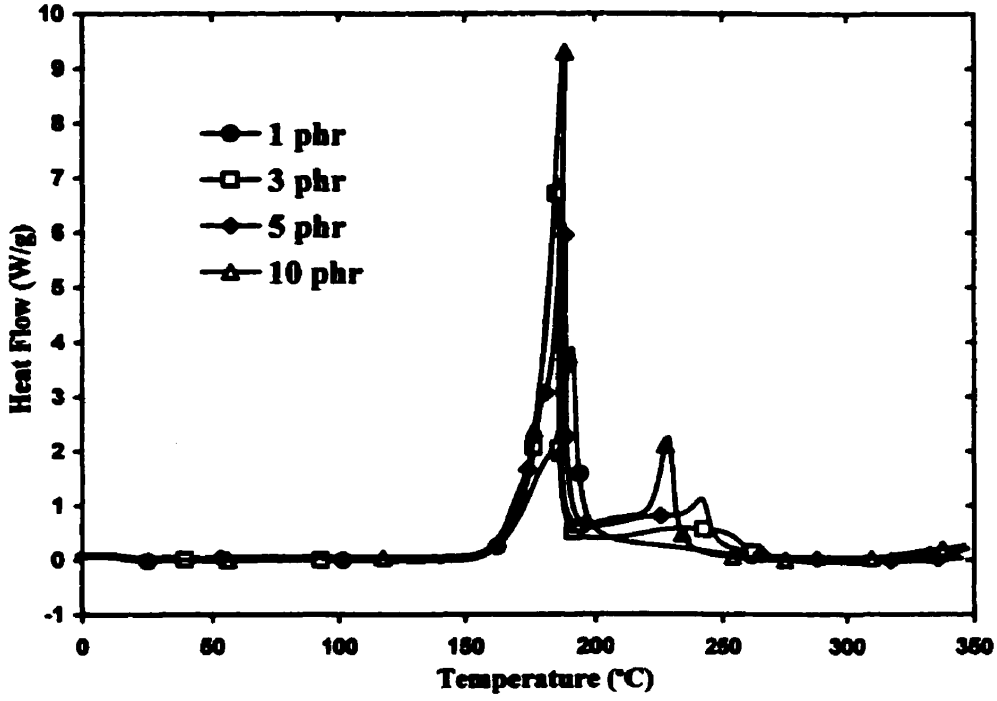

Figure 6.15: DSC exotherms for resin with varying OPPI concentration

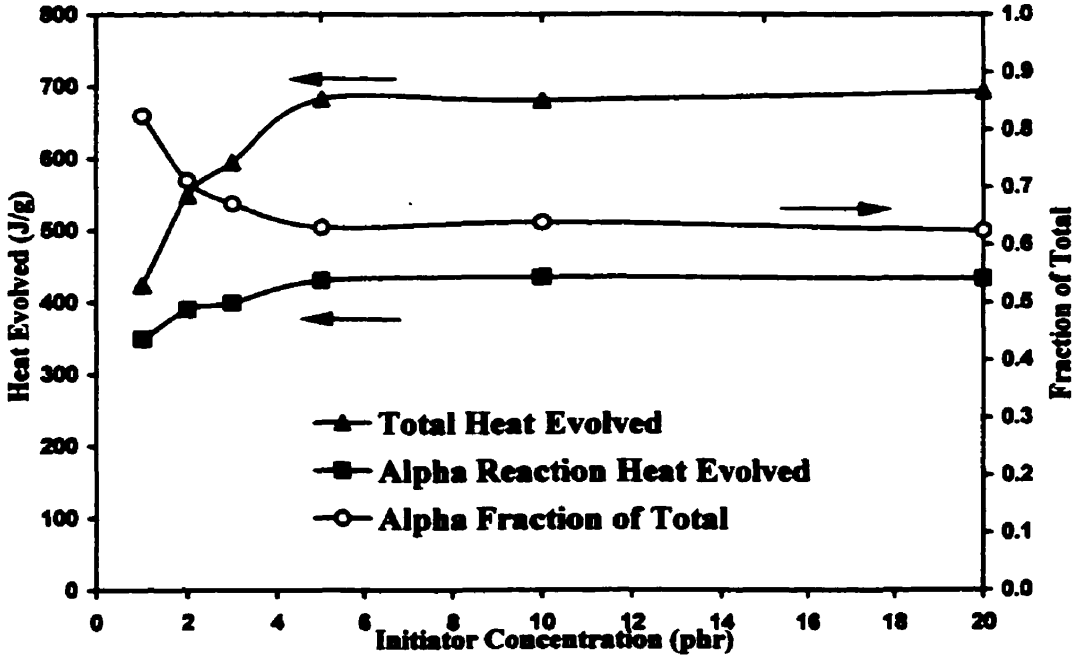

Figure 6.16: Influence of initiator concentration on heat evolved for thermal curing

(including gamma) reaction decreased from 82 % at 1 phr to only 62 % at 5 phr. This confirms that the beta reaction is more sensitive to initiator concentration. Increases in the total exothermic heat evolved during the curing reaction generally leads to gains in properties such as modulus and strength. Since the minimum initiator concentration for the highest total heat of reaction observed was the onset of the plateau the **optimum initiator concentration for thermal curing of the formulation** was determined to be:

$$[I]_{opt.}\text{ (thermal)} = 5\text{ phr.}$$

To investigate the influence of initiator concentration on **radiation curing**, the gamma cell method used by the CRADA on EB curing (described in previous chapters) was used. The gamma cell temperature-versus-dose data was acquired for various 1E/OPPI initiator concentrations. This data is plotted in Figure 6.17. The surprising result of this analysis was that instead of showing a minimum dose for peak temperature rise as observed by Singh [23] and Lopata [53], the dose for peak temperature continued to decrease for increasing initiator concentration. The data of Figure 6.17 was analyzed to determine the dose at peak temperature for each initiator concentration. This information is displayed in Figure 6.18. From this plot, it appears as though increases in initiator concentration up to approximately 3 phr show a significant reduction in the location of the dose for peak temperature. There is an additional reduction in dose when the initiator concentration is increased to 5 phr. Beyond 5 phr, the reduction in dose for peak temperature with increasing initiator concentration is very slight. For this reason, **the limiting value of initiator concentration for effective gamma cell curing** is determined to be $[I]_{opt.}$ **(gamma) = 5 phr**. This confirms the optimum concentration determined for thermal curing. In this way, the gamma cell data has been utilized even

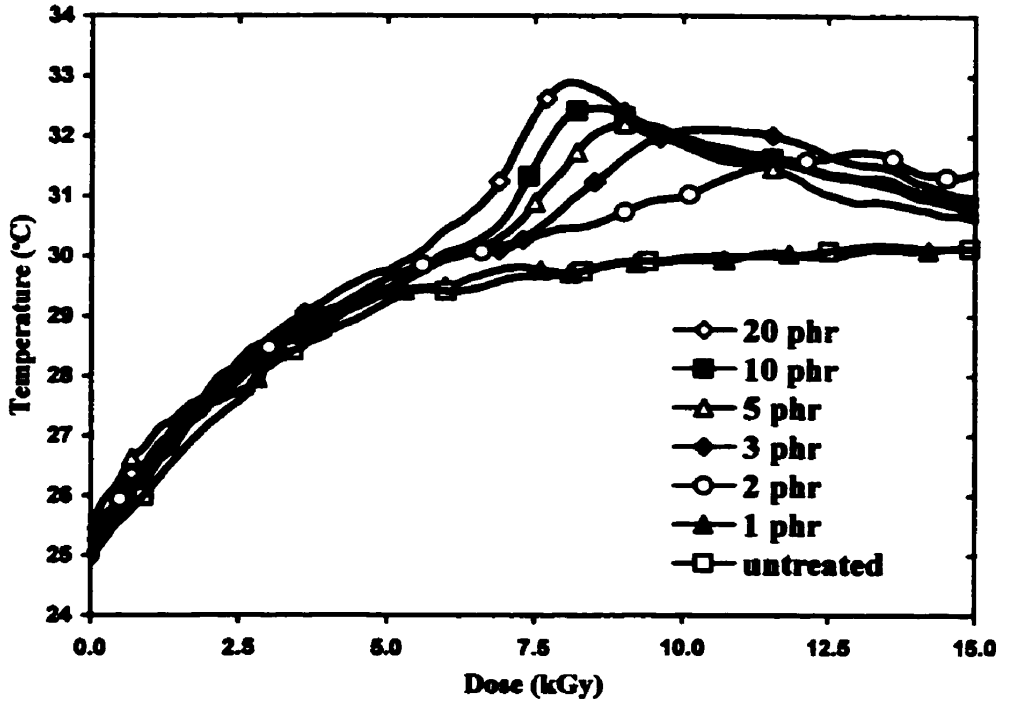

Figure 6.17: Gamma cell temperature data for varying initiator concentration

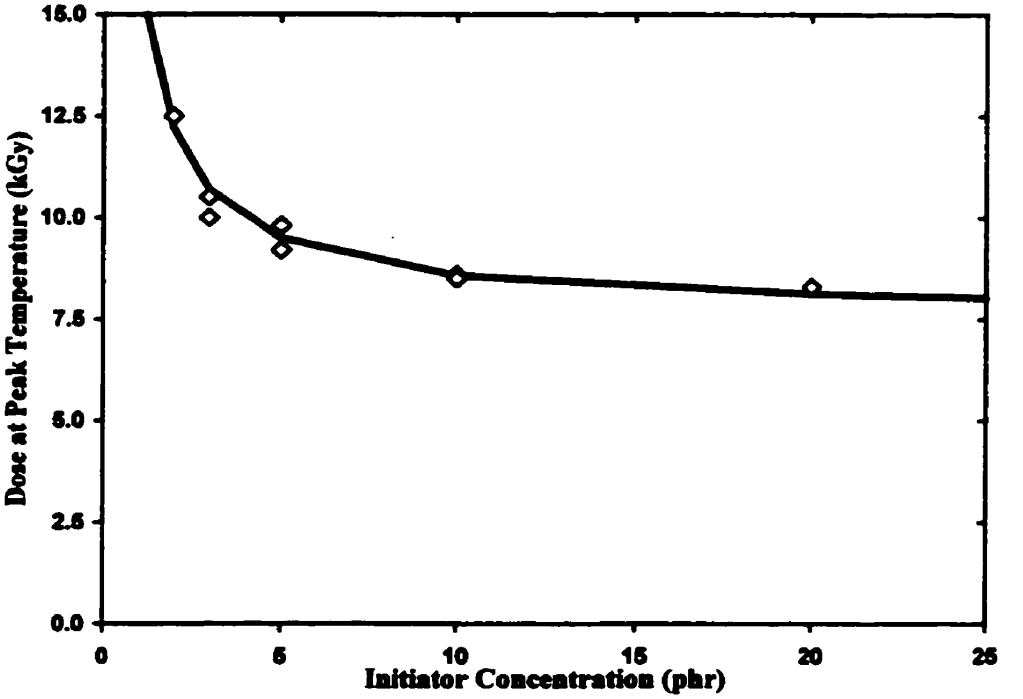

Figure 6.18: Influence of OPPI concentration on Gamma cell dose for peak temperature

though the CRADA method of the selection of an optimum initiator concentration for minimum curing dose could not be applied to this resin system.

A further investigation of initiator concentration was conducted by progressively curing resin samples of 1, 3 and 5 phr by **EB irradiation**. Samples were subsequently ramp cured in the DSC to measure residual exotherms. The results for EB doses of 25, 50 and 250 kGy are shown in Figures 6.19 to 6.21. From these figures, the character of the residual exotherms can be compared. It should be noted that the processing of each sample occurred at the same ambient temperature (T_{amb}=0°C) and had approximately equal maximum temperature (T_{max}=40°C). Following EB irradiation to 25 kGy (Figure 6.19), the 1 phr sample still has a prominent alpha peak, while the alpha peak for the 3 and 5 phr samples has lost is prominence. This is an indication that **as the concentration of initiator increases, the EB radiation is more effective in activating the initiator**. It is also noted that the beta peak is highly dependent on initiator concentration, and is much more prominent for higher concentrations. In Figure 6.21, by 250 kGy, the beta peak has just begun to disappear, implying that the EB radiation has only a weak influence on the beta reaction.

In Figures 6.22 and 6.23, the exotherms from Figures 6.19 to 6.21, along with the exotherms for intermediate dose values have been integrated and replotted. In Figure 6.22, the cure extent is plotted for increasing dose, for each concentration. In the following figure, Figure 6.23, the cumulative absolute amount of curing during EB processing (determined indirectly by subtraction of the residual heat from the known total heat of reaction) is plotted for increasing EB dose. The 5 phr resin reaches a higher cure extent (68%), and the reaction proceeds further (450 J/g) under the influence of EB than

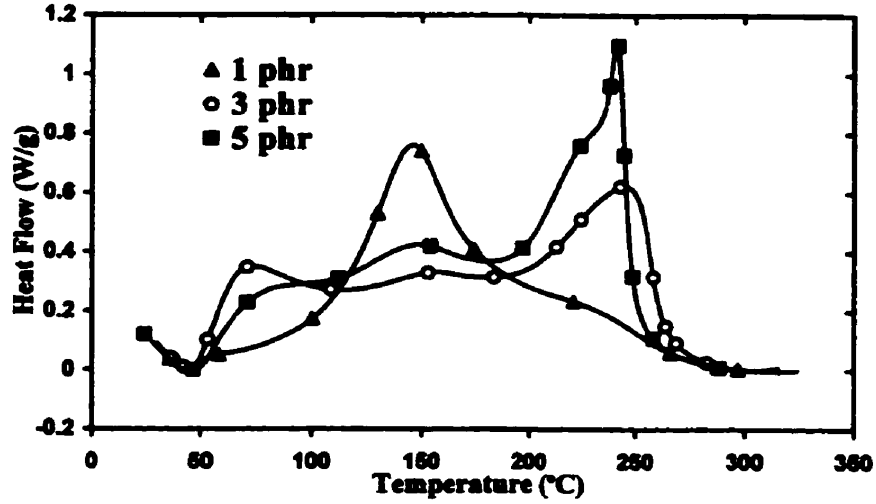

Figure 6.19: Residual exotherms for varying initiator concentration 25 kGy

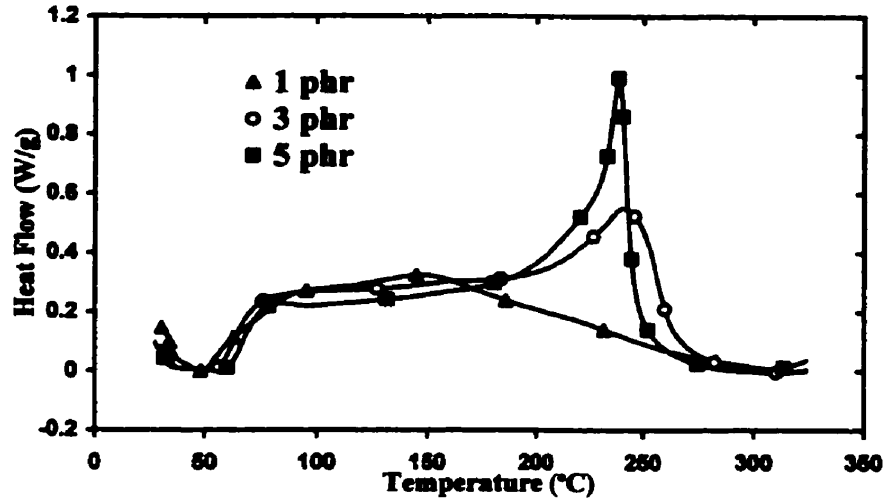

Figure 6.20: Residual exotherms for varying initiator concentration 50 kGy

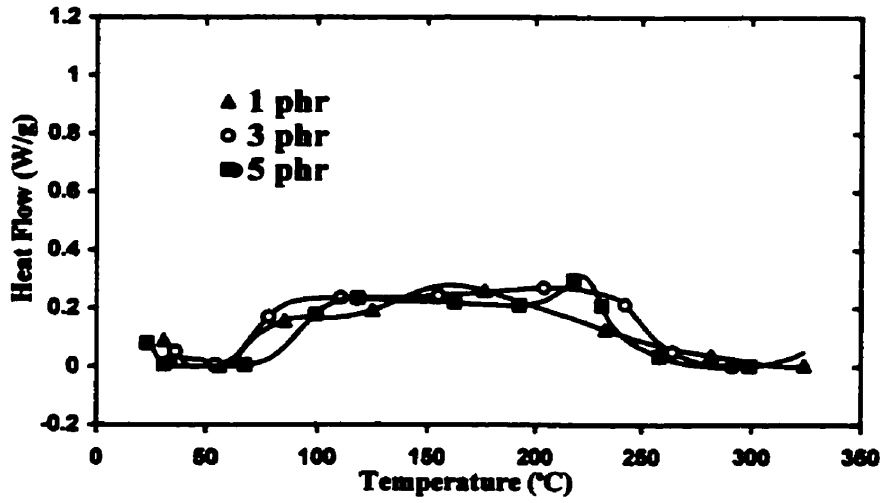

Figure 6.21: Residual exotherms for varying initiator concentration 500 kGy

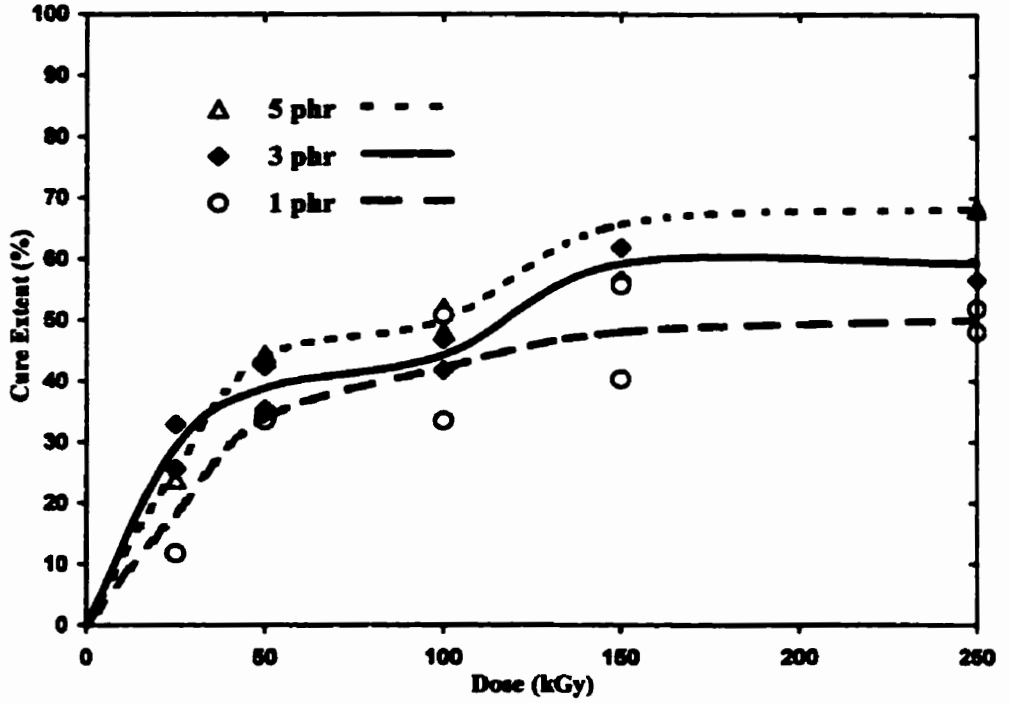

Figure 6.22: Influence of initiator concentration on EB cure extent

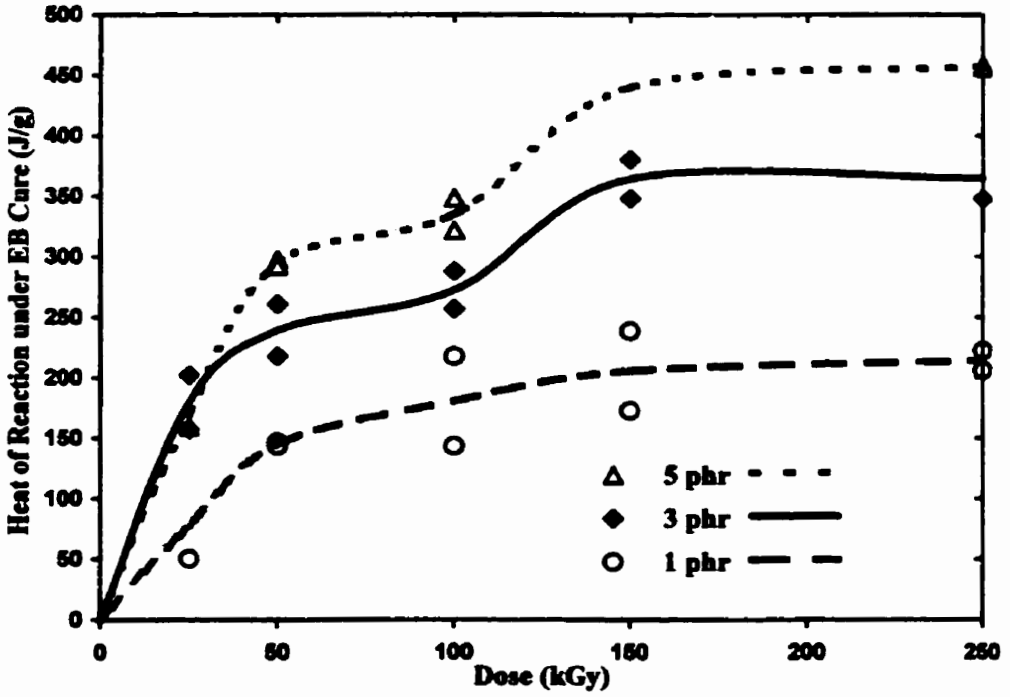

Figure 6.23: Influence of initiator concentration on EB heat of reaction

either the 1 or 3 phr samples. For this reason, and based on the evidence from thermal and gamma analysis, **the optimum initiator concentration for EB curing of 1E/OPPI is suggested to be:**

$$[I]_{opt.}\ (EB) = 5\ phr.$$

It may also be observed in Figures 6.22 and 6.23 that there is an initial plateau in the amount of curing for all initiator concentrations after approximately 50 kGy, and then a second plateau after approximately 150 kGy. These two plateaus in cure extent were repeatedly observed for all experimental work and are likely due to, as previously suggested, diffusional limitations and the difference in reactivity between the alpha and beta reaction. The first (lower temperature) plateau is due to the completion or waning contribution of the alpha reaction to the progression of cure extent. The increase in cure extent beyond this plateau is due to the growing influence of the beta reaction to cure extent, and when this reaction becomes restricted by diffusion the second plateau is reached.

6.4 Influence of Temperature

The influence of temperature on the EB curing process has not been purposefully examined in previous EB studies. A number of authors have suggested that temperature plays an important role, but no data has been published. The fact that the EB formulation studied can be thermally cured is an indication that a significant temperature rise due to exothermic heat of reaction and/or radiation heating may lead to simultaneous thermal

curing. More importantly, any diffusion related phenomena caused by EB irradiation in the glassy state would be influenced by a temperature increase. Re-examining Figure 6.10 and 6.11 it can be observed that the onset temperature (first sign of exothermic heat produced) of residual thermal curing decreases with increasing EB dose. The onset of residual curing drops from 130°C for the untreated resin to 45°C for a sample irradiated to 25 kGy. This is evidence that even low temperature rises approaching 45°C would significantly add to cure extent via thermal means.

On-line temperature measurements were made during all irradiation to observe and establish typical values for temperature rises during EB processing. Sample results from three EB curing runs are shown in Figures 6.24, 6.25, and 6.26. Figure 6.24 shows a (typical) curing cycle for a 3 mm thick composite sample with a volume fraction of fibres of 0.58. The sample was approximately 30 cm by 30 cm in area, and was cured on an Aluminium plate of approximately 3 mm in thickness. Each curing pass, labelled on the figure corresponds to one 25 kGy pass under the EB horn. After the significant exothermic temperature rise during pass #2, the sample was allowed to cool away from the influence of the beam, before the next curing pass. Passes #3 to #8 are done in succession with no cooling time. The temperature rise during these passes is due to the radiation heating of interaction of the beam with the composite and the caul plate, as much as due to chemical reaction of curing. From the figure, it can be seen that T_{max} = 70°C. It is noted here for completeness that the radiation heating may be predicted by using the imparted dose and the thermodynamic relationship:

$$D\ (J/kg) = C_p\ (J/kg \cdot K) \cdot \Delta T\ (K)$$

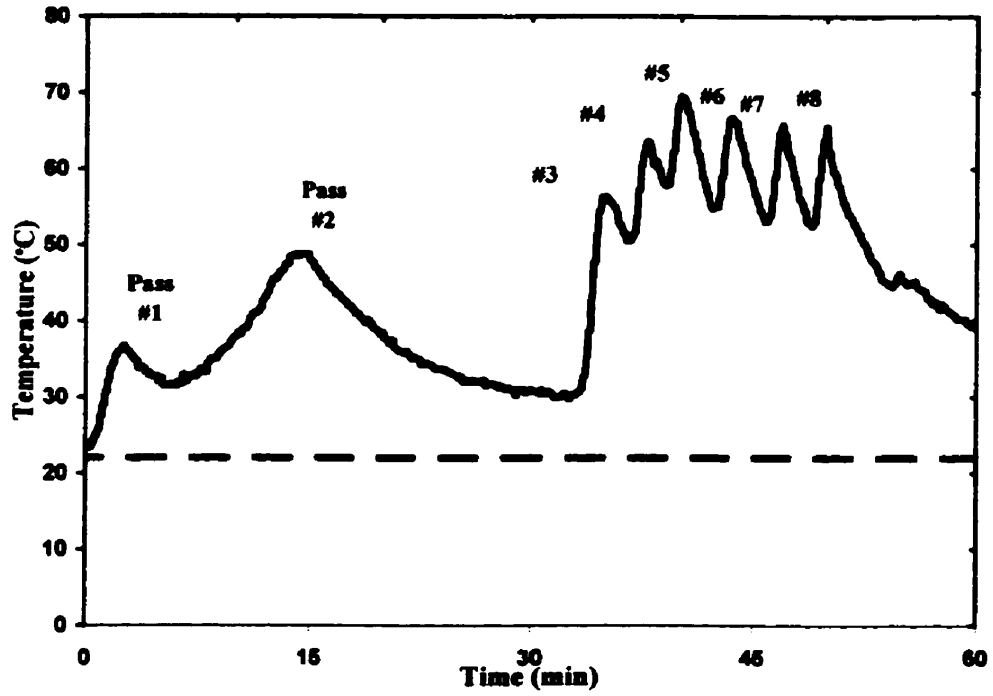

Figure 6.24: Temperature rise for 25 kGy/pass EB curing of composite (Composite: 3mm thick, Vf=55%; Aluminum caul plate 3 mm thick, T_a=22°C)

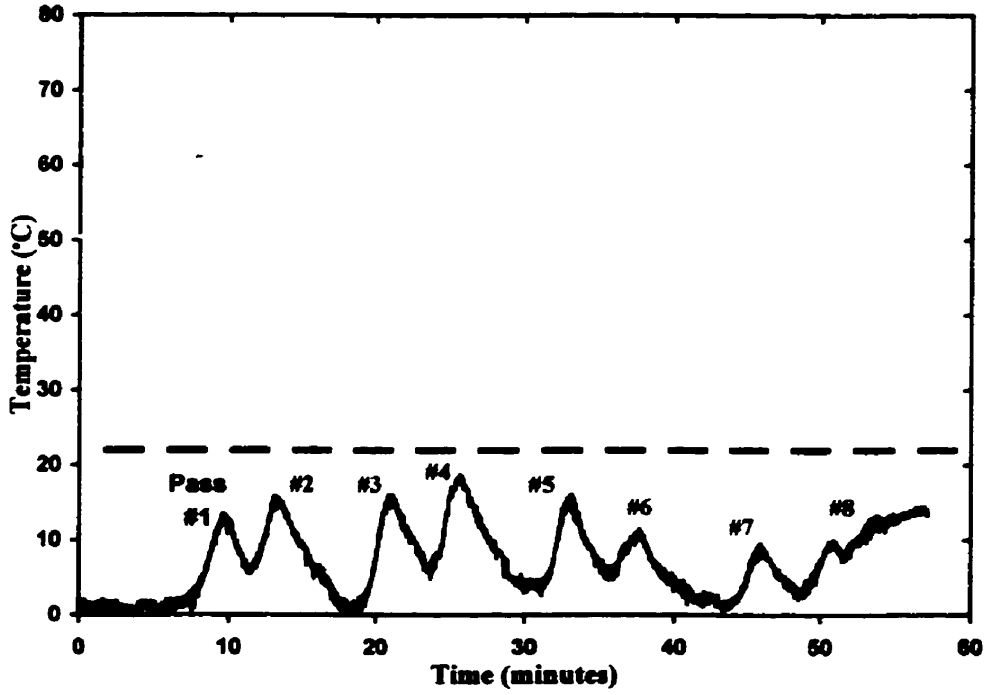

Figure 6.25: Temperature rise for 25 kGy/pass EB curing of small resin sample (approximately 1 g resin sample, T_a=0°C)

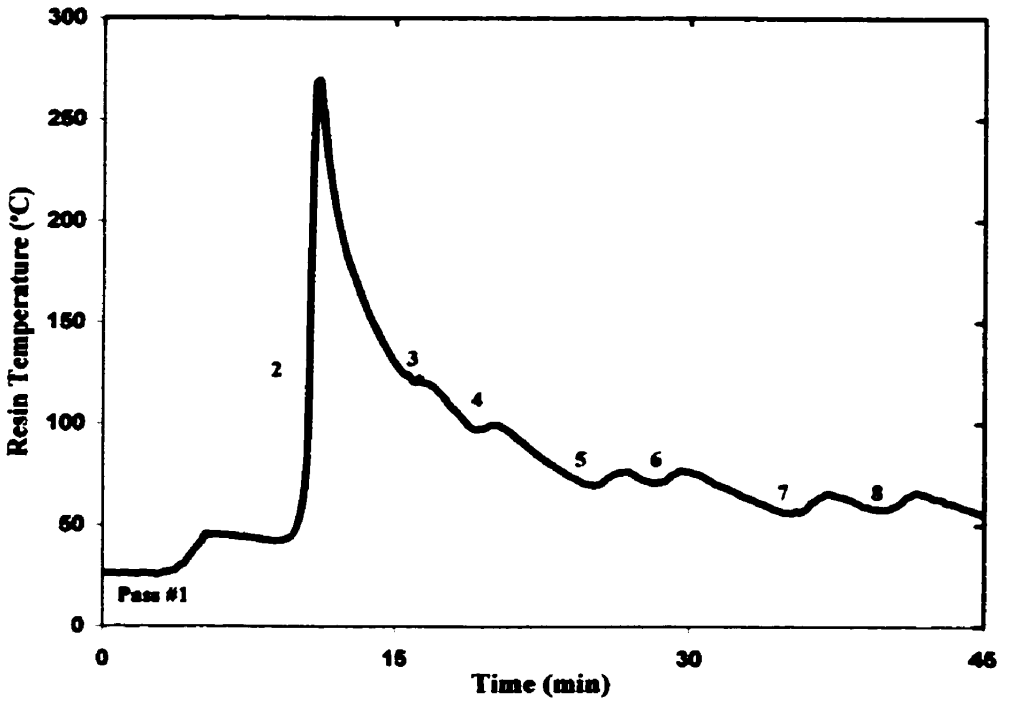

Figure 6.26: Temperature rise for25 kGy/pass EB curing of large resin sample (approximately 3 g resin sample; $T_a = 22°C$)

In Figure 6.25 a temperature plot for a resin sample in a 1 ml syringe EB cured on an ice pack (i.e. at an ambient temperature of $T_a = 0°C$) is shown. The dose per pass was again 25 kGy/pass. The maximum temperature experienced by the sample was approximately $T_{max} = 18°C$. In Figure 6.26, the temperature during EB curing of a 3 ml syringe of resin is shown. This sample was cured at a dose per pass of 25 kGy/pass, and at ambient room temperature. It can be observed that the **exothermic heat produces a large temperature rise** resulting in a maximum temperature of approximately 275°C. The high temperature occurs because the resin sample is large and compact. This result indicates that during EB curing of a thick, resin-rich composite part, temperature rise and consequently thermal curing could be very significant.

Figure 6.27a shows the comparative influence of ambient cure temperature, T_a, on the progressing cure state of resin samples. The final cure state after 250 kGy of EB radiation is drastically affected by ambient temperature. The RT (T_a=22°C) samples end up in a cure state of 70%, but the samples cured with an ambient temperature of T_a=0°C (cured on ice), end up in a cure state of only 55%. The samples cured on dry ice (T_a=-78°C) end up in a cure state of only 27 %. This data is plotted another way in Figure 6.27b. The cure states for the three different ambient temperatures are plotted for four different doses (25, 50 100 and 250 kGy). It is apparent from this figure that the divergence in cure state occurs most significantly after 25 kGy and that up to 25 kGy, the ambient cure temperature does not significantly affect the cure state. This may imply that the ambient temperature does not strongly influence the kinetics of the chemical reaction of crosslinking (i.e. excitation and activation) under EB. As the cure extent proceeds, the diffusion of reactive species becomes restricted due to higher amounts of crosslinking (an

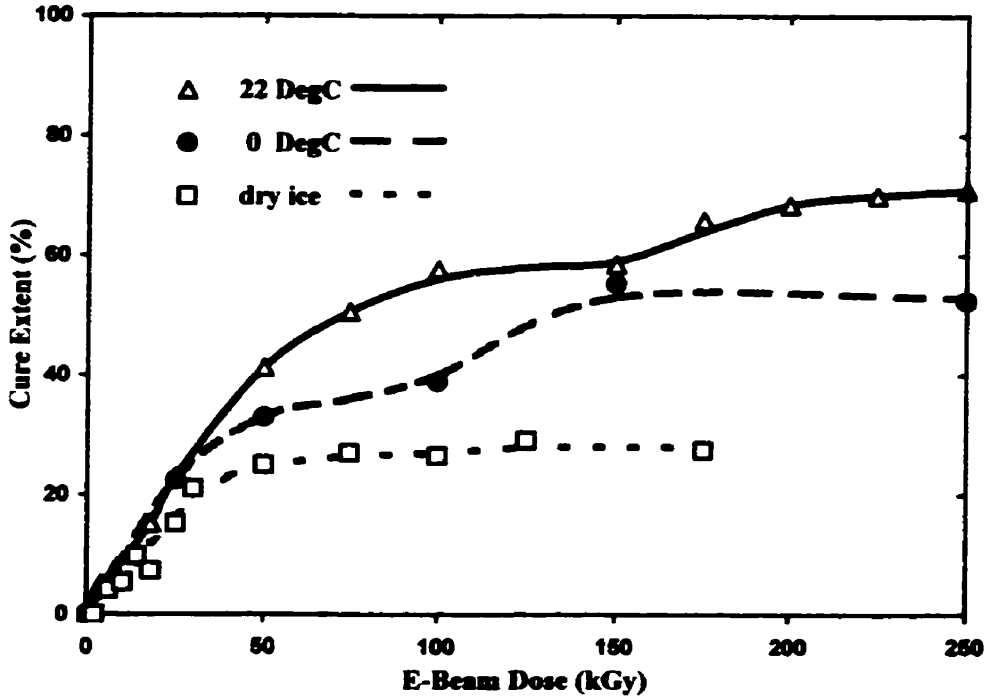

Figure 6.27a: Influence of ambient temperature on cure extent for increasing EB dose

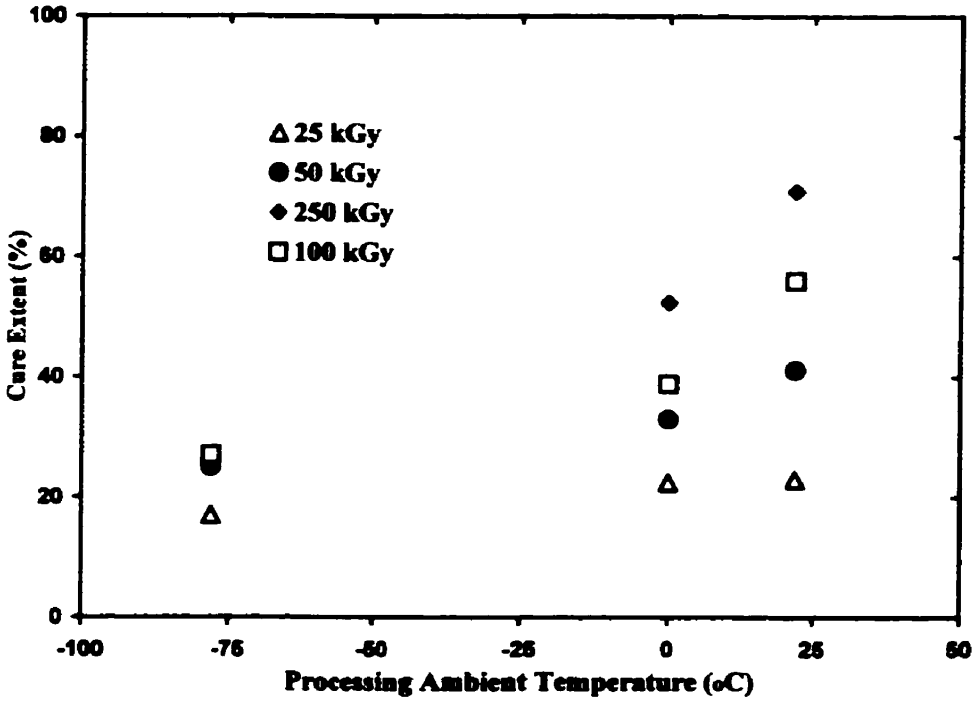

Figure 6.27b: Influence of dose on cure extent for increasing ambient temperature

increasing difference between T_{cure} and T_g) and the ambient temperature becomes more influential. After EB doses of 25 kGy, and certainly for EB doses greater than 50 kGy, the formulation is in the transition stage and is under the combined influence of three phenomena: **Advances made in cure extent from this point on are produced by the declining effects of EB radiation influencing the reaction kinetics, the increasing effects of temperature influencing the diffusion of reactive species, and the increasing possibility of thermal curing of excited initiator species.**

A significant observation can be made by examining the T_a= -78°C data, where the influence of temperature is minimized. At this temperature, there is only a restricted contribution of diffusion and thermal activation of excited species towards curing. The cure extent achieved at this temperature suggests that **the maximum cure extent for EB curing alone with no thermal curing, and limited diffusion is less than 25%.**

Another important observation noted was that the onset temperature (the lowest temperature at which exothermic heat is first observed) for residual curing decreases with increasing dose. At doses grater than 50 kGy, the onset temperature decreased to 0°C for those samples cured at sub-RT values. This is further evidence that the OPPI is dissociated and has become available for crosslinking reactions, but is trapped by limited mobility in the glassy state of the polymer. An increased amount of thermal energy is required to impart enough kinetic energy to the reactive species to complete the reactions.

These results clearly show that **temperature plays a very significant role during EB curing.** With increasing EB dose, the initiator is increasingly excited, and modest temperature rises cause thermal activation and curing. The assumption that has been made by previous researchers that crosslinking during EB processing is strictly due to EB

interaction with the formulation is doubtful. As well, since diffusion of EB activated species is required for crosslinking reactions to occur, the ambient temperature during EB curing is an influential parameter that cannot be independently selected.

6.5 Influence of Reinforcement

The same analysis of examining DSC residual exotherms for increasing EB dose was undertaken to ascertain the influence of the presence of reinforcing fibres on the EB curing process. Volume fraction of approximately 58% composite samples were given EB doses in 25 kGy increments up to 500 kGy, and the resulting residual exotherms are shown in Figures 6.28 and 6.29. The ambient temperature for irradiation of these composite samples was T_a=22°C, and the temperature rise during processing caused the maximum temperature that the samples reached at times during irradiation to be approximately T_{max}=70°C. Figure 6.28 shows the residual exotherms compared to the untreated composite sample. After irradiation, the exotherms are better examined on the expanded scale of Figure 6.29. The alpha peak is prominent up to an EB dose of 100 kGy, and has not moved to as low a temperature as it did for the resin samples (165°C versus 140°C). This may indicate a difference in the reaction kinetics between composite and resin samples.

In Figure 6.30, the cure extent versus EB dose is plotted for the composite and compared to the data for neat resin. From this figure, it is evident that the EB radiation is most effective below 100 kGy, and at doses above 150 kGy has a negligible effect on cure extent. **In comparison to the neat resin, the composite cures to a further extent**

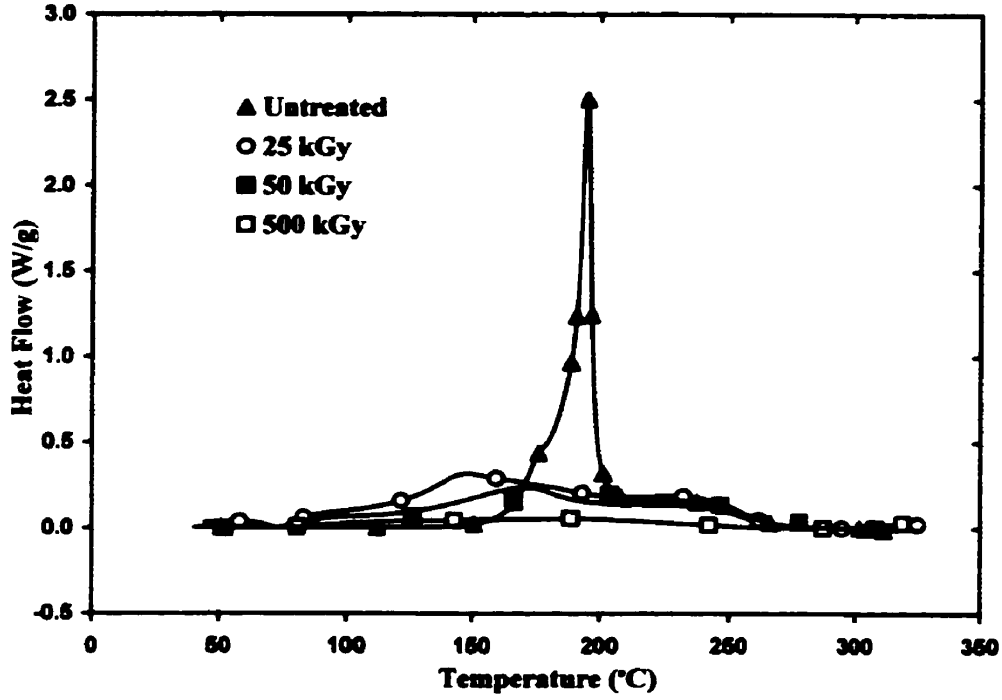

Figure 6.28: Cure progression for EB treated composite (0-500 kGy)

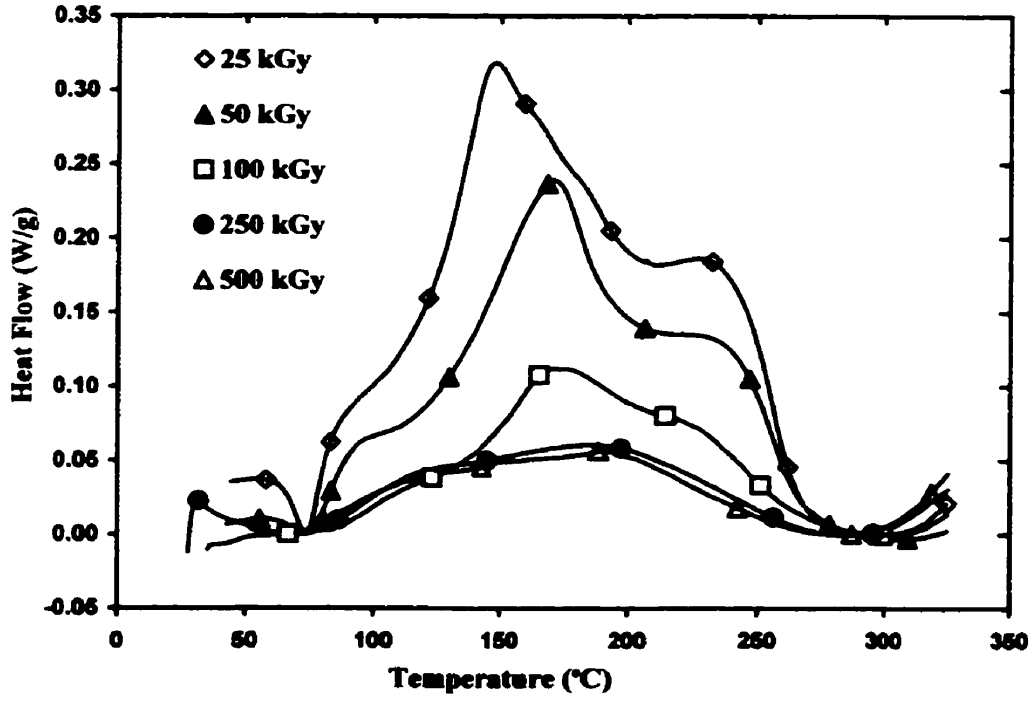

Figure 6.29: Cure progression for EB treated composite (25-500 kGy)

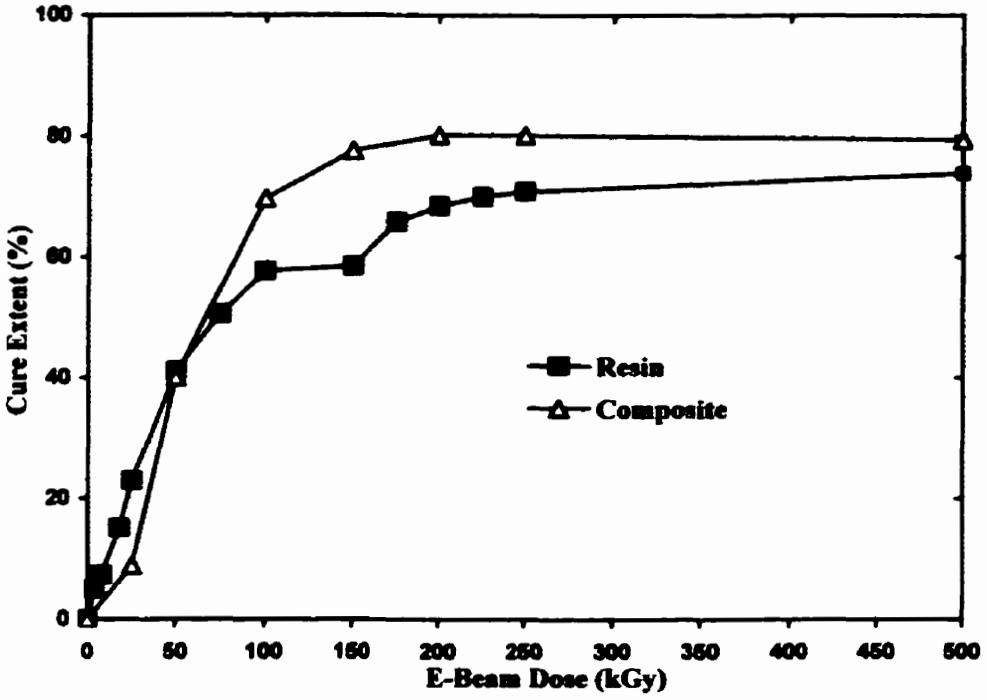

Figure 6.30: Influence of reinforcement on cure extent for increasing EB dose (composite: Vf = 58 %; both resin and composite cured at T_a=22°C)

(80% vs. 73%) at 500 kGy. Generally, the presence of reinforcement in the matrix has previously been thought by other authors to inhibit the EB processing, as mentioned in chapter 4. This has meant that a higher dose has been applied to composite samples (approximately 30 kGy higher) in an effort to advance the final cure state to the same level. Evidence that may support this assumption is that the alpha peak requires a higher dose before it loses its prominence over the other peaks for composite than for neat resin. However, the plot of Figure 6.30 implies that **the presence of reinforcement serves to decrease D_{cure} and increase the maximum cure extent**. A more rigorous examination of the effect of reinforcement could be undertaken which would account for varying the volume fraction (V_f) of fibres, type of fibres (glass vs. graphite), and fibre sizing (the microthin polymer coating deposited on fibres following their fabrication). A study of such factors would be beneficial, but is outside the scope of this study.

6.6 Influence of Dose Rate

The experimental observation of dose rate effects for EB curing is complicated by the constantly pulsing and scanning electron beam and moving conveyor. However, an investigation of different peak dose rates as defined by the author in chapter 3, and different dose per pass values during EB irradiation was undertaken and results in some significant observations. These observations have important implications on the practical selection of spatial parameters such as scan width, conveyor speed, and height above the conveyor.

In Figure 6.31, the cure extent as a function of dose is plotted for three different dose per pass values, $d^{\bullet}$, all cured at T_a=0°C (ice packed) to reduce the influence of temperature. The 2 and 5 kGy/pass samples exhibited very little temperature rise up to 50 kGy (approximately T_{max}=5°C), while the 25 kGy per pass samples exhibited a maximum temperature of approximately T_{max}=20°C. It is apparent that there is virtually no cure extent difference between the 2 kGy/pass and 5 kGy/pass samples; however, the cure extent of the 25 kGy/pass samples is much greater at the same value of dose. There are two possible explanations for this difference. It is possible that this difference is due to an influence of the process parameter of dose per pass on cure extent. That is, the higher the dose per pass, the higher the cure extent for a given dose. An alternative explanation is that the small difference in temperature rise during EB curing at different dose per pass values is responsible for the different cure extents. If the former explanation were true, it would be expected that there would be a difference in cure extent values between 2 kGy and 5 kGy, but no difference was observed. It is likely that the difference in temperature rise between the 25 kGy passes and 2 and 5 kGy passes that has affected the cure extent at least to some extent. Unfortunately it is not possible to completely delineate temperature and dose per pass effects and therefore **not possible to determine whether it is the incremental dose per pass or the associated temperature rise that influences cure extent.**

Another method employed to investigate dose rate effects was to vary the peak scanning average dose rate. Resin samples were cured at 0°C, at the same conveyor height (15 cm) and the same dose per pass (20 kGy). The only difference in processing was the scan width, and hence the **peak scanning average dose rate, d_3,** as described in

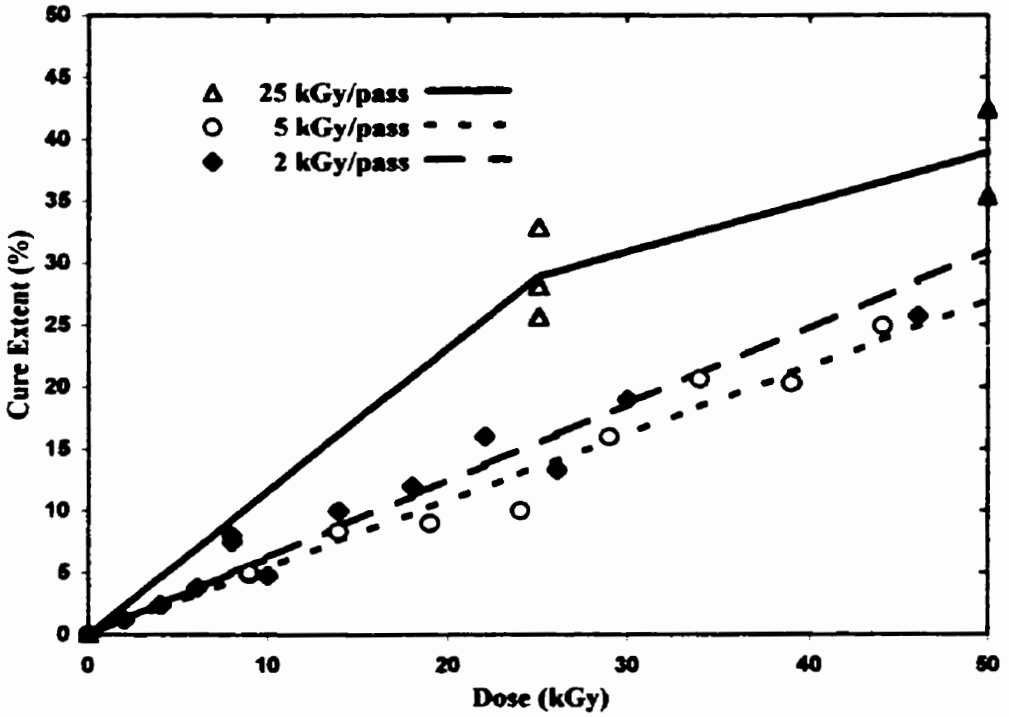

Figure 6.31: Influence of dose per pass on cure extent for increasing dose

chapter 3. A scan width of 30 cm corresponding to a peak scanning average dose rate of 0.65 kGy/s, and a scan width of 60 cm, corresponding to a peak scanning average dose rate of 0.32 kGy/s were used. Figure 6.32 shows the progression of cure extent for the two different scanning average dose rates. It can be observed that **the lower scanning average dose rate (wider scan width) cures to a further extent.** At the plateau at about 80 kGy, the 0.32 kGy/s sample exhibits an ultimate conversion of approximately 50 %, while the 0.65 kGy/s sample exhibits an ultimate conversion of only 45 %. This is a very significant phenomenon. It implies that the dose rate has severe implications on cure extent, and that low dose rates are more favourable to high dose rates. Temperature rise during these two dose rate experiments was very similar (T_{max}=20°), however the time for which each sample was exposed to that temperature was different. The **time of influence, parameter t***, is doubled when the scan width is doubled, so that the lower dose rate experienced elevated temperatures for longer periods than the higher dose rate. It is likely that **the difference in ultimate cure extent for different peak scanning average dose rates is a result of a combination of the influence of t* and d_3 factors.**

A similar investigation of dose rate was undertaken that made use of the change in instantaneous dose rate with height from the conveyor. Resin samples were progressively cured in increments of 20 kGy/pass, at scan widths of 30 cm, but at different scan heights (15 cm and 45 cm). At z=15 cm, the peak instantaneous dose rate is 2.1 MGy/s and the peak duty cycle average dose rate is 2.1 kGy/s. At z=45 cm, the peak instantaneous dose rate is 5.4 MGy/s and the peak duty cycle average dose rate is 6.5 kGy/s. Figure 6.33 shows the cure extent progression for the two different scan heights, cured at the same dose per pass. The scan width was the same for both scan

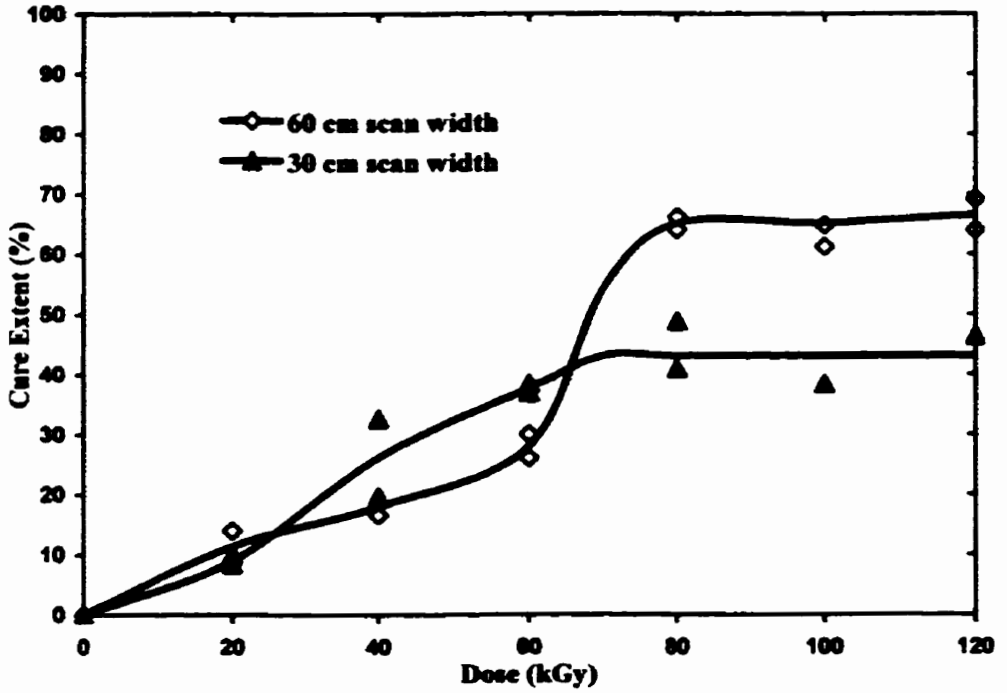

Figure 6.32: Influence of peak scanning average dose rate (scan width) on cure extent for increasing EB dose

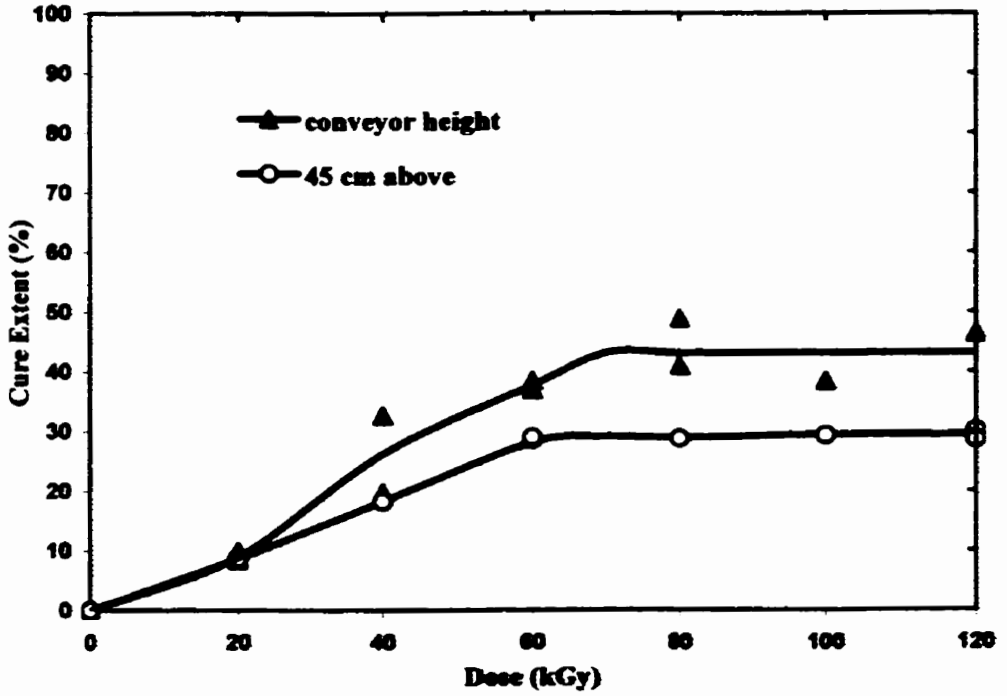

Figure 6.33: Influence of instantaneous dose rate (scan height) on cure extent for increasing EB dose

heights, but since the peak instantaneous dose rate duty cycle average dose rate changes, both the scanning average dose rate and the duty cycle average dose rate change. At z=15 cm, the peak scanning average dose rate was 0.65 kGy/s, and at z=45 cm, the peak scanning average dose rate was 1.7 kGy/s. It is evident from Figure 6.33 that the lower instantaneous dose rate cures to a higher extent. Once again, the maximum temperature rise experienced for both experiments was approximately T_{max}=20°C, but the time of influence, t* is almost tripled between the two scan heights. It is evident from this and the previous investigation that a **'slow' EB curing at a low dose rate results in a higher cure extent than 'fast' curing at a high dose rate for the same applied total dose.** Research by radiation chemists such as Czvikovsky [57], in other applications of EB irradiation of polymers have suggested the same phenomenon.

The differences in cure extent for different peak dose rates may be solely attributed to time-of-influence differences, rather than an actual dose rate dependence. Evidence for this conclusion can be justified by suggesting that increased time at an elevated temperature causes increased diffusion. That is, reactive species trapped in the glassy state show increased migration to reactive sites and complete crosslinking reactions with increased time at slightly elevated temperatures. However, since temperature effects cannot be completely delineated from dose rate effects, it can only be concluded that as a practical matter, simple differences in dose delivery significantly affect EB curing reactions.

6.7 Kinetic Analysis

To develop a better understanding of the phenomenon of EB radiation curing, an investigation of the curing reaction kinetics was initiated. Since it is not possible to accurately measure the rate of heat evolution during EB processing (i.e. an EB calorimeter does not exist) the EB reaction was studied by thermal kinetic analysis following EB irradiation. From this type of analysis, characteristics of the EB curing reaction can be inferred. There were two specific objectives of this analysis. The first goal was to investigate the decrease in residual curing onset temperature caused by EB irradiation. The second, and more ambitious goal was to model the kinetics of the residual thermal curing reaction and to use this model to delineate kinetic effects from diffusional effects. Although significant observations were made through kinetic analysis, the second objective could not be fulfilled. This shortcoming was due to the complexity of the 1E/OPPI formulation. Since three reactions are observed during curing (alpha, beta, and gamma), a complete model of each reaction would be required to distinguish diffusion from reaction kinetics. For the untreated formulation, the three reactions can be distinguished from one another, but with increasing EB dose, it is increasingly difficult, to completely distinguish (and hence analyze) each reaction. Hence, the kinetic investigation to follow is a simplified analysis performed solely to determine the influence of dose on residual thermal curing kinetics.

Isothermal cure monitoring of **untreated** 1E/OPPI resin at different temperatures was performed, the results of which are shown in Figure 6.34. In these tests, the alpha and gamma reactions are observed, the alpha reaction to the right of the gamma reaction. For the test at 160°C, only the alpha reaction is readily observed. For all isothermal

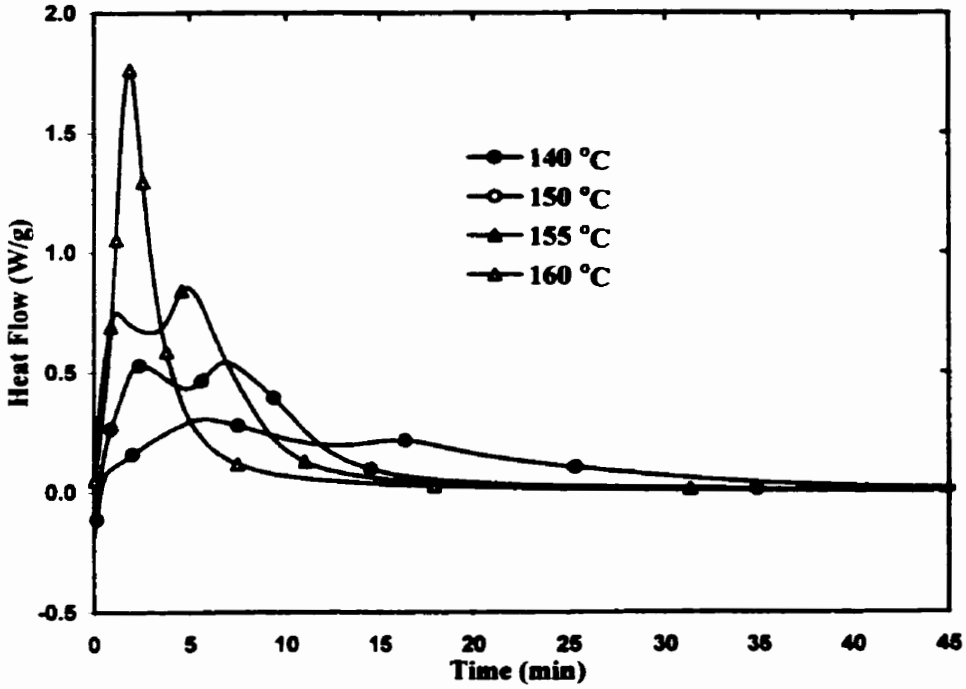

Figure 6.34: Isothermal curing of untreated resin

Temperature (°C)	k (1/min)	n	m
140	0.154	1.15	0.85
150	0.386	1.25	0.75
155	0.600	1.29	0.71
160	1.12	1.39	0.61

Table 6.3: Average rate constants for neat resin

analysis, the beta reaction could be ignored since it was not observed for the isothermal temperatures selected. From these multiple DSC tests, it is apparent that both the alpha and gamma peaks are shifted along the time axis with decreased isothermal temperature. This suggests that the kinetics of both reactions are autocatalytic in nature and hence are described by equation 5.2:

$$dc/dt = k c^m (1 - c^n)$$

The alpha reaction was selected for analysis since it is the primary (highest exothermic heat) reaction. By fitting equation 5.2 to the alpha peak of the isothermal tests and forcing m + n = 2 (an assumption commonly used to simplify the kinetic analysis), the rate constants k, m, and n, shown in table 6.3 were determined.

The isothermal parameters obtained were then used to generate an Arrhenius plot (Figure 6.35, previous page), which exhibits the relationship of equation 5.3:

$$k(T) = Z e^{-E/RT}$$

For the neat resin, the results of the Arrhenius fit were:

Activation energy: $E = 147.1$ **(kJ/mol)**

Arrhenius frequency factor: $\ln(Z) = 40.9$ **(1/sec)**

This same method of thermal kinetic analysis was employed on resin samples that had been EB treated. Low EB dose levels were selected so that the glass transition temperature was lower than the onset of the residual curing reaction, to avoid diffusion related effects. The dose levels that met this criteria were 6, 10, and 14 kGy. The exothermic heat of reaction for each of the alpha beta and gamma reactions was

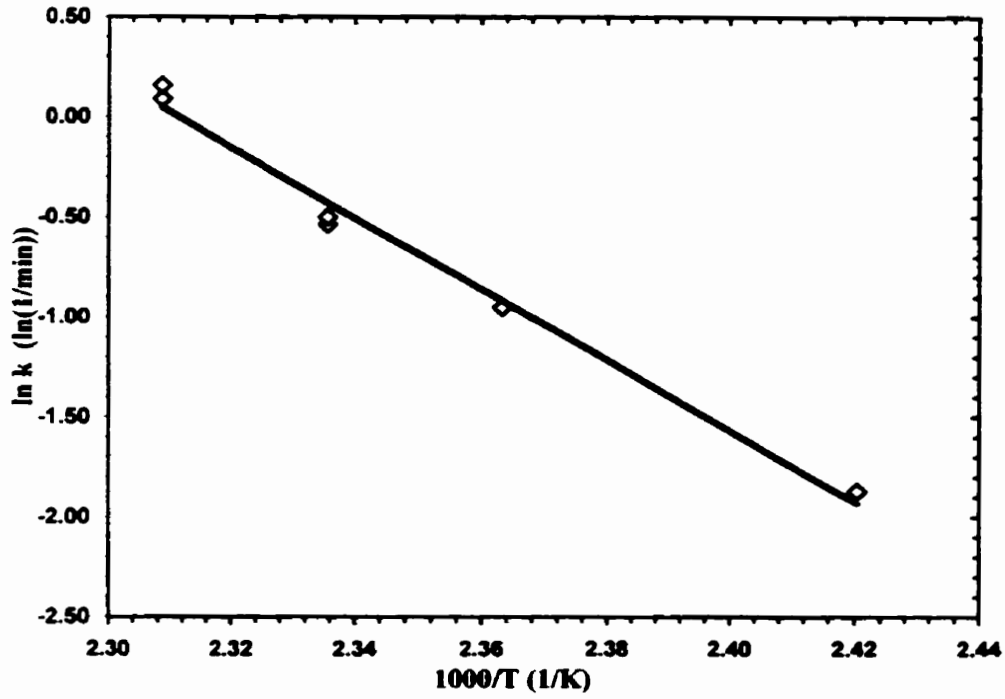

Figure 6.35: Arrhenius plot of untreated resin

determined by a trial and error method of fitting a Gaussian curve to each reaction peak. These results are summarized in Table 6.4.

To limit the effect of thermal activation and curing, the resin samples were EB cured on dry ice, at an ambient temperature of approximately T_a = -78°C, and experienced a maximum temperature of only T_{max} = -40°C. The DSC isothermal tests and Arrhenius plots obtained are shown in Figures 6.36 to 6.41. It should be noted that the kinetic analysis of Figures 6.36 to 6.41 is not an investigation of EB reaction kinetics, rather it is an analysis on the *residual* thermal cure reaction kinetics. However, from this type of investigation it is possible to determine how EB radiation treatment changes the kinetics of the alpha reaction.

EB Treatment (kGy)	Total Enthalpy (J/g)	alpha (J/g)	gamma (J/g)	beta (J/g)
0	615	350	55	210
6	593	340	43	210
10	571	320	41	210
14	555	300	40	210

Table 6.4: Enthalpy of reactions for residual thermal curing following each EB treatment

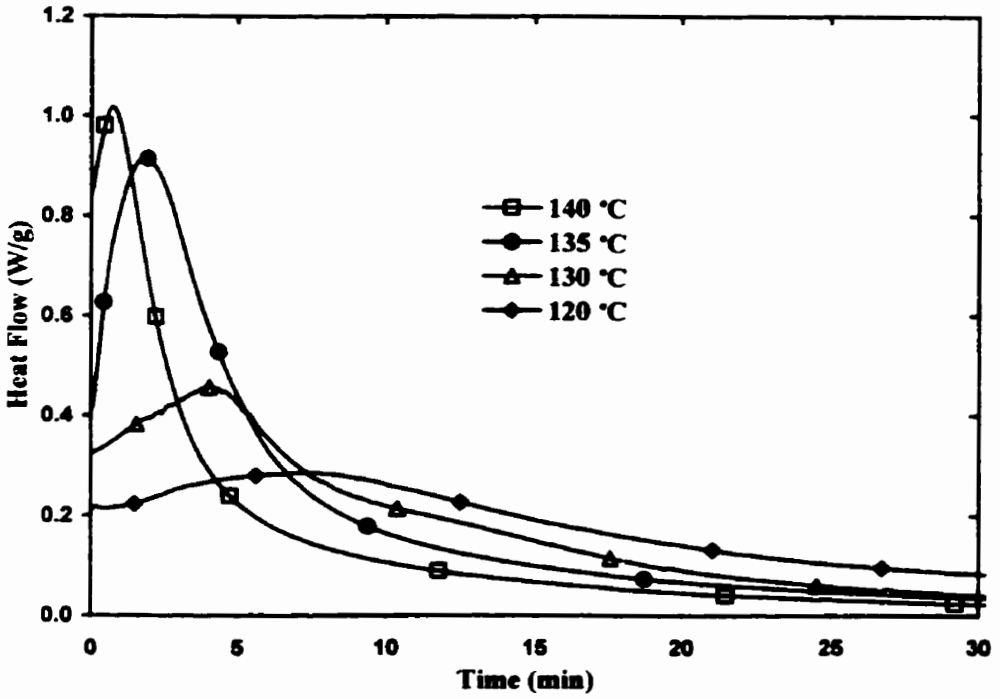

Figure 6.38: Isothermal curing of 10 kGy resin

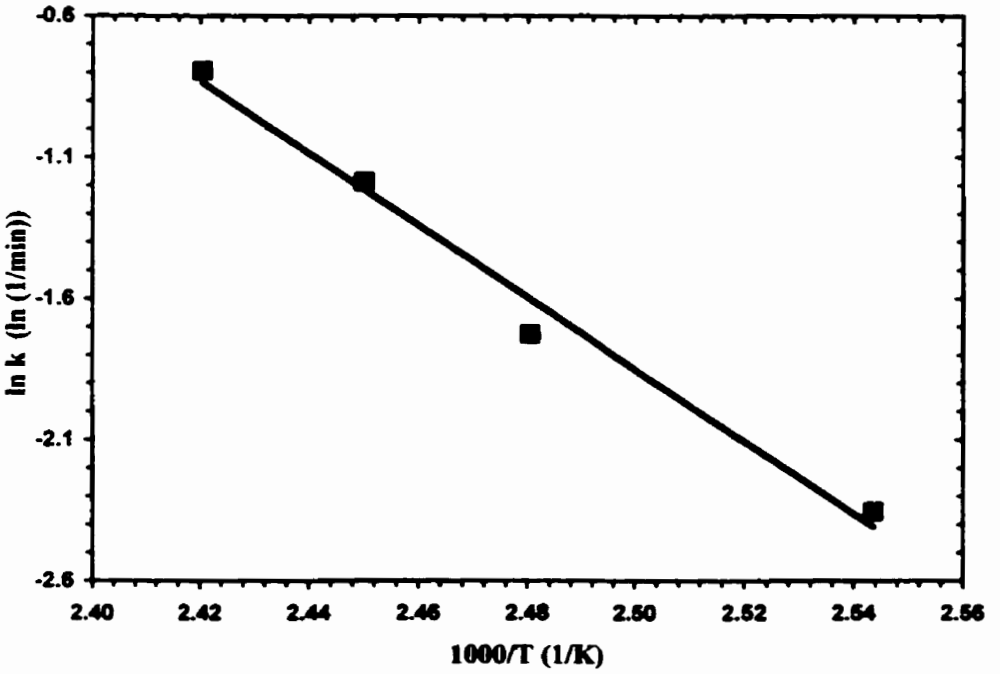

Figure 6.39: Arrhenius plot for 10 kGy resin

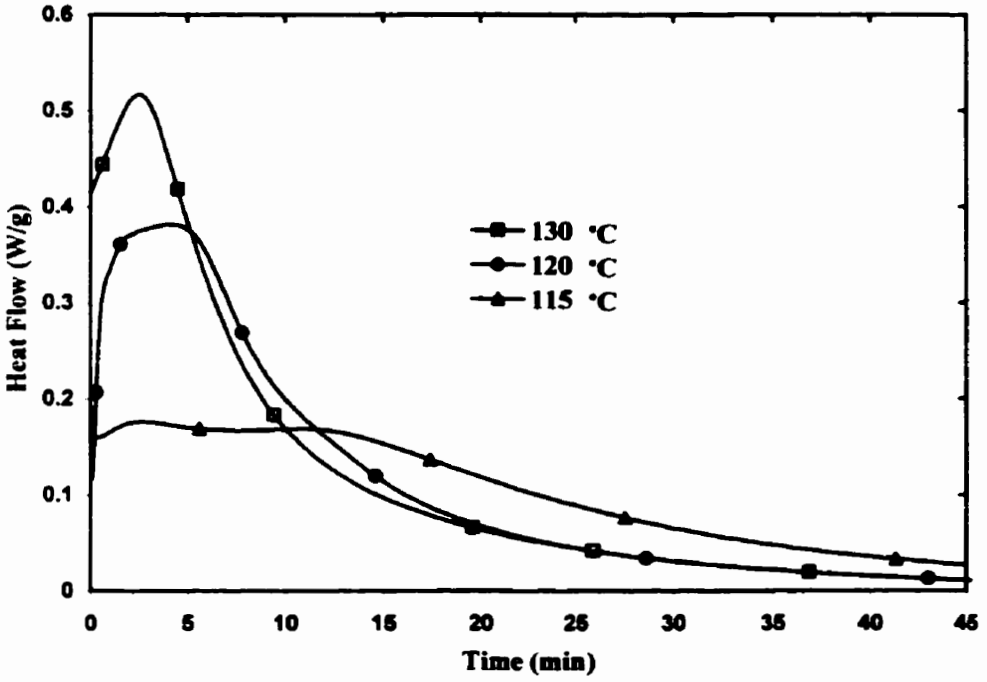

Figure 6.40: Isothermal curing of 14 kGy resin

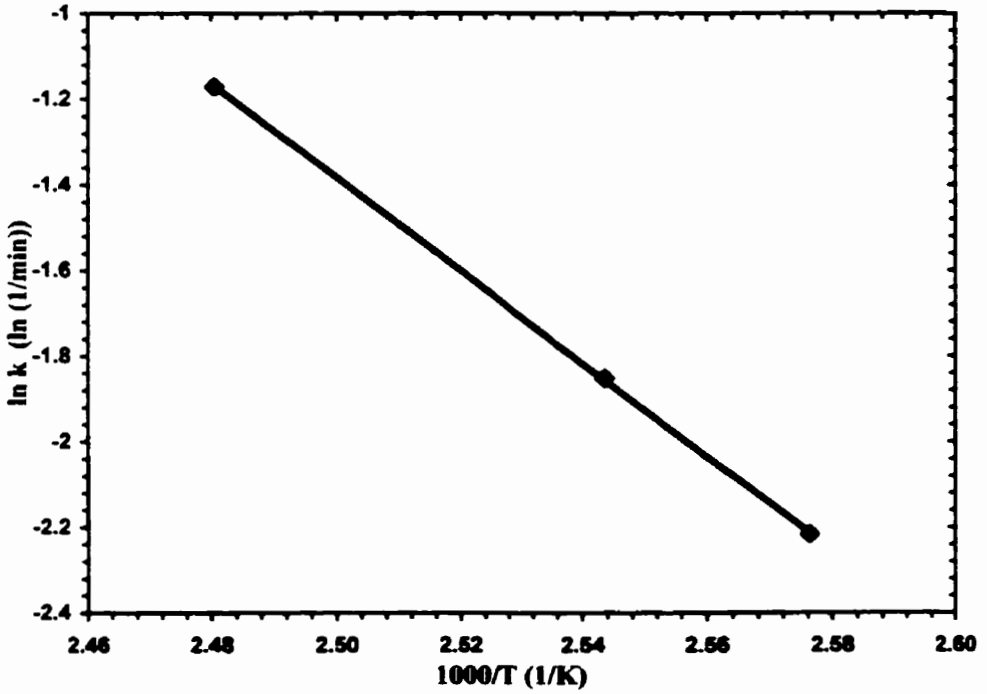

Figure 6.41: Arrhenius plot for 14 kGy resin

From the results of these isothermal tests, the influence of dose on activation energy for low EB doses can be observed (Figure 6.43). It is evident from this figure that small increases in EB dose at low total dose values act to reduce the activation energy for residual thermal curing with a linear tendency. Because of this trend, a simple modification of the Arrhenius equation is suggested for low EB doses:

$$k(T) = Z\, e^{-(E - f D)/RT} \qquad \textbf{(eq. 6.1)}$$

Where the constant **f is introduced as the EB dose factor**, the slope of the data plotted in Figure 6.42. This dose factor has units of::

dose factor, f (units) = (kJ / mol) / kGy

or simply, **f (units) = g / mol**

For 1E/OPPI, the calculated value of this dose factor is:

f (1E/OPPI) = 4.12 g/mol

In developing a simple mathematical model of EB curing (alpha reaction only), it is evident from the results that the influence of temperature must be included in that model. The existence of the relationship between dose and reduced activation energy reinforces the conclusion that for low dose levels, EB irradiation serves to excite the initiator so that a reduced amount of thermal energy is required for activation. The relationship of equation 6.1 applies only for low doses (less than 14 kGy), and has not been verified beyond this range. This analysis demonstrates how simultaneous thermal and EB curing can be accounted for in modelling EB processing.

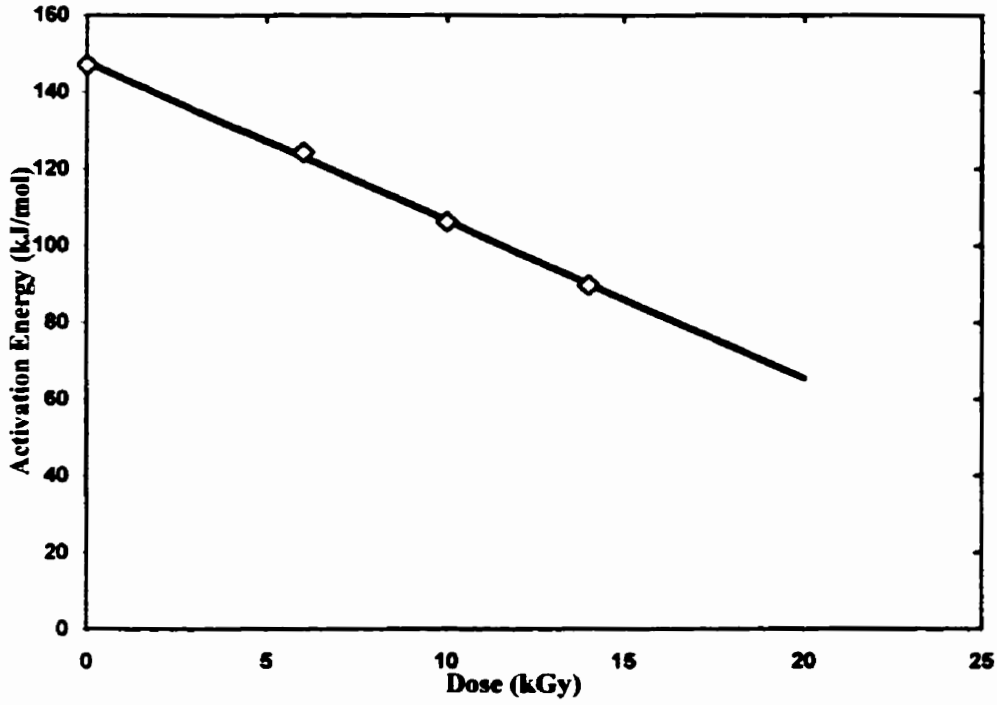

Figure 6.43: Influence of dose on activation energy for residual thermal curing (alpha reaction only)

6.8 Mechanical Properties

The previous evidence presented on the influence of process and material parameters produces the reoccurring certainty that there is a significant amount of undercuring associated with EB processing. This being said, the thermal reactivity of the 1E/OPPI EB formulation makes it suitable for thermal postcuring to complete curing to the furthest extent (highest degree of crosslinking). It has been shown that this thermal postcuring advances the 'B' glass transition from approximately 150°C to 370°C, or in essence causes the 'B' transition to disappear. The challenge undertaken in the mechanical property comparison was to quantify the effect of undercure on the mechanical properties of the resin and to compare thermal and EB cured resin samples. To investigate this, some straightforward mechanical testing was employed.

Cured 1E resin is very brittle and shows no plastic deformation, typical of many epoxies. Three different types of resin samples were prepared and tested:

1) EB cured at room temperature (T_{amb} = 22°C) to 200 KGy;
2) Thermally cured at 177°C for 3 hours and postcured at 232° for 2 hours;
3) EB cured at RT to 200 kGy, and postcured at 232° for 2 hours.

A minimum of ten samples of each type were tensile tested at room temperature to investigate any differences in modulus, strength, and ultimate strain. The average and standard deviation of the results of these tests are presented in table 6.3.

Although the extremely brittle nature of the partially cured resin caused the standard deviation of measured mechanical properties to be significant, a number of general observations can still be made. For instance, a drop in modulus was observed after postcuring. There is a difference in ultimate strength and strain between EB and

	T_g / Service Temp. (°C)	RT Tensile Modulus (GPa)	RT Tensile Strength (MPa)	RT Ultimate Strain (%)
EB 200 kGy	130	3.94 ● 0.12	21.0 ● 8.7	0.48 ± 0.19
EB 200 kGy Thermal postcure: 232°C for 2 hrs	370	3.46 ± 0.08	18.8 ± 1.7	0.50 ± 0.01
Thermal cure cycle: 177°C for 3 hrs 232°C for 2 hrs	370	3.54 ± 0.16	13.2 ± 1.7	0.37 ± 0.08

Table 6.5: Summary of Mechanical Properties

thermally processed samples. The difference in ultimate strength between EB cured and postcured samples falls with the margin of error created by the high deviation from test to test and cannot be considered as a significant difference.

The reduction in room temperature modulus between EB and postcured samples is surprising. It is expected that more crosslinking would result in a higher modulus value. This result may suggest that there is a reduction in residual stresses during postcuring. The difference in strength between EB and thermally cured resin may suggest that there are differences in the structure of the cured resin between the EB treated and untreated samples. A thorough investigation into the mechanical properties of cured resin and composite was not the focus of this investigation. However these initial results serve as an indication that significant differences arise in mechanical properties and further study in this area is warranted.

Chapter 7

Conclusions

Over the course of the previous six chapters, a complete description of EB curing has been provided. Aspects of the history, commercial development, and chemistry of EB curing have been outlined. Processing facilities, EB accelerators, and functional characteristics of the process have been described. A meaningful contribution to high-energy EB research has been made by defining the important process parameters of the technology, including the original concepts of duty cycle average dose rate and scanning average dose rate. Most importantly, on the basis of this work a better understanding of the influence of material and process parameters on high-energy electron beam curing of polymer composites has been developed. Armed with this increased knowledge a number of conclusions can be drawn about the potential merits of EB curing.

To fulfil the specific objectives laid out at the end of Chapter 4, a summary of the primary discoveries and conclusions made on each material and process parameter is useful:

1) **Dose:** An improved method of predicting the dose for maximum curing, D_{cure}, has been developed by examining DSC residual exotherms. The ultimate cure extent achieved by EB curing at room temperature was quite low (approximately two thirds). Either **thermal postcuring** or manipulation of other material and process parameters is required to avoid this undercure. EB Dose is effective at exciting and activating the initiator for crosslinking reactions, however the extent of crosslinking is limited by diffusion.
2) **Temperature**: Of critical importance was the discovery that temperature strongly influences the EB curing process. As irradiation proceeds, thermal curing and EB curing are complementary phenomena. Also, since EB curing becomes more diffusion dependent with increasing dose, both the ambient (applied) temperature and the time-temperature history during processing play a major role in the overall cure extent achieved during irradiation.
3) **Initiator concentration**: Three independent methods of optimizing the initiator concentration were used, all of which indicate a value of 5 phr, higher than the value currently accepted as the industry standard (3 phr).
4) **Dose Rate**: From a practical point of view, dose rate has a strong influence on cure extent. This implies that parameters such as conveyor speed and scan width must be selected carefully when EB curing. Although results are influenced by other parameters, it was observed that low dose rates lead to higher cure extents than high

dose rates. This is thought to be due to temperature and time affecting diffusion and thermal curing.

5) **Reinforcement**: EB curing shows similar behaviour for composite samples as for resins. However, for 1E/OPPI, the composite achieved a higher cure extent than neat resins

6) **Kinetics:** Based on the kinetic analysis of the primary curing reaction, it can be concluded that the interaction between the EB and formulation causes a reduction in the activation energy required for thermal curing. This is the most convincing proof that thermal curing plays an important role during EB processing. A straightforward adjustment to the Arrhenius equation was determined that indicates that modelling of thermal and EB curing simultaneously is possible.

7) **Mechanical Properties:** EB cured resin samples have as good or better properties than thermally cured resin samples, even before postcuring.

These observations serve to answer the specific objectives set out for the experimental research. Collectively, these discoveries lead to a number of **important implications** for the commercial potential and research direction for EB curing:

- Formulations (selection of resin-initiator pair) need optimization to eliminate curing reactions that are only weakly dependent on EB.
- Thermal and EB curing can occur simultaneously during EB processing and therefore must be must be modelled together.
- Diffusion is limiting factor in achieving high cure extents
- EB curing not temperature selectable, which may curtail some of the proposed advantages such as co-curing

- T_gs much higher than cure temperature are achievable, although the ultimate T_g is influence by temperature

A few suggestions are made for future research:

- identify and compare EB and thermal reactions
- investigate fibre-matrix interface for EB versus thermal curing
- investigate residual stresses caused by rapid curing in the glassy state

References

1 J.V. Crivello, M. Fan, D. Bi, "The Electron Beam-Induced Cationic Polymerization of Epoxy Resins", *Journal of Applied Polymer Science 44* (1992), 9-16

2 T.Q. Cao, A. Falcone, J.R. Beymer, D.A. Russell, C.E. Vicks, E.D. Smith-Hicks, "Feasibility Study of Electron Beam Cured Composites", *International SAMPE Technical Conference 28* (1996), 862-876

3 C.J. Janke, G.F. Dorsey, S.J. Havens, V.J. Lopata, "Electron Beam Curing of Epoxy Resins by Cationic Polymerization", *International SAMPE Symposium 41* (1996), 196-206

4 D. Beziers, B. Capdepuy, "Electron Beam Curing of Composites", International SAMPE Symposium 35 (1990), 1220-1232

5 C.B. Saunders, V.J. Lopata, W. Kremers, T.E. McDougall, M. Tateishi, A. Singh, "Electron Curing of Fiber-Reinforced Composites; Recent Developments", *International SAMPE Symposium 38* (1993), 1681-1689.

6 K. Fisher, "Curing with Electron Beams", *High Performance Composites*, September/October 1996, 27-34

7 R.B. Vastava, et al., "E-Beam Processing of Composite Structures", *International SAMPE Symposium 42* (1997), 526-535

8 F. Abrams, T.B. Tolle, "An analysis of E-Beam Potential in Aerospace Composite Manufacturing", *International SAMPE Symposium 42* (1997), 548-557

9 A. Yen, R. Vastava, "Evaluation of E-Beam Cured Composites", *International SAMPE Symposium 42* (1997), 498-508

10 R.B. Vastava, et.al., "An Assessment of E-Beam Technology for Aircraft Applications", *International SAMPE Symposium 43* (1998), 1681-1691

11 M.E. Roylance, C.J. Janke, J.M. Tuss, "Affordable Composite Structures via Electron Beam (E Beam) Curing", *International SAMPE Symposium 43* (1998), 1660-1671

12 M.R. Cleland, A.S. Herer, "New Facilities for High-Power, High-Energy Electron Beam Processing, *International SAMPE Symposium 44* (1999), 259-268

13 C.B. Saunders, V.J. Lopata, W. Kremers, M. Chung, A. Singh, D.B. Kerluke, "Electron Curing of Fibre-Reinforced Composites; An Industrial Application for High-Energy Accelerators", *9th International Meeting on Radiation Processing*, Istanbul, Turkey (1994).

14 D.L. Goodman, C.A. Byrne, G.R. Palmese, "Advanced Electron Beam Curing Systems and Recent Composite Armored Vehicle Results", *International SAMPE Symposium 42* (1997), 515-525

15 D.L. Goodman, C.A. Byrne, "Advanced Electron Beam Curing and Bonding of Ground Vehicles", International SAMP Symposium 43 (1998), 1691-1701

16 J.D. Farmer, C.J. Janke, V.J. Lopata, "The Electron Beam Cure of Paste Adhesives", International SAMPE Symposium 43 (1998), 1639-1645

17 R. Foedinger, D. Rea, R. Grande, C. Davis, T. Walton, R. Norris, C. Janke, T.L Vandiver, "Electron Beam Curing of Filament Wound Composite Pressure Vessels", *International SAMPE Symposium 44* (1999), 248-258

18 A. Hoyt, L.A. Harrah, R. Allred, R. Pittman, "Novel Resins for E-Beam Manufacturable Composite Space Structures", *International SAMPE Symposium 42* (1997), 509-514

19 D.L. Goodman, C.A. Byrne, G.R. Palmese, S. Sarmah, "Composite Curing With High Energy Electron Beams: Novel Materials and Processes", *International SAMPE Symposium 42* (1997), 911-920

20 T.C. Walton, J.V. Crivello, "Recent Advances in Electron-Beam Rapidly Cured Composite Polymers", *International SAMPE Symposium 42* (1997), 537-547

21 K. Van Camp, *Composite Materials Handbook*, Institute for Technological Development, University of Manitoba,, 1993

22 J.M. Margolis, *Advanced Thermoset Composites,* Van Nostrand Reinhold Cmpany, NewYork,1986

23 A. Singh, L.W. Dickson, "Radiation Processing: An Overview", in A. Singh, J. Silverman (Eds.), *Radiation Processing of Polymers*, Munich: Hanser Publishers, 1992, Chap. 1.

24 D.B. Kerluke, C.B. Saunders, A.J. Stirling, "Electron Curing – A New Technology for Polymer Matrix Composites", *International Conference on Advanced Composites*, Wollongong, Australia, 1993.

25 C.J. Janke, G.F. Dorsey, S.J. Havens, V.J. Lopata, "Toughened Epoxy Resins Cured by Electron Beam Radiation", *International SAMPE Technical Conference 28* (1996), 877-889

26 A. Chapiro, "Historical Outline of the Radiation Chemistry of Polymers", in J. Kroh (Ed.), *Early Developments in Radiation Chemistry*, Royal Society of Chemistry, Cambridge, 1989

27 W.D. Coolidge, *Science 62*, 1925, 441

28 W. Mund and W. Koch, *Bull. Soc. Chim. Belge 34*, 1925 119

29 A.O. Allen, "The Story of the Radiation Chemistry of Water", in J. Kroh (Ed.), *Early Developments in Radiation Chemistry*, Royal Society of Chemistry, Cambridge, 1989

30 J. Guillet, Polymer Photophysics and Photochemistry, Cambridge University Press, Cambridge, 1985

31 P. Dufour, "State-of-the-Art Trends in the Radiation-Curing Market", in J.P. Fouassier, J.F. Rabek, *Radiation Curing in Polymer Science and Technology* Vol I, Elseview Applied Science, London, 1993

32 A. Charlesby, "A Physicist Intrudes into Radiation Chemistry", in J. Kroh (Ed.), *Early Developments in Radiation Chemistry*, Royal Society of Chemistry, Cambridge, 1989

33 J.P. Fouassier, "An Introduction to Basic Principles of UV Curing", in J.P. Fouassier, J.F. Rabek, *Radiation Curing in Polymer Science and Technology* Vol I, Elseview Applied Science, London, 1993

34 J.P. Fouassier, "Excited-State Reactivity on Radiacl Polymerisation Photoinitiators", in J.P. Fouassier, J.F. Rabek, *Radiation Curing in Polymer Science and Technology* Vol II, Elseview Applied Science, London, 1993

35 C.B. Saunders, L.W. Dickson, A. Singh, "Gamma and Electron Beam Curing of Polymers and Composites", AECL internal document, circa 1998

36 C.B. Saunders, L.W. Dickson, A. Singh, A.A. Carmichael, V.J. Lopata, "Radiation-Curable Prepreg Composites", *Radtech Syposium*, New Orleans, U.S.A 1988.

37 L.W. Dickson, A. Singh, "Radiation Curing of Epoxies", *Proceedings of the 6th International Meeting on Radiation Processing*, Ottawa, Canada, (1987).

38 A. Singh, "Radiation Curing of Epoxies and Ethers", AECL document, circa 1988

39 V.J. Lopata, M. Chung, T.E. McDougall, V.A. Weinberg, "Electron Curable Adhesives for High Performance Structures", *International SAMPE Symposium 39* (1994).

40 A. Singh, V.J. Lopata, W. Kremers, T.E. McDougall, M. Tateishi, C.B. Saunders, "Electron-Cured Fibre-Reinforced Advanced Composites", *Proceedings 2nd Canadian International Composite Conference – CanCom* (1993), 277-289.

41 T.F. Williams, "Radiation Induced Polymerization", in P. Ausloos (Ed.), *Fundamental Processes in Radiation Chemistry*, 1968 Interscience, New York, 515-598

42 S.I. Omel'chenko, G.A. Bokalo, "Radiation-Chemical Transformations of Epoxy Compounds", *Novye Metody Poluchesniya I Issledovaniya Polimerov*, Naukova, Kiev, 1978, 165-184

43 V.P. Laricheva, "Epoxy Compositions, Solidifying Under Radiation Action", *Lakokras Mater. Ikh Primen. 1*, 1982, 19-20

44 "Electron Beam Curing of Polymer Matrix Composites CRADA Information (1994-1997), Oak Ridge National Laboratory website document

45 "AECL's Industrial Accelerator Program – an Overview", AECL Brochure, circa 1990

46 "The I-10/1 Industrial Electron Accelerator", AECL Brochure, 1991

47 J.R. Lamarsh, *Introduction to Nuclear Engineering*, 2nd Ed., Addison Wesley, Reading Mass., 1983

48 J.D. Lawson, *The Physics of Charged Particle Beams*, Clarendon Press, Oxford, 1988

49 A.J. Singh, C.B. Saunders, "Radiation Processing of Carbon Fiber-Acrylated Epoxy Composites", in A. Singh, J. Silverman (Eds.), *Radiation Processing of Polymers*, Munich: Hanser Publishers, 1992, Chap. 9.

50 A. Singh, C.B. Saunders, J.W. Barnard, V.J. Lopata, W. Kremers, T.E. McDougall, M. Chung, M. Tateishi, "Electron Processing of Fibre-Reinforced Advanced Composites", *Radiation Physical Chemistry 48* (1996), 153-170

51 J.V. Crivello, T.C. Walton, R. Malik, "Fabrication of Epoxy Matrix Composites by Electron Beam Induced Cationic Polymerization", American Chemical Society 1997

52 J.V. Crivello, "Cationic Polymerization – Iodonium and Sulfonium Salt Photoinitiators", Advances in Polymer Science 61 (1984), 1-48

53 V.J. Lopata, M. Chung, C.J. Janke, S.J. Havens, "Electron Curing of Epoxy Resins: Initiator and Concentration Effects on Curing Dose and Rheological Properties", International SAMPE Technical Conference 28 (1996), 901-910

54 Farhataziz and M..Rodgers, Radiation Chemistry: Principles and Applications, VCH Publishers, New York, 1987

55 G.N. Whyte, Principles of Radiation Dosimetry, John Wiley and Sons, Inc., New York, 1959

56 C.J. Janke, "Electron Beam Curable Cationic Epoxy Resin Systems And Composites", Presented at the Electron Beam Curing of Composites Workshop, Oak Ridge, Tennessee, Sept. 1996

57 T. Czvikovszky, "Radiation Processing of Wood-Plastic Composites", in A. Singh, J. Silverman (Eds.), *Radiation Processing of Polymers*, Munich: Hanser Publishers, 1992, Chap. 1.

58 W.J. Skraba, J.W.Lynn, "Radiation-Induced Graft Polymerization of Flexible Polyurethane Foam", in R.F. Gould, Advances in Chemistry Series 66 – Irradiation of Polymers, American Chemical Society, Washington, 1967, Chp. 15

59 D. Campbell, J.L Williams, V Stannett, "Radiation Grafting of Vinyl Monomers to Wool", in R.F. Gould, Advances in Chemistry Series 66 – Irradiation of Polymers, American Chemical Society, Washington, 1967, Chp. 16

60 M. Tavlet, H. Schonbacher, R. Cameron, and C.G. Richardson, "Assessment of Radiation Damage to a Halogen-Free Cable Jacket", in R.L. Clough, S.L. Shalaby, Radiation Effects in Polymers, American Chemical Society, Washington, 1991

61 J.D. Farmer, C.J. Janke, V.J. Lopata, "The Electron Beam Cure of Fiberglass/Epoxy Prepregs", *International SAMPE Technical Conference 29* (1997)

62 C.J. Janke, R.E. Norris, K. Yarborough, S.J. Havens, V.J. Lopata, "Critical Parameters for Electron Beam Curing of Cationic Epoxies and Property Comparison of Electron Beam Cured Cationic Epoxies versus Thermal Cured Resins and Composites", International SAMPE Symposium 44 (1997), 477-486

63 C. Saunders, V. Lopata, W. Kremers, "Electron Curing of Composite Structures for Space Applications", Executive Summary Submitted to Phillips Laboratory by AECL Technologies Inc., 1997

64 V.J. Lopata, C.J. Janke, G. Wrenn, G.F. Dorsey, S.J. Havens, "Electron-Beam-Curable Epoxy Resins for the Manufacturing of Advanced High Performance Composites", *International SAMPE Symposium 42,* 1997

65 G. Wisanrakkit and J.K. Gillham,"The Glass Transition Temperature as an Index of Chemical Conversion for a High-T_g Amine/Epoxy System", *Journal of Applied Polymer Science 41*(1990), 2885-2929

66 A.S. Crasto, R.Y. Kim, B.P. Price, "Electron Beam Cure of Composites for Aerospace Structures", *International SAMPE Symposium 42* (1997), 487-497

67 D.L. Goodman, C.A. Byrne, R. Moulton, D. Dixon, A. Yen, R.C. Costen, "Automated Tape Placement with In-Situ Electron Beam Cure", *International SAMPE Symposium 44* (1999), 269-280

68 J.R. Crivello, "Photocurable Monomers and Polymers for Space Applications", *International SAMPE Symposium 43* (1998), 1190-1194

69 J.V. Crivello, J.L. Lee, "Alkoxy-Substituted Diaryliodonium Salt Cationic Photoinitators", Journal of Polymer Science: Part A: Polymer Chemistry 27 (1989), 3951-3968

70 C.J. Janke, G.F. Dorsey, S.J. Havens, V.J. Lopata, International SAMPE Symposium 41 (1996), 216-226

71 M.Schwartz, Composite Materials Handbook, McGraw-Hill, New York, 1992

Appendix A

An Introduction to Polymers and Composites

A.1 Polymers and Plastics

The words polymer and plastic are often used interchangeably in everyday English, without much confusion. Indeed, in scientific literature they are also used in place of one another, but strictly speaking the two terms have quite different meanings. For example, the biological molecule DNA is a polymer but certainly not a plastic. So it is often left to the reader to implicitly know what is meant by each usage of the words. This being the case, some elaboration is presented here.

A **polymer** is a large molecule (*poly* meaning many) composed of repeating units, or 'mers' (from the Greek word *meros* – part), connected by covalent bonds. Covalent bonds are those chemical bonds in which atoms share electrons with other atoms to form stable molecules. Polymers are considered their own class of materials, distinct from other classes such as metals or ceramics. Polymers may be (and are sometimes classified as) naturally occurring or synthetic. Naturally occurring polymers include wood, bark, leaves, bone, skin, natural rubber, and silk. Synthetic polymers are easily recognizable as

human-made, and include PVC, polystyrene, synthetic rubber, and polyethylene. The term **plastic** refers to certain synthetic polymers and their formulations, which may include filler material, anti-oxidants, colouring agents, plasticizers, or other additives. Plastics may have a variety of appearances and properties, but in general may be defined by their ability to undergo continuous deformation under an applied force. Plastics are a subgroup of the polymer class of materials. Other subgroups of polymers include rubbers (also known as elastomers), textiles (e.g. fabric like rayon, nylon, etc.), adhesives, paints, and biopolymers (e.g. DNA).

Plastics are usually named by the manufacturer (a brand name) or given a generic name. Sometimes plastics are referred to by the primary polymer they contain, despite differences in their additives. Polymers always have a scientific, chemical name based on strict chemical naming conventions that describe their structure. Some polymers are also given names by the chemical company that synthesizes them, or person who discovers them. **Although the term polymer encompasses all of the subgroups and examples listed, it is often used instead of the more specific term plastic, especially by engineers and materials scientists.**

Most plastics are organic polymers, meaning they are made up of carbon and hydrogen atoms. Familiarity with the principles of organic chemistry is necessary to understand the specifics of bonding and structure in plastics. Although engineers must be knowledgeable in chemistry, they are generally less concerned with the mechanisms of polymerization and more with the resultant properties and usefulness of a polymer.

Most synthetic or engineered polymers (plastics, elastomers, textiles) have been developed in the last 50 to 60 years. Early polymers were created by modifying natural

polymers, but these days the trend has shifted to the production of totally synthetic polymers. These polymers are usually created from materials of low molecular weight hydrocarbons from oil or the pyrolysis (chemical change caused by heat) products of coal and wood. A very small percentage of polymers are created from the recycling of used polymers. The processing of engineered polymers involves taking the raw material created from pyrolysis, blending various additives, and inducing polymerization to form a useful material. Sometimes parts are shaped during the polymerization, and sometimes at a subsequent processing stage.

A.2 Thermosets, Thermoplastics and Processing

There are two distinct classifications in plastics: Thermoset plastics (thermosets) and thermoplastics. **Thermoplastics** can be heated to their softening or melting point, reshaped by pressure or in a mold, and cooled to retain that shape. This can be done repeatedly without significantly changing the properties or microstructure of the polymer. **Thermoset** polymers may only be shaped and cooled once. The process of **curing** thermosets causes permanent crosslinks to form between molecules, which will not allow subsequent reshaping. When thermosets are subjected to ensuing heat and pressure, only degradation or charring of the polymer occurs.

Polymers such as polyvinylchloride (PVC) and polyethylene are thermoplastics, while epoxies and polystyrene are thermosets. Thermoplastics are generally fairly impact resistant, or tough, and usually melt at lower temperatures, which are properties one usually associates with all plastics (plastic food containers don't break when you drop

them, but they melt if you get them close to the stove). Conversely, thermoset polymers can be brittle and glassy, but also have very good temperature resistance – up to 350°C and beyond.

Polymerization is a reaction that creates chemical linkages between relatively small molecules, or **monomers**, to form very large molecules made up of repeating monomer units. If the chemical linkages form a rigid, cross-linked molecular structure, a thermosetting plastic results. If a flexible molecular structure is formed, either linear or branched, a thermoplastic results. The term **polymerization** is usually reserved for thermoplastics while the term **curing** is generally reserved for thermosets. Polymerization reactions can occur by bulk, emulsion, suspension or solution polymerization. The chemical reaction of curing is a form of bulk polymerization. The term **resin** is commonly used to describe a polymer before it has been completely processed and in general refers to a high molecular weight organic material with no sharp melting point. Resins consist of the building blocks of a polymer – namely monomers and **oligomers** (polymers containing only a small number of repeating units). The term pre-polymer may be used to refer to any of these terms - resin, monomer, or oligomer.

There are a wide variety of ways that a plastic may be formed into a part such as casting, extruding, thermoforming, and blown molding. The specifics, advantages, limitations and relative costs of each will not be discussed here. In general, a plastic part is produced by a combination of cooling, heating, flowing, deformation, and chemical reaction. The processes differ, depending on whether the material is a thermoset or thermoplastic. The usual sequence of processing a thermoplastic is to heat the already polymerized material so it softens and flows, force the material in the desired shape

through a die or a mold and chill the melt into its final shape. By contrast, a thermoset is usually processed by starting out with a partially processed material, which is softened and activated by heating. While soft, the thermoset is forced into the desired shape by pressure, and held it at an elevated curing temperature until the polymerization reaction proceeds to the point where the part hardens and *sets* into its permanent shape.

A.3 Epoxies

Epoxies are a thermoset polymer of enormous importance to engineers. They can have a range of chemical structures, but they are based on the epoxide ring of two carbons and an oxygen in a linked ring. We generally think of epoxy as being used for adhesive or repair, for example a two-part epoxy that you buy in the hardware store. In fact, a great many of the applications of epoxies are in adhesion and repair. A two-part epoxy is actually a low molecular weight epoxy in one container, and a hardening agent in the other. The hardening agent causes the epoxy rings to open, and for each of the individual epoxy monomers to crosslink or bond to adjacent molecules. Eventually the system becomes highly crosslinked and hardens from a viscous liquid to a solid 3D polymer network. Catalysts may be used in addition to (or in some cases in place of) hardeners to facilitate the curing reaction.

This curing process depends on the hardener and the epoxy chemical structure. For some resin systems, the hardening can take place at room temperature. For other epoxy systems, the application of heat is necessary to help initiate and sustain the

crosslinking reaction. In either case, the chemical reaction of crosslinking is **exothermic** in nature, meaning that the reaction releases heat as it is proceeds.

A.4 Composites

A composite material is a substance made up of two or more distinct components, materials which do not mix, but exist together to form a material with enhanced properties and expanded capabilities. The history of composite materials extends back to ancient times when it was discovered that the addition of straw to clay made stronger bricks. Concrete, invented by the Romans, is a composite made up of aggregate and cement. Steel reinforcing bars used in modern concrete structures are merely an additional layer of reinforcement. In the last fifty years, with the advent of synthetic polymers, composites have evolved to become dominate in many fields of engineering, including the construction, aerospace, and biomedical industries.

Typically, an engineered composite is typically made up of a **matrix** or binder material, within which **reinforcement** is embedded. This reinforcement can take the shape of particles, whiskers or fibres. One of the most common modern composites is fibreglass, which has chopped strands of glass which are very strong, but also brittle, and a resin or plastic matrix, which is durable, tough and distributes external loads evenly to the glass fibres. Carbon fibre composites are relatively new, within the last 30 years. Carbon, or in its crystalline form, graphite, is very strong, with both a high modulus of elasticity (it resists stretching) and a high ultimate strength (it won't easily break in tension). Carbon fibres are also very light for their strength, when compared to other

materials. Carbon or graphite fibres embedded in a polymer matrix creates a material with superior properties – light, strong, tough and durable.

Polymers make up the matrix material of a vast majority of modern composites, which are called polymer matrix composites (PMCs), or fibre reinforced plastics (FRPs). Metal and ceramic matrix composites (MMCs and CMCs) are used to a lesser degree for specific applications. The matrix serves to bind, protect and transfer stress to the reinforcement, as well as give the component its shape. The majority of matrices currently in use are thermoset polymers, with the majority of those being epoxies. Epoxies offer ease of manufacturing, adhere well to reinforcement, shrink little, and are strong and durable.

Reinforcement for composites is usually in the form of long, thin fibres. Because of microscopic flaws present in all materials, homogeneous materials such as steel or glass rods usually only achieve approximately 10 % of their theoretical strengths (based on inter-atomic bonding). By drawing a material down to a fine thread, the stress (load per unit area) that a material is capable of withstanding can rise exponentially to one quarter or more of the theoretical value. As well, by using multiple fibres in a matrix instead of a bulk material, when one fibre fails, the crack does not automatically spread to the other fibres. Graphite/carbon, aramid (Kevlar) and glass fibres, embedded in epoxy matrices, make up the composites with the most superior properties and are often called advanced composites.

A.5 Advanced Composites and Their Properties

Advanced composites are so-named because they are used in advanced or high-tech industries and exhibit advanced or especially desirable properties. The aerospace industry is a very big user of advanced composites because strong and light materials make it easier and cheaper to get into the sky. The Boeing 757, 767, and 777, and Airbus 320 planes all use carbon fibre PMCs extensively. The X-34 Reusable Launch Vehicle (space shuttle replacement) will have an airframe that is almost 95% graphite/epoxy. Improving the properties of advanced PMCs to improve the performance characteristics of such applications is an important field of study.

There are two factors that contribute to performance of a PMC – **materials and processing**. Materials can be improved by developing better resins and fibres, and by optimizing both new and old formulations. In a similar manner, processing can be improved by developing new processes, and by optimizing process conditions. Improvement in materials and processing are evaluated by composite qualification testing. Standard test methods are used to characterize **mechanical properties** such as tension (ASTM D3039), compression (ASTM D3410), in-plane shear (SACMA 8-77), short-beam shear (ASTM D2344) and flexural properties (ASTM D790). These properties are tested both at dry room temperature and at hot and wet conditions before they are analyzed. In addition, **physical properties** such as void and fibre volume fraction must be used in evaluating composites.

Thermo-mechanical properties of polymers are often also called **rheological properties**. Rheology is the study of the change in form and flow of matter, particularly of the plastic flow of solids. A rheological property of significant importance is the glass

transition temperature (T_g) of thermoset polymers and their composites. The glass transition point is the temperature at which a material changes from glass-like behaviour to rubber-like behaviour (i.e. from a rigid to a softened state). Both mechanical and electrical properties degrade significantly at this point, which is characterized by a narrow transition range rather than a sharp point as in freezing or boiling. For advanced applications that are subjected to temperature extremes, the glass transition temperature is an important parameter. Both material and process parameters are often evaluated based on the T_g of the resulting composite parts.

Appendix B

Thermal Analysis and Differential Scanning Calorimetry

The expression 'thermal analysis' suggests the measurement of heat. In fact, the measurement of heat is only one part of thermal analysis laboratory practice. Thermal analysis encompasses measurement of phenomena associated with heat and heat transfer, and even more generally speaking, the investigation of temperature dependent events.

B.1 Differential Scanning Calorimetry

The actual measurement of heat, one of the most prominent thermal analysis techniques, is the objective of calorimetry. To measure heat, one must exchange heat. The exchanged heat tends to effect a temperature change in a body, which can be used as a measure of the heat exchanged. The process of heat exchange involves the flow of heat, which leads to local temperature differences along its path, which may also serve as a measure of the flowing heat.

Chemical transitions, and many physical transitions, are associated with the generation or consumption of heat. Calorimetry is the universal method for investigating

such processes. Measuring devices in which an exactly known amount of heat is input into a sample and the temperature change in the sample is measured, are also referred to as calorimeters. Differential Scanning Calorimetry (DSC) is defined as follows:

> *A technique in which the heat-flow rate (power) to the sample is monitored against time or temperature while the temperature of the sample, in a specified atmosphere, is programmed.*

There are two different types of DSCs: the power compensating DSC and the heat flux DSC. The power compensating DSC belongs to the class of heat-compensating calorimeters. Two specimens (a sample under investigation and a reference) are heated in separate identical furnaces. The differential temperature between the sample and reference is converted to differential heat flow by measuring the power required to return the temperature difference to a constant value (theoretically zero). The **heat flux DSC** belongs to the class of heat-exchanging calorimeters. Two specimens are subjected to controlled heating in the same furnace. The measurement signal is the temperature difference between samples. A temperature difference develops if there is any difference between the heat flow rates to the sample and to the reference. The magnitude of the temperature difference describes the intensity of the exchange and is proportional to the heat flow rate.

B.2 The Heat Flux DSC

The analysis in the body of this thesis has utilized a heat flux DSC, and so its operation will be described in more detail. The characteristic feature of this measuring system is that the main heat flow from the furnace to the samples takes place through a disk of good thermal conductivity. The samples, or more precisely the sample containers, are positioned symmetrically on the disk. The thermocouples are positioned directly below each sample, and are built right into the disk structure. Each temperature sensor covers an area that is approximately equal to the area of the sample container, so that the position of the sample inside the container (usually called the sample pan) does not matter. To keep the error in measurement as small as possible, the arrangement and exact location of the sample and reference should always be the same.

Figure B.1 shows a schematic of a DSC cross section. A constantan disk is the primary means of transferring heat to the sample and reference positions. The differential heat flow, Φ, is monitored by area thermocouples formed by the junction of the constantan disk and chromel wafers, which cover the underside of the platforms. Chromel and alumel wires attached to the chromel wafers form thermocouples, which directly monitor the sample temperature. The furnace is made of silver to provide the high thermal conductivity needed for exceptional temperature stability.

When the furnace is heated, heat flows through the disk to the samples. When the arrangement is ideally symmetric and the samples are identical, equaliy high heat flow rates flow into the sample and the reference. The differential temperature signal ΔT (differential voltage from thermocouples) is zero at this point. When this steady-state equilibrium is disturbed by a transition within one of the samples, a differential signal is

generated which is proportional to the difference between the heat flow rates to the sample and to the reference sample:

$$\Phi_s - \Phi_r = -\Delta T \qquad (\Delta T = T_s - T_r) \qquad \text{(eq. B.1)}$$

In practice it is not possible to have thermally identical samples nor is it possible to have exact thermal symmetry of the measuring system at all operating temperatures. Therefore there is always a signal ΔT, even if there is no transition taking place, which depends on the temperature and sample properties. This baseline heat flow, Φ_{bl} must be compensated for during the analysis.

The measurement signal ΔT is obtained as an electrical voltage. The measured heat flow rate Φ_m is assigned to the signal ΔT by an internal calibration:

$$\Phi_m = -k \cdot \Delta T \qquad \text{(eq. B.2)}$$

The measurement signal output by the DSC is Φ_m in mW or μW.

There are two obvious ways to check Φ_m as compared to Φ_{true}. The first method is made by measuring the steady-state heat flow into a sample of known heat capacity C, under a constant temperature scan rate dT/dt:

$$C \cdot dT/dt = \Phi_{true} = K_\Phi \cdot \Phi_m \qquad \text{(eq. B.3)}$$

The second method is to compare the integral over a transition peak of a reference sample with the expected (known) heat of transition Q_r:

$$Q_r = Q_{true} = K_Q \cdot I(\Phi_m - \Phi_{bl})\, dt \qquad \text{(eq. B.4)}$$

Where Φ_{bl} is the baseline curve, as previously mentioned.

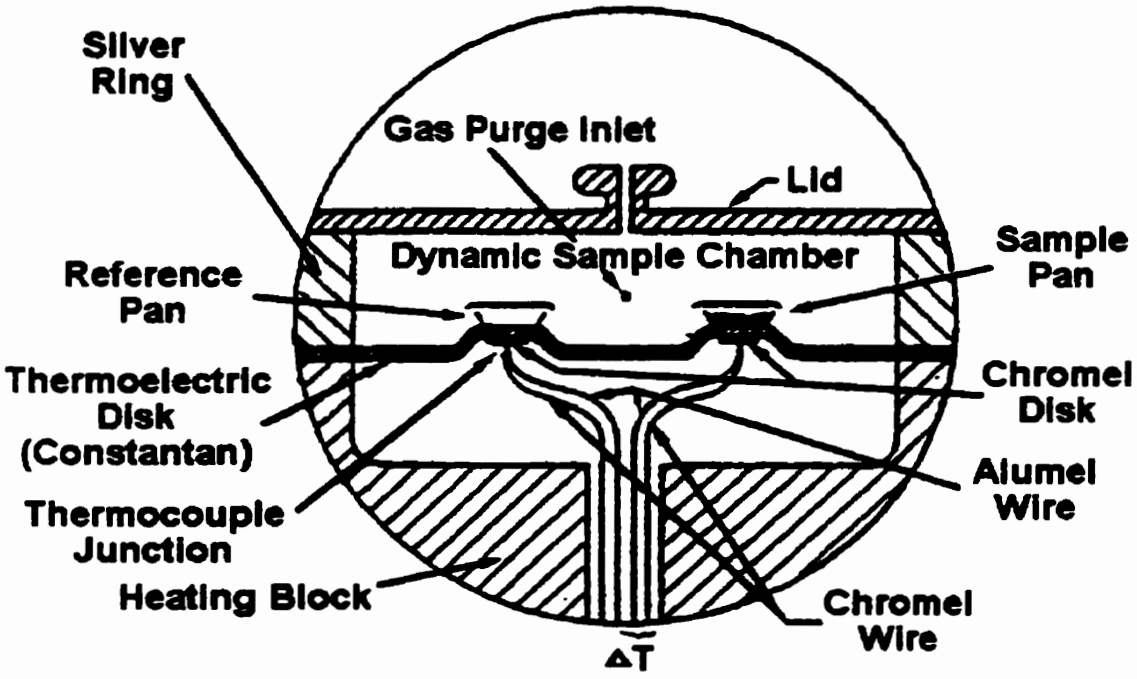

Figure B.1: Heat flux DSC cross section

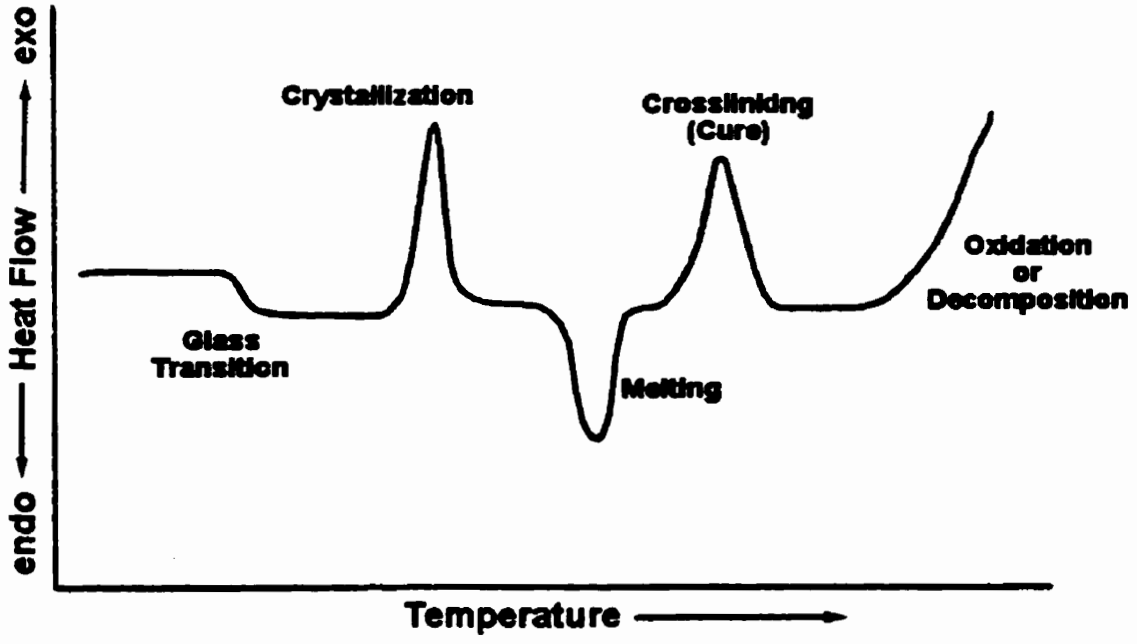

Figure B.2: Thermal events on the DSC

B.3 DSC Operation and Testing

The most common mode of operation is to scan the temperature of the furnace at a constant rate, and measure the resulting heat flow. The sample pans available are made out of aluminium, copper, graphite, gold or platinum. For most applications, aluminium pans are used. A sample can be sealed hermetically within the pan if desired. Purge gas is admitted to the furnace chamber automatically through an orifice in the heating block. The gas is preheated by circulation through the block before entering the sample chamber. Any purge gas may be used, but is most common to use Nitrogen. The reference is most often simply an empty pan. Sometimes an extra pan lid or portion thereof is encapsulated in the reference pan to match the mass of reference with sample. This is done to improve baseline performance.

The characteristic shapes of some transitions are displayed in Figure B.2. In endothermic events, heat is absorbed by the sample relative to the reference. For exothermic events, heat is released by the sample relative to the reference. Typical applications of DSC are glass transition, degree of cure (thermoset resins), and specific heat capacity measurements.

The glass transition is a step-change in the mobility of polymer molecules in the amorphous region of the polymer. At temperatures below the glass transition, mobility is restricted resulting in a hard, rigid structure. Above the glass transition the material is viscous or rubbery. Physical properties change significantly at the glass transition temperature, T_g. Above the transition materials have a higher heat capacity, higher coefficient of thermal expansion, and a lower modulus. Since there is a step-increase in heat capacity at T_g, an endothermic shift in the baseline occurs when heating. Typically,

the temperature of the inflection point of the transition is used for T_g. The accepted standard test method for measurement of T_g is covered by ASTM standard E1356.

Measurement of the degree of cure (or crosslinking) applies to thermosetting polymers such as epoxies and phenolics. It is a measure of the extent of chemical reaction in the polymer system, usually expressed as a percent. It is often determined from the glass transition temperature, which increases with increased crosslinking. It may also be determined by a comparative study of curing exotherms. An important area of study with DSC is the kinetics of these crosslinking reactions. Obviously, optimization of the curing process is desired for the manufacturing process of polymer materials. A review of DSC kinetic methods will not be presented here.

It should be noted that sensitivity and resolution of thermal events are affected by the heating rate and sample mass. As can be seen from equation B.3, for a large measured signal (higher sensitivity), a high heating rate and high sample mass should be used. Since heat transfer is a time dependant phenomenon, the best resolution is observed with a lower heating rate and smaller sample mass.

B.4 DSC Specifications

The University of Manitoba's Thermal Analysis Model 2910 Differential Scanning Calorimeter has the following specifications:

Sample Size:		.5 to 100 mg	
Sample Volume (max):		10 mm^3	
Atmosphere:		Non-corrosive inert, reducing or oxidizing	
Dynamic Gas Purge (preheated):		Up to 100 ml/min at pressures from 266 Pa to atmospheric	
Thermocouples:		Sample:	Chromel/Alumel
		Control:	Platinel II
		ΔT:	Chromel/Constantan
Temperature Range:	Air/Oxygen Environment:		Ambient to 600° C
	Inert Gas Environment:		Ambient to 725° C
	Liquid Nitrogen Cooling Accessory:		As low as -150°
Temperature Accuracy:		+/- 1° C or 1 % whichever is greater	
Temperature Reproducibility (using metal standards):			+/- 0.1° C
Programmable Heating Rate:		0.01 to 200° C/min	
Maximum Sensitivity:		1 μW (2:1 signal-to-noise RMS)	
Calorimetric Precision:		+/- 1 % (based on metal samples)	

B.5 Dynamic Mechanical Analysis

Dynamic mechanical analysis (DMA) is a thermal analysis technique that measures the mechanical properties of materials as they are deformed under periodic stress. Especially useful for polymers and PMCs, DMA is usually performed by scanning the temperature (warming or cooling) to determine thermal dependence of the material properties. A variable sinusoidal stress is constantly applied to a material specimen, and the resulting strain is measured with respect to time and temperature. If the material is purely elastic, then the phase difference between the stress and strain sine waves is 0° (i.e. they are in phase). If the material is purely viscous, the phase difference is 90°. Most materials including polymers are viscoelastic and exhibit a phase difference, δ, between those extremes. This phase difference, along with the amplitudes of stress and strain, is used to determine a number of fundamental material properties, including storage and loss modulus, tan δ, complex and dynamic viscosity, transition temperatures, creep, and stress relaxation (see Figure B.3).

A typical mode of operation of the DMA is to use a dual cantilever clamp, in which a long, thin wafer is held by fixed clamps at either end, while a middle clamp applies the periodic stress. Most DMA measurements are made using a single frequency and constant deformation (strain) amplitude, while the temperature is varied. DMA measures the viscoelastic properties of materials and provides, in graphic form, a picture of the relationship between temperature and modulus (Figure B.4). Standard practice and terminology related to DMA operation are described in ASTM standards D4065 and D4092.

There are several components that are critical to the design and resultant performance of a dynamic mechanical analyzer. These components are the drive motor (which supplies the sinusoidal deformation force to the sample material), the drive shaft support and guidance system (which transfers the force from the drive motor to the clamps which hold the sample), the displacement sensor (which measures t he sample deformation [oscillation amplitude] that occurs under the applied force), the temperature control system (furnace), and the sample clamps. There are a number of different clamp configurations that allow testing of such properties as flexural & elastic modulus, as well as specific properties of thin films and fibres. The DMA machine at the University of Manitoba (TA model 2980) is able to deliver forces (stresses) of 0.001 to 18 Newtons (4 lbs.), and temperature ranges from –150°C to 600°C.

Observation and measurement of the glass transition temperature is a common use for the DMA. From an engineering perspective, the sweeping drop in modulus at the glass transition has more significance than the change in thermal conductivity observed with the DSC. Referring to Figure B.4, the T_g for a DMA test is usually chosen to be the temperature for the peak value of tan δ or loss modulus. These temperature values are usually in agreement with a few degrees. Sometimes, if the polymer or composite sample is exhibiting complex behaviour, the loss modulus and tan δ do not have a simple peak as in the diagram. In these cases, engineers usually quote the service temperature, T_s rather than the glass transition. The service temperature is often defined as the temperature at which the modulus falls to 50 % of its value at room temperature. Often, T_s is very nearly at the same temperature as the T_g, and it is easier to determine, so is used in place of a T_g value.

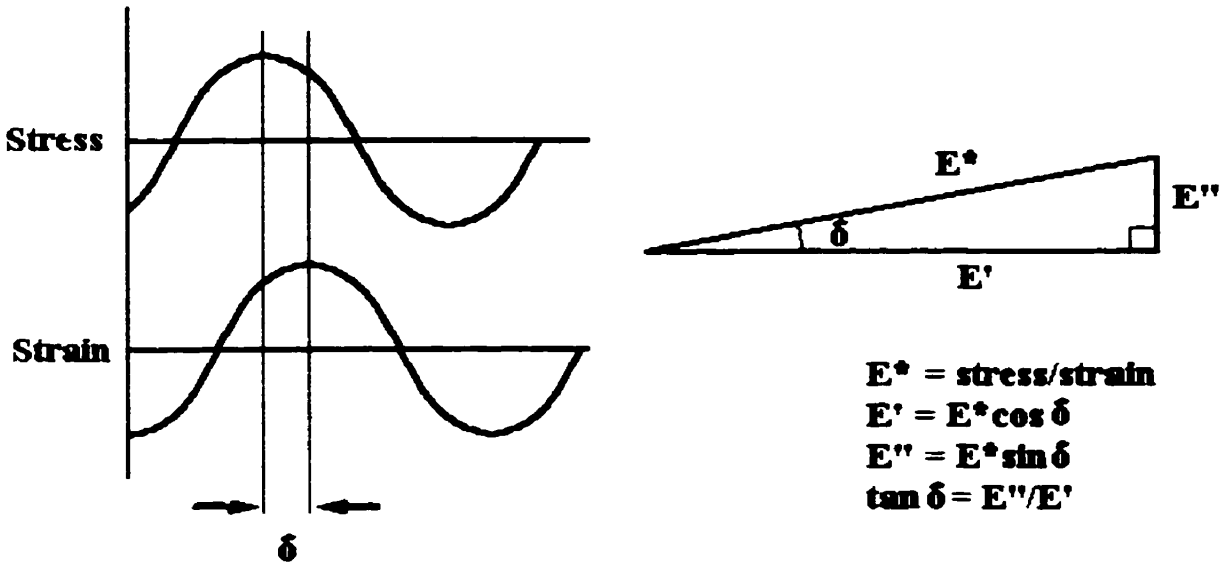

Figure B.3: Complex modulus of a viscoelastic material

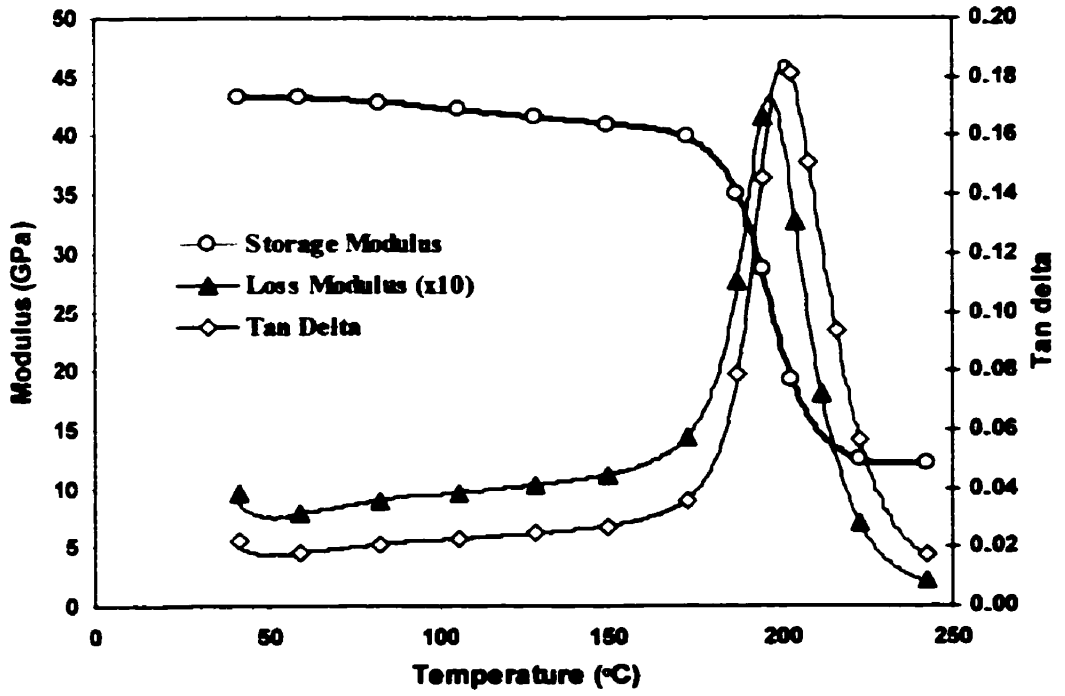

Figure B.4: DMA complex modulus plot showing the glass transition